Part One
Amino Acids as Building Blocks

Amino Acids, Peptides and Proteins in Organic Chemistry.
Vol.3 – Building Blocks, Catalysis and Coupling Chemistry. Edited by Andrew B. Hughes

ISBN: 978-3-527-32102-5

1
Amino Acid Biosynthesis

Emily J. Parker and Andrew J. Pratt

1.1
Introduction

The ribosomal synthesis of proteins utilizes a family of 20 α-amino acids that are universally coded by the translation machinery; in addition, two further α-amino acids, selenocysteine and pyrrolysine, are now believed to be incorporated into proteins via ribosomal synthesis in some organisms. More than 300 other amino acid residues have been identified in proteins, but most are of restricted distribution and produced via post-translational modification of the ubiquitous protein amino acids [1]. The ribosomally encoded α-amino acids described here ultimately derive from α-keto acids by a process corresponding to reductive amination. The most important biosynthetic distinction relates to whether appropriate carbon skeletons are pre-existing in basic metabolism or whether they have to be synthesized *de novo* and this division underpins the structure of this chapter.

There are a small number of α-keto acids ubiquitously found in core metabolism, notably pyruvate (and a related 3-phosphoglycerate derivative from glycolysis), together with two components of the tricarboxylic acid cycle (TCA), oxaloacetate and α-ketoglutarate (α-KG). These building blocks ultimately provide the carbon skeletons for unbranched α-amino acids of three, four, and five carbons, respectively. α-Amino acids with shorter (glycine) or longer (lysine and pyrrolysine) straight chains are made by alternative pathways depending on the available raw materials. The strategic challenge for the biosynthesis of most straight-chain amino acids centers around two issues: how is the α-amino function introduced into the carbon skeleton and what functional group manipulations are required to generate the diversity of side-chain functionality required for the protein function?

The core family of straight-chain amino acids does not provide all the functionality required for proteins. α-Amino acids with branched side-chains are used for two purposes; the primary need is related to protein structural issues. Proteins fold into well-defined three-dimensional shapes by virtue of their amphipathic nature: a significant fraction of the amino acid side-chains are of low polarity and the hydrophobic effect drives the formation of ordered structures in which these side-chains are buried away from water. In contrast to the straight-chain amino

Amino Acids, Peptides and Proteins in Organic Chemistry.
Vol.3 – Building Blocks, Catalysis and Coupling Chemistry. Edited by Andrew B. Hughes

ISBN: 978-3-527-32102-5

acids, the hydrophobic residues have large nonpolar surface areas by virtue of their branched hydrocarbon side-chains. The other role of branched amino acids is to provide two useful functional groups: an imidazole (histidine) and a phenol (tyrosine) that exploit aromatic functional group chemistry.

This chapter provides an overview of amino acid biosynthesis from a chemical perspective and focuses on recent developments in the field. It highlights a few overarching themes, including the following:

i) The chemical logic of the biosynthetic pathways that underpin amino acid biosynthesis. This chemical foundation is critical because of the evolutionary mechanisms that have shaped these pathways. In particular, the way in which gene duplication and functional divergence (via mutation and selection) can generate new substrate specificity and enzyme activities from existing catalysts [2].
ii) The contemporary use of modern multidisciplinary methodology, including chemistry, enzymology, and genomics, to characterize new biosynthetic pathways.
iii) Potential practical implications of understanding the diverse metabolism of amino acid biosynthesis, especially medicinal and agrichemical applications.
iv) The higher-level molecular architectures that control the fate of metabolites, especially the channeling of metabolites between active sites for efficient utilization of reactive intermediates.

Box 1.1: Nitrogen and Redox in Amino Acid Biosynthesis

Ammonia is toxic and the levels of ammonia available for the biosynthesis of amino acids in most biochemical situations is low. There are a limited number of entry points of ammonia into amino acid biosynthesis, notably related to glutamate and glutamine. Once incorporated into key amino acids, nitrogen is transferred between metabolites either directly or via *in situ* liberation of ammonia by a multifunctional complex incorporating the target biosynthetic enzyme. The main source of *in situ* generated ammonia for biosynthesis is the hydrolysis of glutamine by glutaminases. *De novo* biosynthesis of amino acids, like element fixation pathways in general, is primarily reductive in nature. This may reflect the origins of these pathways in an anaerobic world more than 3 billion years ago.

Box 1.2: The Study of Biosynthetic Enzymes and Pathways

The source of an enzyme for biochemical study has important implications. Most core metabolism has been elaborated by studying a small number of organisms that were chosen for a variety of reasons, including availability, ease of manipulation, ethical concerns, scientific characterization, and so on. These exemplar organisms include the bacterium *Escherichia coli*, the yeast *Saccharomyces cerevisiae*, the plant *Arabidopsis thaliana*, and the rat as a typical mammal. Much of the detailed characterization of amino acid biosynthesis commenced with studies on these organisms. With the rise of genetic engineering techniques, biosynthetic

enzymes from a wide variety of sources are available for scientific investigation, and there has been increasing emphasis on working with enzymes and pathways from alternative organisms.

Metabolic diversity is greatest among prokaryotes. One fundamental change in the underlying microbiology that has affected our understanding of pathway diversity has been the appreciation of the deep biochemical distinctions between what are now recognized to be two fundamental domains of prokaryotes: eubacteria and Archaea [3]. The former bacteria include those well known to be associated with disease and fermentation processes; while the latter include many methanogens and extremophiles (prokaryotes that grow in extreme conditions, such as hyperthermophiles that grow at temperatures above 60 °C or halophiles that grow in high ionic strength environments). Bioinformatics approaches are complementing conventional enzymological studies in identifying and characterizing interesting alternative biosynthetic pathways [4]. The greater understanding of microbial and biosynthetic diversity is presenting exciting opportunities for novel discoveries in biosynthesis.

Much of the focus of biosynthetic enzymology now focuses on enzymes from pathogens and hyperthermophiles. The focus on the study of enzymes from pathogens is predicated on the possibility that inhibitors of such enzymes may be useful as pesticides and therapeutic agents. Since humans have access to many amino acids in their food, they have lost the ability to make "dietary essential" amino acids that typically require extended dedicated biosynthetic pathways [5]. The biosynthetic enzymes of the corresponding pathways are essential for many pathogens and plants, but not for humans; hence, selective inhibitors of these biosynthetic enzymes are potentially nontoxic to humans, but toxic to undesirable organisms. Enzymes from hyperthermophilic organisms, produced by genetic engineering, are scrutinized mainly because of their ease of structural characterization. These enzymes retain their native structures at temperatures that denature most other proteins, including those of the host organism. These proteins are of high thermal stability and simple heat treatment can be used to effect high levels of purification of the desired protein.

1.2
Glutamate and Glutamine: Gateways to Amino Acid Biosynthesis

Glutamate and the corresponding amide derivative, glutamine, are critical metabolites in amino acid metabolism. The biochemistry of these two amino acids also illustrates the distinct chemistry associated with the α-amino and side-chain functional groups, each of which is exploited in the biosynthesis of other amino acids. These amino acids derive from ammonia and α-KG. Glutamate dehydrogenase (GDH) interconverts α-KG and glutamate (Figure 1.1) [6]. Although glutamate is formed in this way by reductive amination, this enzyme is generally not dedicated to biosynthesis; the reverse reaction, an oxidative deamination to regenerate α-KG, is

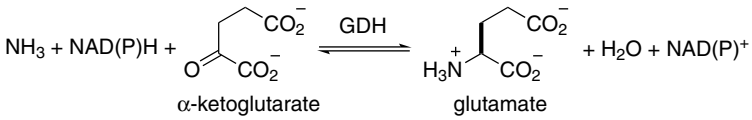

Figure 1.1 Interconversion of α-KG and glutamate catalyzed by GDH.

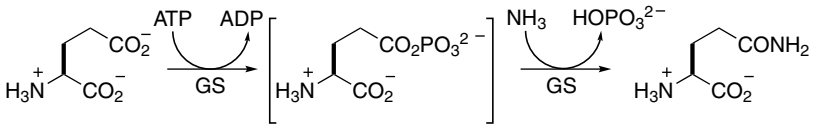

Figure 1.2 Conversion of glutamate to glutamine catalyzed by GS.

often an important *in vivo* role for this enzyme [7]. This deamination chemistry might be a factor in the relatively weak binding of ammonia (e.g., $K_M(NH_3)$ is 3 mM for the *E. coli* enzyme – above normal environmental concentrations). In many organisms there is an additional enzyme, glutamate synthase (GOGAT), dedicated to the biosynthesis of glutamate [8]. GOGAT utilizes ammonia generated *in situ* by the hydrolysis of glutamine and this enzyme will be described after a discussion of the biosynthesis of glutamine.

The conversion of glutamate to glutamine, catalyzed by glutamine synthetase (GS), requires the activation of the side-chain carboxylate as an acyl phosphate, prior to nucleophilic substitution of the resulting good leaving group by ammonia (Figure 1.2). The use of ATP, to produce γ-glutamyl phosphate, assists both the kinetics and the thermodynamics of amide formation: by producing a more reactive carboxylic acid derivative and overturning the intrinsically favorable nature of amide hydrolysis in water.

GS from enteric bacteria, such as *E. coli* and *Salmonella typhimurium*, is an exemplar of an amino acid biosynthetic enzyme; the overall reaction it catalyses is effectively irreversible *in vivo* ($K = 1200$). Being dedicated to biosynthesis, it has evolved tight binding of ammonia ($K_M(NH_3) < 200\,\mu M$) which allows efficient synthesis of glutamine under the low ammonia conditions (much less than 1 mM) found *in vivo*. Its *in vivo* role as an entry point for the biosynthesis of a wide range of nitrogen metabolites is eloquently communicated by the extensive feedback regulation of this enzyme by a range of nitrogen-containing metabolites, including glycine, serine, alanine, and histidine [9–12]. Glutamine is the primary store of ammonia in many cells; the side-chain amide is chemically unreactive, but its favorable hydrolysis can be catalyzed on demand by glutamine amidotransferase (GAT) enzymes [13].

1.2.1
Case Study: GOGAT: GATs and Multifunctional Enzymes in Amino Acid Biosynthesis

In contrast to GDH, GOGAT is a dedicated biosynthetic enzyme. It is the primary source of glutamate in plants, eubacteria and lower animals [14, 15]. These iron–sulfur flavoproteins carry out the reductive amination of α-KG to glutamate via a five-

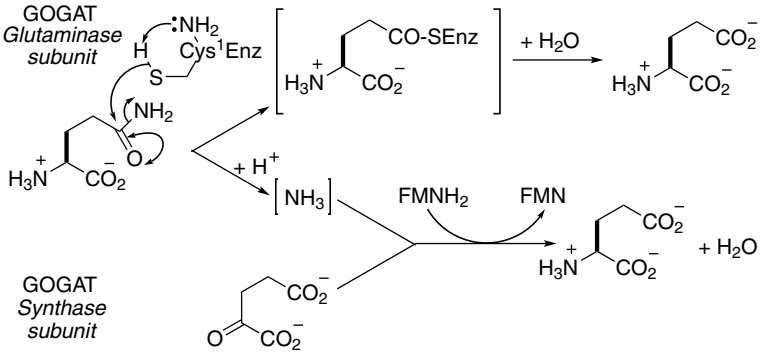

Figure 1.3 The biosynthesis of glutamate mediated by GOGAT.

step process that utilizes the *in situ* hydrolysis of glutamine as the source of ammonia for this reaction (Figure 1.3) [16].

As with many reductive biosynthetic enzymes, there are variants of the enzyme adapted to different electron sources; for example, both ferredoxin- and nicotinamide-dependent enzymes are known, and examples of both of these classes of GOGAT have been studied in detail [15]. They reveal many of the key features of metabolite channeling observed in biosynthetic enzymes utilizing glutamine as a nitrogen donor.

The NADPH-dependent GOGAT from *Azospirillum brasilense* is an α,β-heterodimer [17]. The β-subunit supplies the electrons for the reductive amination process: NADPH reduces FAD and the electrons are passed, in turn, to a 3Fe–4S center on the α-subunit and then on to the FMN cofactor at the active site for glutamate formation. The α-subunit consists of four domains. The N-terminal domain is a type II GAT, in which the N-terminal cysteine attacks glutamine releasing ammonia and generating an enzyme-bound thioester, which is subsequently hydrolyzed (Figure 1.3) (type I GATs, the other variant, utilize a combination of an internal cysteine and a histidine as catalytic residues [18]). When a class II GAT is active, a conserved Q-loop closes over the active site and prevents release of ammonia to the solution; instead the nascent ammonia travels through a hydrophilic internal tunnel approximately 30 Å in length to the third domain which is a $(\beta\alpha)_8$ barrel containing the 3Fe–4S cluster and the FMN active site. The latter site binds the substrate α-KG and carries out the synthesis of glutamate, presumably via reduction of an α-iminoglutarate intermediate. There is a gating mechanism for synchronization of GAT and reductive amination active sites: the glutaminase activity is dependent on the binding of both α-KG and reduced cofactor at the second site (Figure 1.4) [19].

The ferredoxin-dependent GOGAT from the cyanobacterium, *Synechocystis* sp. PCC 6803, has a similar structure to the *A. brasilense* enzyme, possessing a type II GAT domain and a synthase site linked by a 30-Å tunnel, which is gated in an analogous way [21]. The GAT domain exists in an inactive conformation, which can bind glutamine but not hydrolyze it. This is converted to the active conformation on binding of α-KG and reduced cofactor, $FMNH_2$, to the synthase site; this

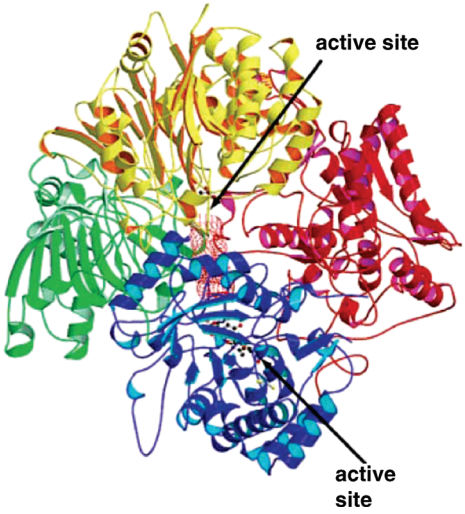

Figure 1.4 Structure of GOGAT showing the internal tunnel for ammonia transfer between the GAT (gold) and synthase (blue) active sites. (Picture taken from [20].)

conformational switch also serves to open the entry point to the ammonia tunnel. A conserved glutamate residue (Glu1013 in the *Synechocystis* enzyme), present at the tunnel constriction, has been shown to be the key residue controlling the cross-regulation mechanism. This glutamate interacts with the N-terminal amino group of the protein, which is the active-site base of the glutaminase, as well as affecting the geometry of the tunnel entry point. Mutation of this residue to aspartate, asparagine, or alanine affected glutaminase activity and the sensitivity of glutaminase action to the binding of α-KG at the synthase site [22].

GOGAT exemplifies our growing awareness of details of glutamine-dependent enzymes, in particular, and biosynthetic pathways, in general. By exploiting the higher-level organization of multifunctional enzyme systems, metabolites can be channeled to the next enzyme of a pathway, thereby controlling their fate. Together with the potential for subtle levels of regulation, this organization ensures the efficient use of biosynthetic intermediates [20].

1.3
Other Amino Acids from Ubiquitous Metabolites: Pyridoxal Phosphate-Dependent Routes to Aspartate, Alanine, and Glycine

1.3.1
Pyridoxal Phosphate: A Critical Cofactor of Amino Acid Metabolism

Once glutamate is available, the α-amino function can be transferred to other α-keto acids via amino acid aminotransferase enzymes (Figure 1.5) [23]. This family of

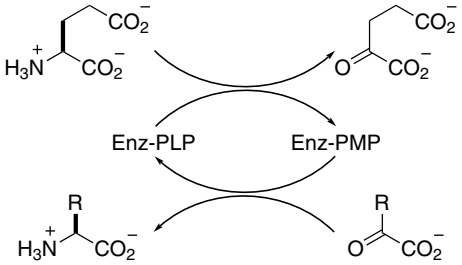

Figure 1.5 Overall interconversion mediated by most aminotransferase enzymes (e.g., for AATases R = $CH_2CO_2^-$).

enzymes exploit the catalytic versatility of the cofactor pyridoxal 5′-phosphate (pyridoxal phosphate PLP), one of the active forms of vitamin B_6, which is interconverted with pyridoxamine phosphate (PMP) during the overall transformation [24, 25].

The aldehyde of PLP readily forms Schiff bases with amines and this cofactor is generally tethered to the active site of enzymes via a link to a lysine side-chain. Amino acid substrates bind to the cofactor by Schiff base exchange with the enzyme lysine, which is thereby liberated as a potential active-site base. The critical feature exploited in amino acid metabolism is the ability of PLP to act as an electron sink, stabilizing negative charge build up at C^{α} of the substrate (Figure 1.6). By delocalizing negative charge at this center PLP is able to mediate chemistry at the α-, β-, and γ-centers of appropriately functionalized amino acids (see Box 1.3).

Pyridoxal-dependent enzymes have been classified into five fold-types and the aspartate aminotransferase (AATase) family of enzymes belong to Fold-Type I [26, 27]. The cytosolic and mitochondrial AATases were the first PLP-dependent enzymes for which detailed structural information was obtained [28–30]. These enzymes interconvert glutamate and oxaloacetate with α-KG and aspartate (Figure 1.7). Glutamate is activated by binding to the PLP and the displaced Schiff base Lys258 acts as an acid–base catalyst to transfer a proton between C^{α} and C4′ of the PLP [31]. An aspartate residue (Asp222) interacts with the protonated nitrogen of the cofactor,

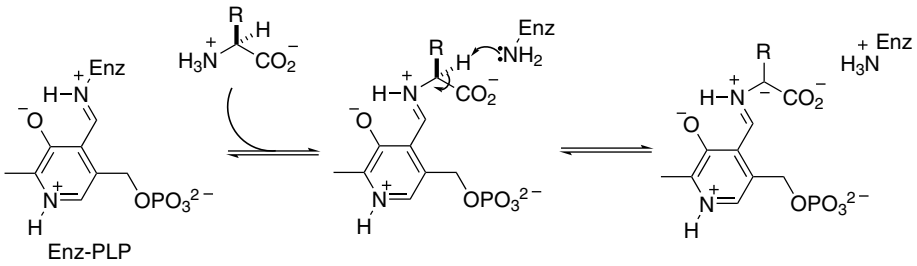

Figure 1.6 Schiff base formation and anion stabilization by PLP-dependent enzymes.

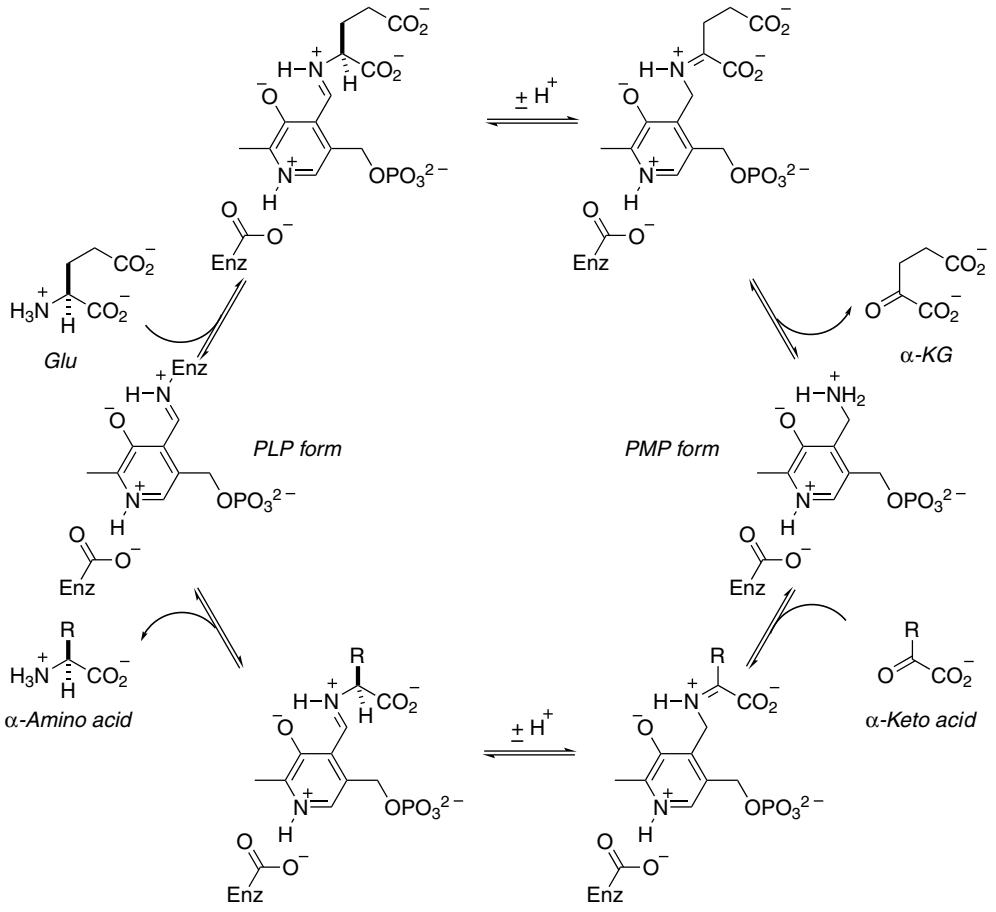

Figure 1.7 Mechanism of aminotransferase catalysis (for AATases R = $CH_2CO_2^-$).

stabilizing the pyridinium form and facilitating deprotonation of the substrate. Once a proton has been transferred from C^{α} to C4′, hydrolytic cleavage of the ketimine linkage liberates α-KG and leaves the PMP form of the cofactor. Binding of oxaloacetate and running the reaction in reverse leads to regeneration of the original enzyme and production of aspartate. Aminotransferase enzymes provide a general mechanism for interconverting α-amino acids and α-keto acids, illustrating a second route by which nitrogen is transferred between metabolites.

1.3.2
Case Study: Dual Substrate Specificity of Families of Aminotransferase Enzymes

Aminotransferase enzymes pose an intriguing challenge for substrate specificity since they bind two different substrates successively at the same site and must

Box 1.3: The Mechanistic Versatility of PLP: A Biochemical Electron Sink

Amino acids bind to PLP by forming a Schiff base. Once bound, the ability of PLP to stabilize a negative charge at the α-center of bound amino acids has been harnessed by a range of amino acid biosynthetic enzymes to mediate chemistry at the α-, β- and γ-centers of suitably functionalized amino acids.

α-Center Reactivity

Cleavage of any of the three substituent bonds to the α-center can lead to a carbanionic species (Figure 1.8). Deprotonation of the α-proton, by the lysine liberated on Schiff base exchange, is used in transamination chemistry where the α-proton is relocated to the benzylic position of PLP *en route* to PMP as described above (and in some amino acid racemases). Decarboxylation provides a related anion, which can be protonated; this is the source of biological amines and is exploited in the biosynthesis of lysine via decarboxylation of the D-amino acid center of *meso*-diaminopimelate (DAP). Finally, when the amino acid side-chain contains a β-hydroxyl function, retro-aldol chemistry provides a way of cleaving this C−C bond. This is exploited in the biosynthesis of glycine, for example, by

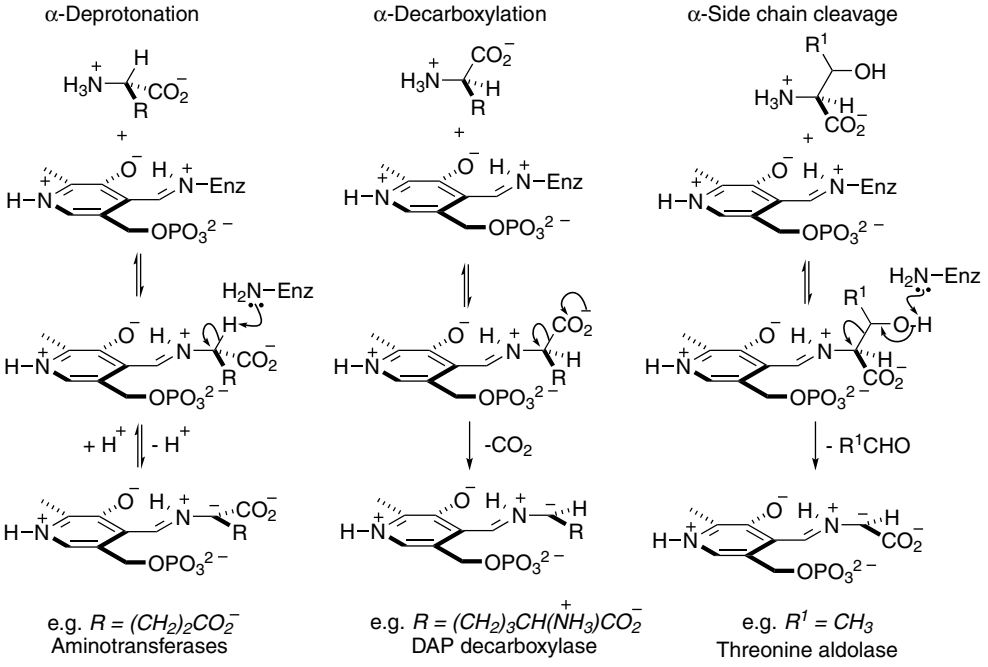

Figure 1.8 Stereoelectronic control of α-center reactivity by PLP-dependent enzymes illustrated by enzymes involved in amino acid biosynthesis. As noted in the text, the decarboxylation example, DAP decarboxylase, utilizes a D-amino acid substrate.

threonine aldolase. Enzymes control the identity of the bond that is cleaved by exploiting stereoelectronic factors as originally proposed by Dunathan [32]. The cleaved bond must align with the delocalized π-orbitals of the PLP cofactor. By specific recognition of the α-amino acid functionalities, the enzyme can control the orientation of the substrate and hence its fate [33].

β,γ-Center Reactivity

Amino acids that contain a leaving group at the β-position can undergo elimination chemistry from the α-deprotonated intermediate. Nucleophilic attack on the aminoacryloyl intermediate leads to overall nucleophilic substitution, via an elimination–addition mechanism (Figure 1.9). This is exploited in the biosynthesis of cysteine and related amino acids. More extended proton relays can extend this chemistry to the γ-center (Figure 1.10) as observed in γ-cystathionine synthase.

recognize these substrates but not others. AATases selectively bind glutamate and aspartate. Two active-site arginine residues (Arg292 and Arg386) bind to the two carboxylates of these substrates, one of these, Arg292, controls the specificity forming an ion pair with the carboxylate side-chain of each substrate (Figure 1.11). Mutation of this arginine to an anionic aspartate depresses the activity (k_{cat}/K_M) of the enzyme with respect to anionic substrates by a factor of more than 100 000 [34].

Other families of aminotransferases face greater challenges with the dual substrate specificity that is a general feature of all these enzymes. Since glutamate is a common amino donor in these systems, these enzymes must accommodate the negatively charged γ-carboxylate of glutamate while also accepting side-chains of the alternative substrate with different sizes, polarities, and charges. Two different strategies are employed to deal with the issue: an "arginine switch," whereby the key arginine undergoes a conformational shift to accommodate the new side-chain, and the use of an extended hydrogen bond network to mediate substrate recognition, rather than the cationic charge of arginine (Figure 1.11) [35].

PLP-mediated β-substitution chemistry

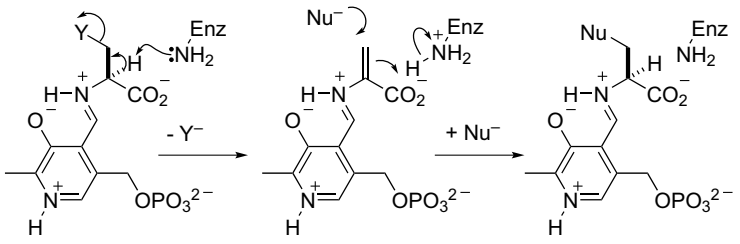

Figure 1.9 PLP-mediated nucleophilic substitution at the β-center of amino acids.

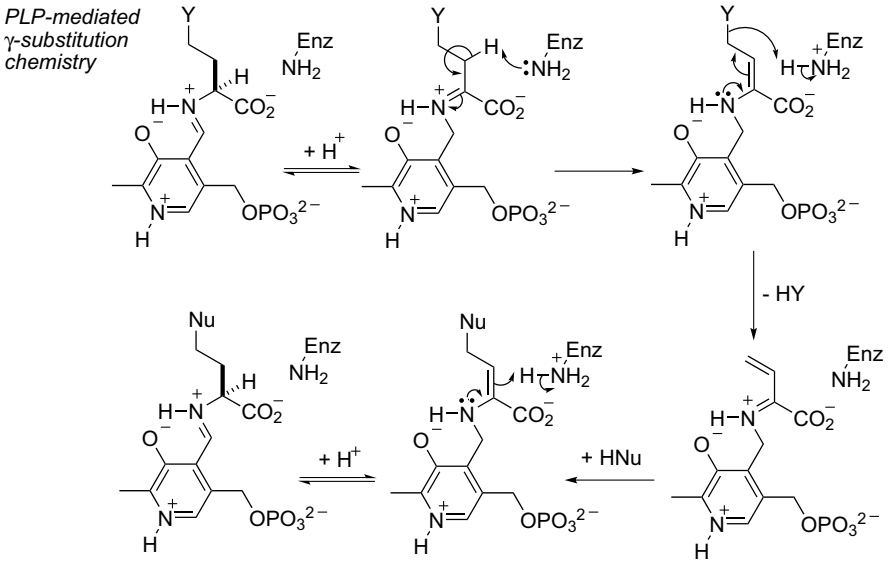

Figure 1.10 PLP-mediated nucleophilic substitution at the γ-center of amino acids.

Tyrosine aromatic amino transferases (TATases) utilize glutamate or aspartate as amino donors to produce the aromatic amino acids tyrosine, phenylalanine, and tryptophan. The TATase from *Paracococcus denitrificans* provides a clear example of an arginine switch [36]. The binding of a series of inhibitors to this enzyme shows that the active site utilizes Arg386 for specific recognition of the α-carboxylate and the

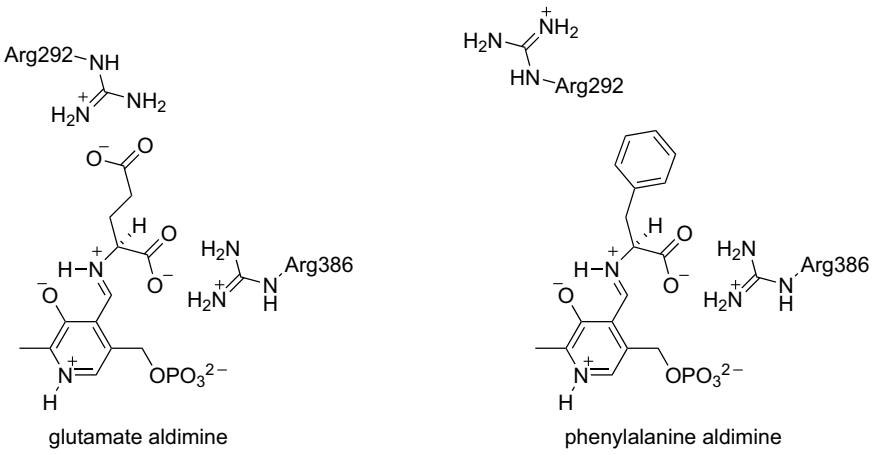

Figure 1.11 The arginine switch in the substrate specificity of aminotransferases: in *P. denitrificans* TATase Arg292 forms an electrostatic attraction to the glutamate γ-carboxylate; reorientation of Arg292 away from the active site allows binding of a nonpolar side-chain. (Adapted from [31].)

surrounding region, in the vicinity of the α- and β-centers of the substrate, is rigid. However, active-site residues that bind the large hydrophobic substituent are conformationally flexible and Arg292 moves out of the active site to accommodate bulky uncharged substrates [37]. The arginine switch has been engineered into AATase by site-directed mutation of six residues, thereby allowing transamination of large aromatic substrates [38]. The crystal structure of the resulting mutant provided the first structural evidence for the arginine switch [39].

Aspartate aminotransferase and tyrosine aminotransferase from *E. coli* are paralogs that share 43% sequence identity. It is likely that they evolved by gene duplication of an ancestral AATase gene. The role of gene duplication and evolution of new substrate specificities is an area of general interest [40]. Directed evolution, which mimics the action of natural selection, is a powerful strategy for tailoring protein properties [41]. It has been used to test these ideas. Repeated mutation of AATase, with selection for aromatic aminotransferase activity, leads to mutants with broadened substrate specificity [42], validating this evolutionary analysis. The first reports on the directed evolution of aminotransferases with modified substrate specificity were of the conversion of AATases to branched-chain aminotransferases [43]. In this case a mutant with 17 amino acid changes, remote from the active site, resulted in an arginine switch that allowed Arg292 to switch out of the active site. This change accommodates bulky hydrophobic side-chains (e.g., the catalytic efficiency (k_{cat}/K_M) of valine is increased by 2.1×10^6) [44, 45]. It appears that the arginine switch is readily accessible to evolution and that directed evolution strategies may provide a general tool for the development of new enzymes with tailored specificities.

The other mechanism for dual substrate specificity is the employment of an extended hydrogen bond network (Figure 1.12). The AATase [46] and TATase [47] from *Pyrococcus horikoshii* both use this strategy, as does the branched-chain aminotransferase from *E. coli* [48]. Binding glutamate at the active site without the

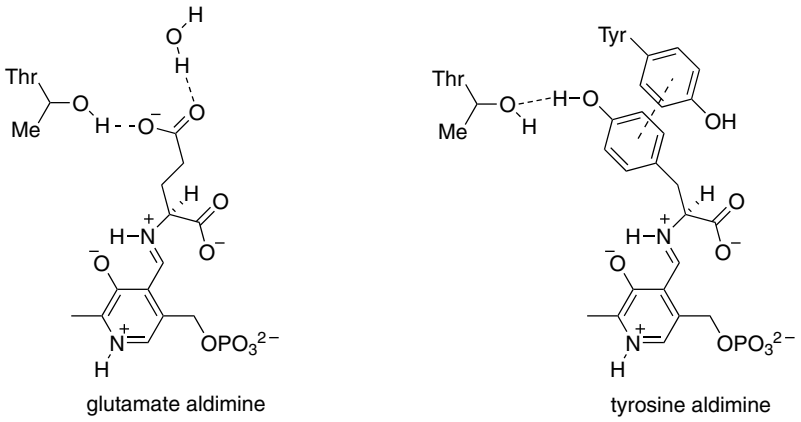

Figure 1.12 Extended hydrogen bond and π-stacking interactions in side-chain recognition of TATase from *P. horikoshii*. (Adapted from [31].)

presence of a cationic residue to recognize the side-chain reduces the electrostatic complexities for dual specificity. Interestingly, by using smaller, less flexible, residues than arginine for recognition, the branched-chain aminotransferase can more accurately distinguish between aspartate and glutamate.

1.3.3
PLP and the Biosynthesis of Alanine and Glycine

Two more of the protein amino acids, alanine and glycine, are biosynthesized by direct exploitation of α-center PLP chemistry. Essentially any α-amino acid can be created from the corresponding α-keto acid if an appropriate aminotransferase is available. Pyruvate is a ubiquitous metabolite and the corresponding amino acid, alanine, is readily available by transamination using aminotransferases of appropriate specificity (Figure 1.13).

There are three biosynthetic routes to glycine (Figure 1.14). Some organisms, such as the yeast *S. cerevisiae*, utilize all three. In organisms, such as *S. cerevisiae*, that have access to glyoxalate, transamination provides glycine directly. In this case the amino donor is alanine [49, 50].

The other two routes to glycine involve PLP-mediated cleavage of the protein β-hydroxy amino acids serine and threonine by the enzymes serine hydroxymethyltransferase (SHMT) and threonine aldolase. Enzymes of this class often have relaxed substrate specificity and can cleave the side-chain from a number of β-hydroxy-α-amino acids. Threonine aldolase is an important source of glycine in

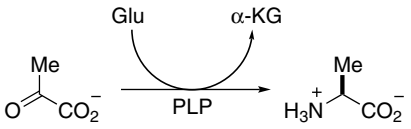

Figure 1.13 Biosynthesis of alanine from pyruvate.

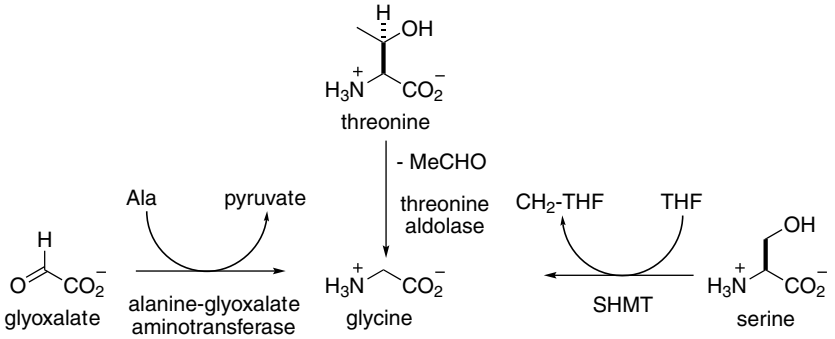

Figure 1.14 Three PLP-dependent biosynthetic routes to glycine.

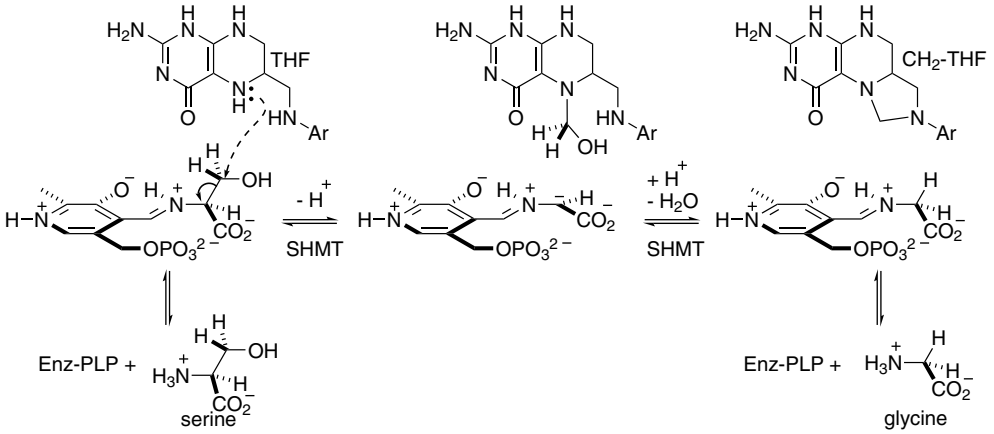

Figure 1.15 Proposed mechanism for SHMT.

S. cerevisiae [51]. Threonine forms a Schiff base with PLP which then catalyses a retro-aldol reaction to remove the side-chain as ethanal (see Box 1.3) [52, 53].

The biosynthesis of glycine in humans occurs primarily via the action of SHMT [49]. This enzyme is a critical source of both glycine and one-carbon units for metabolism [33]. Like threonine aldolase, the enzyme carries out a PLP-mediated side-chain cleavage reaction of a β-hydroxy-amino acid. However, in the case of serine the side-chain of the amino acid is a reactive aldehyde, methanal, and is not produced as a free intermediate. Instead it becomes attached to an essential cofactor as methylene-tetrahydrofolate (CH_2-THF). In this case, the THF cofactor is required in order to bring about the reaction. Extensive studies with isotopically labeled substrates and mutated enzymes, together with X-ray structural information, have attempted to resolve the question of whether the folate cofactor assists the cleavage reaction directly or simply reacts with methanal as soon as it is formed via retro-aldol chemistry (Figure 1.15) [54–58].

1.4
Routes to Functionalized Three-Carbon Amino Acids: Serine, Cysteine, and Selenocysteine

3-Phosphoglycerate is a key metabolite of glycolysis and is the precursor to the three-carbon protein amino acids with β-functional groups: serine, cysteine, and the 21st amino acid of the genetic code, selenocysteine.

1.4.1
Serine Biosynthesis

In Gram-negative bacteria, serine is biosynthesized in three steps from 3-phosphoglycerate [59]. The first step is oxidation to 3-phosphohydroxypyruvate and, as the

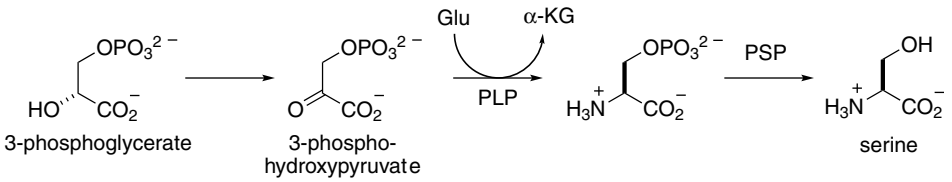

Figure 1.16 Biosynthesis of serine.

point of commitment to the biosynthetic pathway, it is feedback regulated by the end product, serine [60]. The resulting α-keto acid is a substrate for transamination with glutamate acting as the amino donor. Hydrolysis of the resulting serine-β-phosphate catalyzed by phosphoserine phosphatase (PSP) provides the free amino acid (Figure 1.16).

Systematic protein crystallography, exploiting the use of reactive intermediate analogs, has provided a detailed series of "snapshots" of intermediates in the catalytic cycle of the PSP from *Methanococcus jannaschii*, allowing the reaction to be visualized in three-dimensional detail (Figure 1.17) [61]. A conserved aspartate residue at the end of the active-site tunnel is a nucleophilic catalyst, attacking the serine-β-phosphate to generate an acyl phosphate intermediate. Release of serine allows the binding of a water molecule to mediate hydrolysis of the labile aspartate-β-phosphate to regenerate the starting enzyme.

The PSP from *Pseudomonas aeruginosa* has evolved the ability to bind homoserine rather than water in the second half of the reaction and transfer the activated phosphate of the aspartate-β-phosphate species to this amino acid providing access to homoserine-γ-phosphate, which is a biosynthetic precursor to threonine (Figure 1.18), as will be described later. This circumvents the need to expend ATP in phosphorylating this alcohol and is a rare example of an enzyme that transfers phosphoryl groups directly between non-nucleotide metabolites. This illustrates again the role of changed substrate specificity in generating new enzyme activities [62].

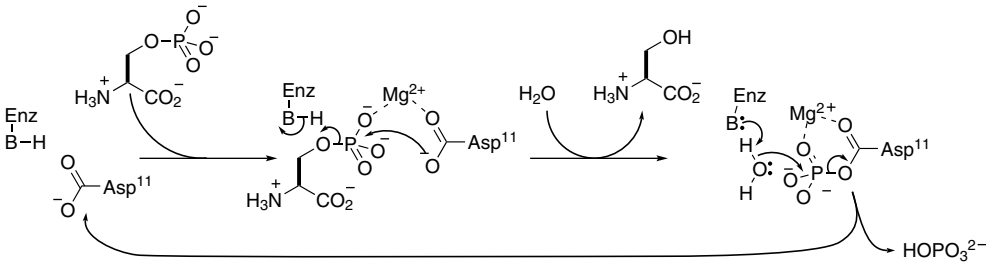

Figure 1.17 Catalytic details of PSP from systematic protein X-ray crystallography.

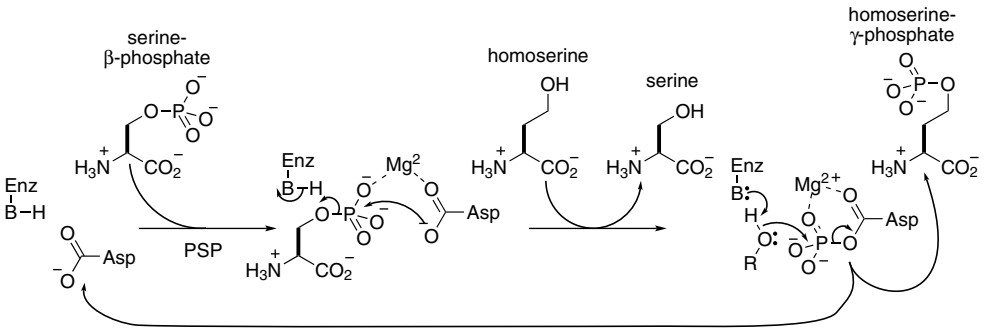

Figure 1.18 *P. aeruginosa* PSP-catalyzed biosynthesis of homoserine-γ-phosphate by phosphoryl transfer.

1.4.2
Cysteine Biosynthesis

Serine is the starting material for the synthesis of the other three-carbon protein α-amino acids. There are two common pathways to cysteine: the sulfur assimilation pathway and the trans-sulfuration pathway. Vertebrates use the latter pathway, which interconverts homocysteine and cysteine. This latter pathway is discussed separately in the section on methionine biosynthesis.

The sulfur assimilation pathway to cysteine is found in plants, eubacteria and some Archaea. The two key steps in this synthesis are mediated by a bifunctional cysteine synthase complex [63]. Serine acetyltransferase activates the side-chain hydroxyl group of serine by derivatization with acetyl-CoA and the resulting *O*-acetylserine (OAS) reacts with a sulfur nucleophile, catalyzed by a PLP-dependent enzyme OAS sulfhydrylase (*O*-acetylserine sulfhydrylase, OASS) (Figure 1.19).

In enteric bacteria there are two isozymes of OASS that utilize different sulfur nucleophiles as substrates [64]. One isozyme, produced under aerobic conditions,

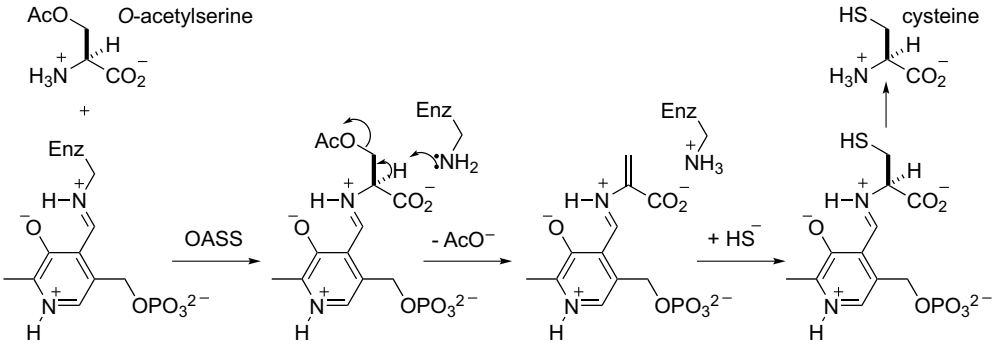

Figure 1.19 Cysteine formation catalyzed by OASS.

utilizes hydrosulfide (formed by a multistep reduction of sulfate) [65]. Under anaerobic conditions a second isozyme is produced which utilizes thiosulfate and produces *S*-sulfo-cysteine, which is transformed to cysteine by reaction with thiols.

The mechanism of OASS from *Salmonella typhimurium* has been studied in detail [65, 66]. This enzyme is a homodimer with an active-site PLP cofactor bound to Lys41. The initial stages of the reaction parallel those of aminotransferase enzymes. The monoanion form of OAS forms a Schiff base with PLP by amino exchange with Lys41, which is thereby liberated to act as an active-site acid–base catalyst. In this case, deprotonation of the α-center of PLP-linked OAS by Lys41 eliminates acetate and forms of a bound aminoacrylyl intermediate. After loss of acetate, hydrosulfide binds, in the second step of this ordered Ping Pong Bi Bi mechanism, and reacts with the aminoacrylate intermediate to produce cysteine. This mechanism is illustrative of a general class of PLP-dependent enzymes that facilitate reaction at the β-center of amino acids by facilitating the loss of a leaving group at that position (see Box 1.3).

1.4.3
Case Study: Genome Information as a Starting Point for Uncovering New Biosynthetic Pathways

With the availability of a large number of genome sequences it is possible to identify the likely biosynthetic pathways operating in particular organisms based on the presence or absence of particular genes for biosynthetic enzymes. This has proved a powerful tool in expanding our understanding of the diversity and distribution of metabolic pathways. Genome analysis of the biosynthesis of cysteine and its incorporation into cysteinyl-tRNA have led to the discovery of two new pathways for the biosynthesis of this amino acid. These findings, in turn, have led to developments in our understanding of the biosynthesis of selenocysteine in humans [67]. This area presents a nice case study in the emerging use of genome analysis to identify new variants in biosynthetic pathways.

1.4.3.1 Cysteine Biosynthesis in *Mycobacterium Tuberculosis*

Amino acid biosynthesis in *Mycobacterium tuberculosis* is under active investigation because of the growing health threat posed by tuberculosis. Inhibitors of distinctive essential metabolic pathways in this organism may be useful as antibiotics. The complete genome sequence of *M. tuberculosis* is known [68]. *M. tuberculosis* carries out cysteine biosynthesis via the sulfur assimilation pathway and adjacent genes, *cysE* and *cysK1*, encode the serine acetyltransferase and OASS activities of the cysteine synthase complex [69]. However, genome analysis revealed the presence of two other genes homologous to OASS, *cysK1* and *cysM*. Furthermore, *cysM* was found clustered with two other genes related to sulfur metabolism. One of these genes, now called *cysO*, is homologous to a family of small sulfide carrier proteins, such as ThiS, which play a role in thiamine pyrophosphate biosynthesis [70]. A thiocarboxylate derivative of the C-terminal group of these proteins is the sulfide carrier. The protein is activated by ATP, to form an acyl phosphate, and then converted to the corresponding

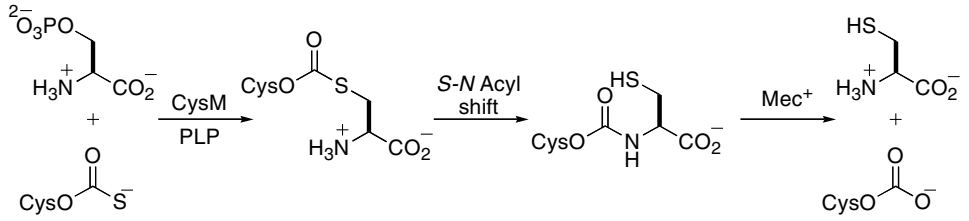

Figure 1.20 Biosynthesis of cysteine in *M. tuberculosis*.

thiocarboxylate via nucleophilic substitution. Reaction of this thiocarboxylate, and hydrolysis of the resulting acyl derivative leads to overall transfer of sulfide. A second gene in this cluster, *mec*$^{+}$, encodes a potential hydrolase and this gene had previously been linked to sulfur amino acid metabolism in a *Streptomyces* species. This genome analysis led Begley *et al.* to investigate CysO as a potential sulfur source for cysteine biosynthesis (Figure 1.20). *In vitro* assays, making extensive use of protein mass spectrometry, confirmed this role [71]. CysO reacts with a suitably activated serine derivative to form a thioester, which rearranges to generate the corresponding peptide bond. Mec^{+} is a zinc-dependent carboxypeptidase that removes the newly created cysteine from the temporarily homologated protein.

Subsequent studies have shown that CysO is part of a fully independent pathway to cysteine in this organism (Figure 1.20) [72]. The activated form of the serine substrate for CysM is *O*-phosphoserine rather than the *O*-acetylserine utilized by the sulfur assimilation pathway. This is the biosynthetic precursor to serine as described previously.

Cysteine plays a key role in responding to oxidative stress encountered by *M. tuberculosis* in its dormant phase. The CysO-dependent route to cysteine may be particularly important under these conditions because thiocarboxylate may be used as it is more resistant to oxidation that other sulfide sources. The absence of this biosynthetic route in other organisms, including humans, make inhibitors of these biosynthetic enzymes of great interest for the treatment of the persistent phase of tuberculosis.

1.4.3.2 **Cysteine Biosynthesis in Archaea**

A similar genomics-based approach has uncovered an alternative cysteine biosynthetic pathway in Archaea. When the genome sequences of some methanogenic Archaea were sequenced they were found to lack the gene, *cysS* for the appropriate cysteinyl-tRNA synthetase. In one of these organisms, *Methanocaldococcus jannaschii*, it was found that Cys-tRNA^{Cys} was generated via an alternative pathway (Figure 1.21) [73]. First, the relevant tRNA, tRNA^{Cys}, is ligated to phosphoserine by the enzyme *O*-phosphoseryl-tRNA synthetase (SepRS) which then undergoes a PLP-mediated exchange of the β-phosphate for thiol to generate Cys-tRNA^{Cys}, catalyzed by Sep-tRNA: Cys-tRNA synthase (SepCysS) – a type I PLP-dependent enzyme. When the gene for SepCysS is deleted in the related methanogen, *Methanococcus*

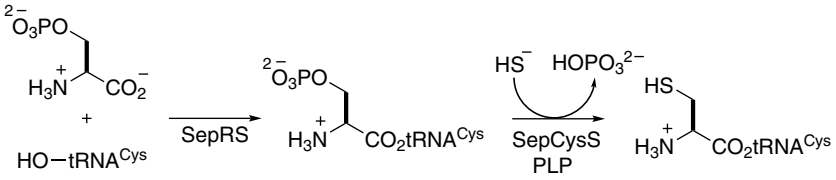

Figure 1.21 Biosynthesis of Cys-tRNA^{Cys} in the methanogenic archaeon *M. jannaschii*.

maripaludis, the organism is a cysteine auxotroph, indicating that this is the sole pathway to cysteine in this organism.

1.4.3.3 RNA-Dependent Biosynthesis of Selenocysteine and Other Amino Acids

Developments in cysteine biosynthesis research have underpinned our understanding of the biosynthesis of the 21st protein amino acid, selenocysteine. Selenocysteine has been known to be an important residue for a range of enzymes since 1976 [74]. This amino acid is incorporated into proteins by the ribosome using a tRNA^{Sec} – a suppressor tRNA that corresponds to a stop codon in the genetic code [75]. The utilization of this suppressor tRNA allows the expansion of the genetic code, but requires an additional elongation factor for the ribosome to insert the amino acid in the growing chain.

The biosynthesis of selenocysteine was first elucidated in *E. coli* and, like the archaeal route to cysteine, it is based on modification of aminoacyl-tRNAs (Figure 1.22). The pathway starts with the ligation of serine to tRNA^{Sec}, catalyzed by SerRS. The resulting ester undergoes PLP-mediated nucleophilic substitution of the side-chain hydroxyl group with a selenium-based nucleophile, selenophosphate, that is produced from selenide and ATP. The mechanism of selenophosphate synthetase from *E. coli* has been established using positional isotope exchange methodology [76, 77]. The reaction of Ser-tRNA^{Sec} with selenophosphate is catalyzed by SelA [78]. The nucleophilic substitution reaction is assumed to follow a mechanism analogous to that of OASS involving an initial elimination of water to form an aminoacrylyl-tRNA$^{[Ser]Sec}$ intermediate that reacts with the selenophosphate and the

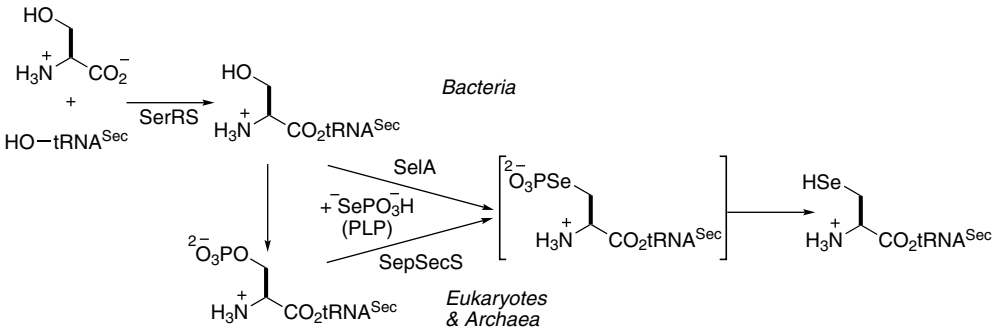

Figure 1.22 Biosynthesis of the tRNA adduct of selenocysteine.

resulting phosphoselenocysteyl-tRNA^{Sec} undergoes hydrolysis to generate selenocysteyl-tRNA^{Sec}.

This biosynthetic pathway was assumed to be common to all selenocysteine utilizing enzymes, but studies in eukaryotes failed to uncover the requisite biosynthetic enzymes. Subsequent studies have shown that selenocysteine biosynthesis occurs by a common pathway in Archaea and eukaryotes that is distinct, but related to that in bacteria. A protein believed to be associated with selenocysteine synthesis coprecipitated with the loaded selenocysteyl-tRNA^{Sec} and bioinformatics analysis showed that the enzyme was a PLP-dependent enzyme [79]. The chemical similarity of cysteine and selenocysteine provided the clue to unraveling the biosynthetic pathway to the latter amino acid in eukaryotes: Sep-tRNA^{Sec} was shown to be a substrate for the RNA-dependent biosynthesis of selenocysteine.

In the eukaryotic and archaeal version of the biosynthetic pathway, the β-hydroxyl group of Ser-tRNA^{Sec} is activated by phosphorylation to form the phosphoserine derivative, Sep-tRNA^{Sec}, which then undergoes PLP-mediated nucleophilic substitution of the β-phosphate leaving group with selenophosphate catalyzed by selenocysteine synthase, SepSecS [80]. Selenocysteine synthase is homologous to OASS both in structure [81] and sequence [82, 83] and the catalytic mechanism is analogous, involving an initial elimination of phosphate to form an aminoacrylyl-tRNA$^{[Ser]Sec}$ intermediate which reacts with the selenophosphate. Despite selenocysteine being an addition to the 20 amino acids found ubiquitously in proteins, the phylogenetic data suggest that its biosynthesis is a primordial process and that selenocysteine has played a role in metabolism since before the divergence of the ancestors to the three kingdoms of life (bacteria, Archaea and eukaryotes) more than 3 billion years ago.

The synthesis of selenocysteine on a specialized tRNA scaffold assists in distinguishing the otherwise similar chemistry of selenocysteine and cysteine; the biosynthetic enzymes recognize structural features of tRNA^{Sec}. Selenocysteine is not the only amino acid synthesized by modification of an aminoacyl-tRNA. *N*-Formyl methionine is the N-terminal residue of proteins in eubacteria and eukaryotic organelles (mitochondria and chloroplasts). It is synthesized via formylation of Met-tRNA^{fMet} in a process that also depends on binding to the tRNA^{fMet} and is specific to this aminoacyl-tRNA species [84]. Interestingly, it has also been found that many organisms produce aminoacylated tRNAs for asparagine and glutamine by amidating aspartyl and glutamyl precursors. Again, genome analysis is proving useful in identifying the pathway(s) present in particular organisms [85]. For example, whereas Gln-tRNA^{Gln} is synthesized from glutamine in the cytoplasm of eukaryotes, the majority of eubacteria and all Archaea make it by the transamidation route [86].

1.5
Other Amino Acids from Aspartate and Glutamate: Asparagine and Side Chain Functional Group Manipulation

Glutamate and aspartate are the parents of six further amino acids that are ubiquitously found in proteins: asparagine, methionine, and threonine are produced

from aspartate; and glutamine, proline, and arginine are derived from glutamate. The conversion of glutamate to glutamine has already been described and illustrates the strategy by which the remaining members of this group of protein amino acids are made. In each case the side-chain carboxylate undergoes functional group manipulation starting with activation to a short-lived acyl phosphate intermediate and then subsequent nucleophilic substitution. The two nucleophiles that are utilized are ammonia and hydride ion (delivered by redox cofactors), and these will be discussed in turn.

1.5.1
Asparagine Biosynthesis

There are two isozymes of asparagine synthetase in *E. coli* [87]. Each enzyme exploits the cleavage of ATP to AMP and pyrophosphate as a means of activating the β-carboxylate of aspartate. The two isozymes differ in their nitrogen source: AsnA utilizes ammonia [88], whereas AsnB uses glutamine. *E. coli* asparagine synthetase B is a multifunctional enzyme. The N-terminal domain is a class II GAT. The C-terminal domain binds aspartate and ATP, and generates β-aspartyl-adenylate as the reactive nucleophile (Figure 1.23). A kinetic model for the multistep reaction has been developed [89].

By producing an inactive mutant with the glutaminase active-site nucleophile, the N-terminal cysteine, changed to an alanine it has been possible to crystallize the enzyme with both glutamine and AMP bound, thus clearly revealing the relative locations of the two active sites (Figure 1.24) [90]. The two active sites are connected by a tunnel that is 19 Å long and lined primarily with low polarity functional groups. Ammonia traverses this tunnel and combines with the β-aspartyl-adenylate that is

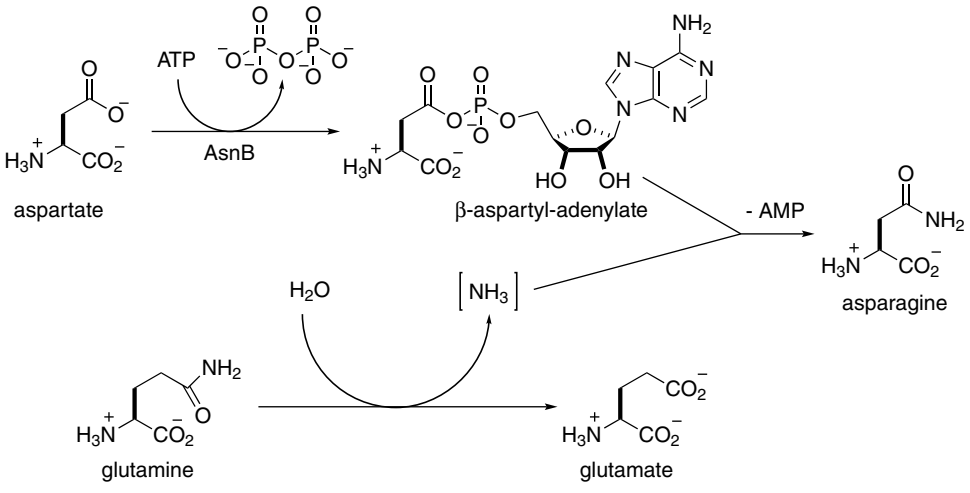

Figure 1.23 Asparagine biosynthesis mediated by bifunctional AsnB.

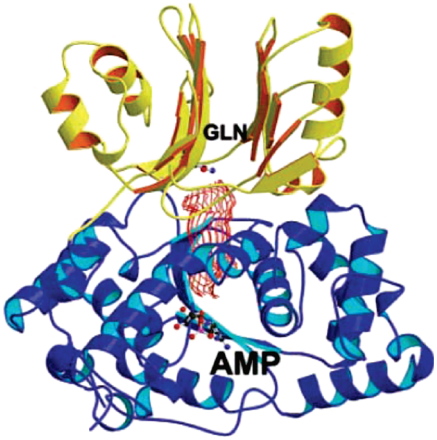

Figure 1.24 Glutaminase (gold) and synthetase (purple) sites of AsnB are linked via an internal tunnel. (Picture taken from [20].)

formed at the second active site. This situation echoes that described for GOGAT and reinforces the pattern of multifunctional GAT-dependent enzymes with internal molecular tunnels for efficient delivery of nascent ammonia [20].

Like AsnB, asparagine synthetases from plants and animals are glutamine-dependent – illustrating the importance of glutamine, rather than ammonia, as a nitrogen carrier in higher organisms. Some leukemia cells have diminished levels of asparagine synthetase. When asparagine levels are reduced further by side-chain hydrolysis, mediated by the enzyme L-asparaginase, these cells become especially sensitive to chemotherapy Hence, L-asparaginase is a component of chemotherapeutic protocols for treating some acute childhood leukemias. Some of these leukemias develop resistance to chemotherapy by increasing their production of asparagine synthetase. For this reason, inhibitors of this enzyme are of potential significance as antileukemia agents and these are being developed based on the mechanistic studies of *E. coli* AsnB [91]. Mimics of the tetrahedral intermediate associated with ammonolysis of the aspartyl-β-adenylate intermediate inhibit the enzyme at submicromolar concentrations and inhibitors of this type (Figure 1.25) are being tested for their efficacy as chemotherapeutic agents [92].

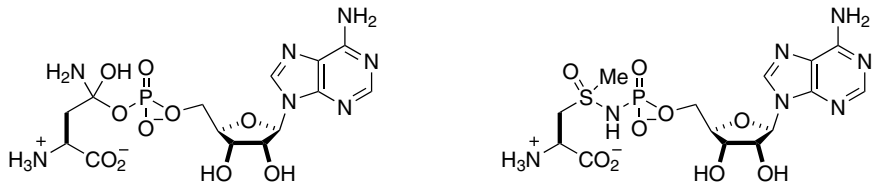

Figure 1.25 Inhibitor of AsnB designed as a tetrahedral intermediate mimic.

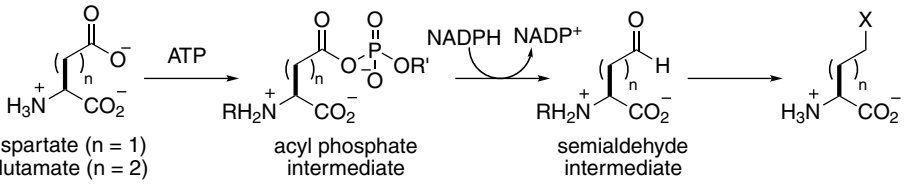

Figure 1.26 Strategy of aspartate and glutamate family amino acid biosynthesis.

1.6
Aspartate and Glutamate Families of Amino Acids

1.6.1
Overview

The remaining four- and five-carbon amino acids are prepared by pathways based around a common chemical strategy (Figure 1.26): ATP-dependent activation of the side-chain carboxylate of the parent amino acid generates a reactive acyl phosphate intermediate that is reduced to the corresponding aldehyde by hydride transfer; the product amino aldehydes are also labile species and these are converted to more durable reduced analogs in the next stage.

These pathways illustrate several common features of amino acid biosynthetic pathways. Enzymes catalyzing analogous reactions in parallel pathways are often homologous in structure. Once enzymes are available that can catalyze a particular set of reactions then gene duplication and substrate specificity modification, via mutation and selection, can generate parallel pathways [93]. This evolutionary mechanism highlights the important role of the underlying chemical logic of the pathways that underpin this organization. A second general feature is that pathways involving reactive intermediates benefit from multifunctional enzyme systems that can efficiently channel metabolites to the active site that catalyzes the next stage in the pathway. This not only increases the yield of the reaction, but also controls the fate of the metabolite when there are competing metabolic uses of the product. For this reason there are often multiple isozymes to catalyze reactions that occur in multiple pathways and these are generally independently regulated [94]. For isozymes that catalyze reactions at branch-points of pathways, where a commitment to one or other final product is made, the pattern of feedback regulation provides a direct confirmation of the *in vivo* role of the specific form of the enzyme.

1.6.2
Aspartate Family Amino Acids: Threonine and Methionine

The first three steps of the biosynthesis of threonine and methionine in plants and microbes are common to both pathways (Figure 1.27) [95]. Aspartokinase (AK) catalyzes the ATP-dependent β-phosphorylation of aspartate, which creates the

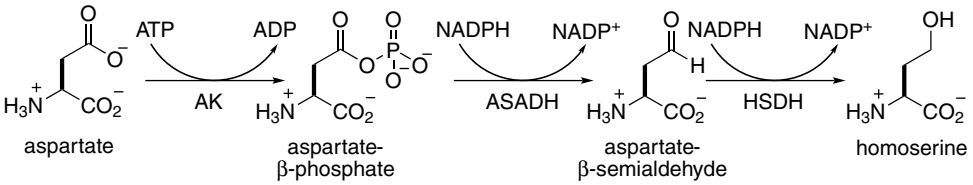

Figure 1.27 Biosynthesis of homoserine.

requisite leaving group for subsequent transformation [96]. The resulting aspartate-β-phosphate is reduced to the corresponding aldehyde by aspartate β-semialdehyde dehydrogenase (ASADH). Homoserine dehydrogenase (HSDH) catalyzes the further reduction of aspartate-β-semialdehyde to homoserine – a key intermediate for the biosynthesis of both threonine and methionine. NADPH is a hydride source for the reduction chemistry. In *E. coli* and other bacteria there are independently regulated isozymes of AK-HSDH for threonine and methionine biosynthesis.

ASADH from several sources has been characterized [97–99]. The mechanism of ASADH (Figure 1.28) is analogous to the oxidation of glyceraldehyde-3-phosphate to glycerate-3-phosphate – one of the key oxidation steps in glycolysis [100]. Aspartate-β-phosphate undergoes initial nucleophilic substitution of phosphate with the active-site thiol of cysteine-136. The resulting thioester is then reduced by a nicotinamide cofactor, NADPH, to aspartate-β-semialdehyde ASA. The resulting aldehyde, ASA, is sufficiently reactive with nucleophiles that the three-dimensional structure of a

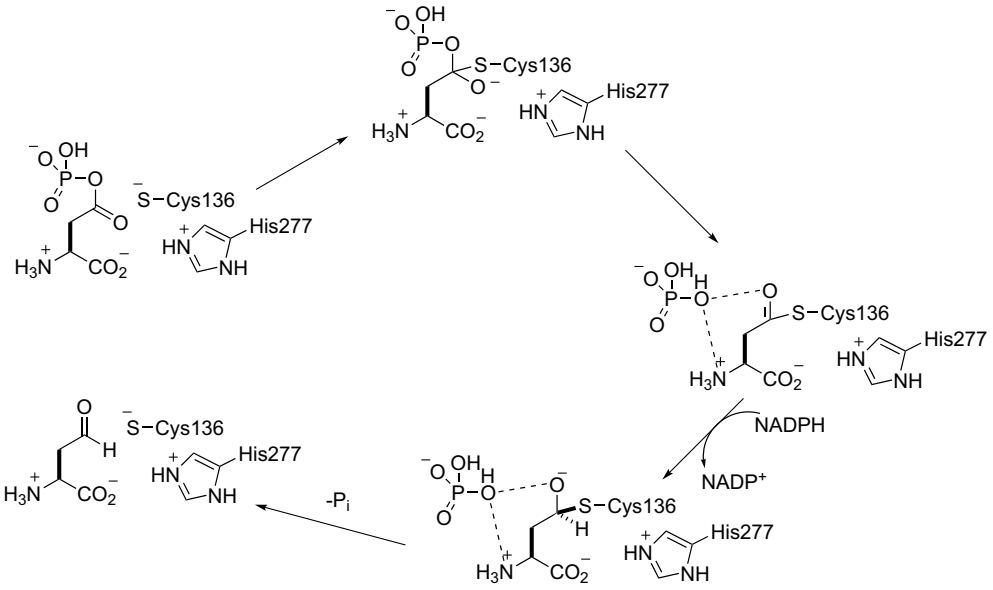

Figure 1.28 Mechanism of ASADH.

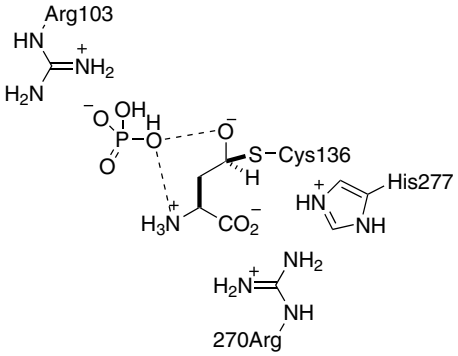

Figure 1.29 Structure of the hemithioacetal intermediate in the mechanism of ASADH.

tetrahedral intermediate of the reduction step has been determined: when ASA and phosphate is incubated with the enzyme a hemithioacetal intermediate accumulates at the active site.

The structure of this intermediate provides a detailed snapshot of the catalytic machinery of the enzyme in action (Figure 1.29) [98]. The α-carboxylate of the substrate is bound to Arg270; a catalytic histidine (His277) is suitably placed for deprotonation of the thiol and one of two bound phosphates occupies the site of the displaced leaving group. As is expected from the Pauling view of enzyme catalysis, ASADH stabilizes a reactive intermediate on the pathway; in this case by hydrogen bonding to the positively charged side-chain of His277, the backbone peptide NH of Asp135 and the phosphate leaving group from the first half of the enzyme-catalyzed reaction.

With two labile species in the pathway, metabolite channeling is a feature of this biosynthetic chemistry. Interestingly, in a number of organisms, including *E. coli*, the first and third reactions are mediated by bifunctional AK-HSDH enzymes but the intervening ASADH reaction is carried out by a separate enzyme. It has proved difficult to provide direct kinetic evidence for the channeling of intermediates through a trifunctional enzyme complex AK-HSDH/ASADH; however, evidence for the presence of such a complex has accrued from a competition experiment [101]. An inactive ASADH mutant was generated by changing the essential active-site cysteine to alanine. When increasing amounts of this mutant were added to mixtures of wild-type AK-HSDH and ASADH the synthesis of homoserine was reduced. The inactive ASADH mutant binds to AK-HSDH in competition with wild-type ASADH and, when bound, prevents the direct flux of metabolites [102]. Channeling of aspartate-β-phosphate increases the efficiency of the pathway by minimizing possible losses from hydrolysis that might occur if this intermediate was freely exchanged with solution.

Homoserine dehydrogenase from *S. cerevisiae* has also been studied in detail and follows an ordered Bi Bi kinetic mechanism. The redox cofactor NADPH binds prior to ASA and homoserine is released before loss of the oxidized $NADP^+$ cofactor. The

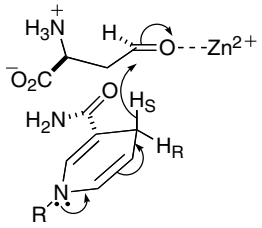

Figure 1.30 Stereospecificity of hydride transfer in the formation of homoserine.

pro-(*S*) hydride of stereospecifically deuterated NADP[^{2}H] is transferred and the reduction is catalyzed by carbonyl polarization by a protonated active-site lysine residue (Lys223) [103, 104] (Figure 1.30).

1.6.2.1 **Case Study: Evolution of Leaving Group Specificity in Methionine Biosynthesis**
For processing to either methionine or threonine, the hydroxyl group of homoserine is converted into a good leaving group. Primary metabolism provides two main alternatives for hydroxyl activation: polyphosphates like ATP can generate phosphate leaving groups; alternatively thioesters (notably TCA cycle metabolites acetyl-CoA and succinyl-CoA) generate carboxylate leaving groups (Figure 1.31). There are variations in the pathway at this point depending on this choice. Phosphorylation of homoserine by homoserine kinase (HSK) to produce homoserine-γ-phosphate is ubiquitously used for threonine biosynthesis [105]. An interesting alternative phosphorylation route, based on the evolution of a novel bifunctional PSP, was described above (Figure 1.18) [62]. Homoserine-γ-phosphate is also the biosynthetic precursor to methionine biosynthesis in plants [95]. Other organisms use homoserine transacylases to activate homoserine for methionine biosynthesis and two different acyl groups are employed: Gram-negative bacteria make *O*-succinyl-homoserine, while yeasts and many clinically important bacteria (e.g., *M. tuberculosis* and *P. aeruginosa*) use an *O*-acetyl-homoserine as a precursor to methionine. Although the choice of leaving group does not fundamentally change the chemistry, it does have implications for the specificity of inhibitors and for the control of the pathways since, with distinct building blocks, the two pathways can be controlled independently.

All homoserine transacylases have a catalytic triad of residues situated at the end of a tunnel. The α-carboxylate of the substrate is recognized by an arginine and an active-site nucleophile (serine or cysteine) is assisted in catalysis by a histidine in

Figure 1.31 Three different activated forms of homoserine.

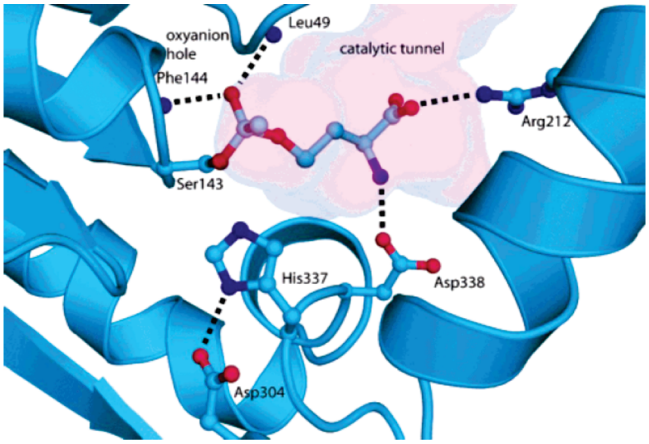

Figure 1.32 Homoserine transacetylase from *H. influenzae*. (From [102].)

conjunction with either an aspartate or glutamate. The structures and sequences of homoserine transacylases group into two families related to the active-site nucleophile. Homoserine transacetylase from *Haemophilus influenzae* is typical of one class [106]. A conserved serine (Ser143) is in a strained conformation and acts as a reactive nucleophile to accept the acetyl group from acetyl-CoA (Figure 1.32). His337 is an adjacent acid–base catalyst and, like the active site of serine proteases, there is an oxyanion hole to stabilize the tetrahedral intermediate. The residues of the tunnel are well placed to direct homoserine to the acetylated active site and thereby assure transesterification outcompetes hydrolysis.

It had been believed that transsuccinylases comprised the cysteine-dependent family of transacylases. However, when one of this family of enzymes from *Bacillus cereus* was fully characterized it was found to be a transacetylase. The structure of this enzyme illustrates both the details of the active-site architecture, with the catalytic triad of Cys142, His235, and Glu237, and the basis for the substrate specificity of the enzyme (Figure 1.33a) [107]. A glutamate residue, Glu111, protrudes into the active

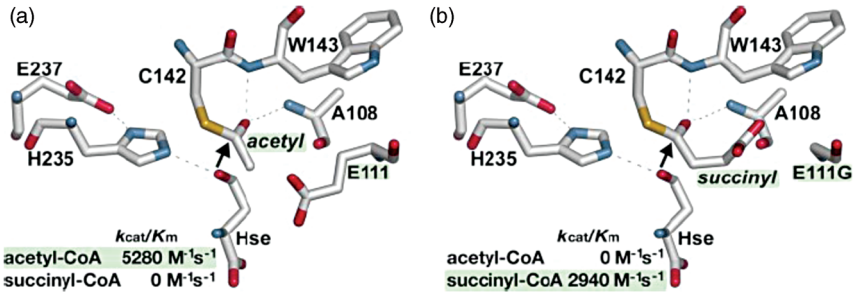

Figure 1.33 Point mutagenesis (E111G) of *B. cereus* homoserine transacylase changes its substrate specificity from that of a transacetylase (a) to a transsuccinylase (b). (From [107].)

site limiting its size, allowing binding of acetyl species but excluding succinyl species on steric and electrostatic grounds. In many other enzymes of this class the corresponding residue is glycine, which presents no such impediments to succinyl derivatives. Making a single point mutation of this glutamate to glycine was sufficient to convert a specific transacetylase into a specific transsuccinylase (Figure 1.33b). This shows again the power of point mutations to engineer modifications to enzyme substrate specificity.

1.6.2.2 **Threonine, Homocysteine, and PLP**

The manipulations of these activated homoserine derivatives to form threonine and homocysteine (*en route* to methionine) both involve catalysis of the loss of the side-chain leaving group. In each case this is catalyzed by a PLP-dependent enzyme. The ability to mediate the chemistry at β-, and γ-centers of amino acids, in addition to the α-center chemistry previously described, illustrates the catalytic versatility of PLP that makes it an indispensible cofactor in amino acid metabolism (see Box 1.3).

1.6.2.3 **Threonine Synthase**

Threonine synthase (TS) catalyzes the conversion of homoserine-γ-phosphate to threonine. Threonine synthases are PLP-dependent enzymes, of type II fold, with a complex mechanism that utilizes the full capacity of PLP to stabilize reactive intermediates [108]. Sequence alignments have identified two subfamilies – class I and class II [109]. Class I enzymes are found in plants and some bacteria and Archaea, and are allosterically activated by *S*-adenosylmethionine [110]. Three-dimensional structures for both classes of enzymes are available [111–113].

Owing to its potential significance for the development of antibiotics to treat tuberculosis [114], the class I TS from *M. tuberculosis* has been studied in detail [115]. In the resting state, the PLP cofactor forms a Schiff base with Lys69. When homoserine-γ-phosphate binds to PLP it displaces Lys69, which then acts as a proton relay in a sequence of acid–base reactions that are shown in Figure 1.34, which gives an overview of the mechanism of the reaction.

Deprotonation of the α-proton of the substrate by Lys69 produces an aza-allyl anion. Reprotonation at the benzylic position of the PLP, by the conjugate acid of Lys69, generates a new iminium ion. Deprotonation at the β-position by the regenerated basic Lys69 leads to elimination of phosphate and the formation of a conjugated iminium ion. Now a proton transfer is required from the benzylic position of the PLP and the terminus of the conjugated system to produce a α,β-unsaturated ketimine ready for reaction with water at the β-position to generate threonine. While Lys69 is well placed to undertake the initial proton transfers, the molecular gymnastics required to also mediate the latter proton transfer is beyond its reach and there has been debate in the literature about the catalytic group required for this chemistry. Recent detailed structural studies show that the most likely acid–base catalyst is the 5′-phosphate of the PLP cofactor (Figure 1.35) [115]. This phosphate moiety is less than 5 Å away from both the benzylic position of the

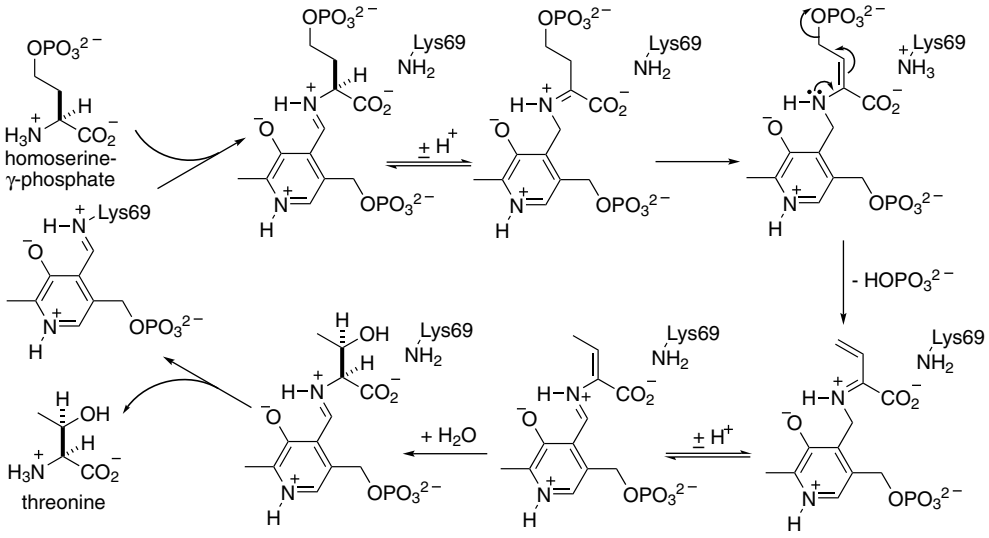

Figure 1.34 Mechanism of threonine synthase.

PLP and the γ-carbon of the substrate. In the final step, Lys69 deprotonates a bound water molecule to generate hydroxide ion that attacks the α,β-unsaturated ketimine and produces threonine, which is released by hydrolysis of the Schiff base linkage to PLP.

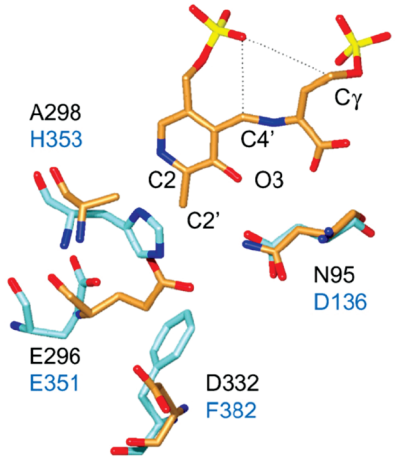

Figure 1.35 Proximity of PLP phosphate to C4′ and Cγ sites at the active site of threonine synthase. (From [110].)

1.6.2.4 Methionine, Cysteine, and Cystathionine

Methionine and cysteine are the two sulfur-containing protein amino acids. The side-chain sulfur is transferred between the two via the adduct, cystathionine. Most plants and microbes transfer the sulfur from cysteine to an activated homoserine derivative to make homocysteine, which is then methylated to produce methionine. In mammals only the reverse process is carried out. Some fungi undertake trans-sulfuration in both directions [116, 117]. The interconversion of cysteine and homocysteine involves facilitating leaving group chemistry at β- and γ-positions in two sequential PLP-dependent processes: cystathionine γ-synthase and cystathionine β-lyase (forward) or cystathionine β-synthase then cystathionine γ-lyase (reverse). The combined actions of cystathionine γ-synthase and cystathionine β-lyase from *E. coli* have been well characterized, and provide an example of the microbial route to homocysteine.

Cystathionine γ-synthase facilitates the loss of succinate from the γ-position of *O*-succinylhomoserine by a mechanism analogous to the first stage of threonine synthase catalysis. Cysteine attacks the bound vinylglycine intermediate in the reverse of the elimination chemistry and the overall result is nucleophilic substitution to produce cystathionine (Figure 1.36) [116].

Cystathionine β-lyase acts at the cysteine end of cystathionine to labilize homocysteine as a leaving group from the β-position. Hydrolysis results in the release of pyruvate as the other reaction product (Figure 1.37) [118].

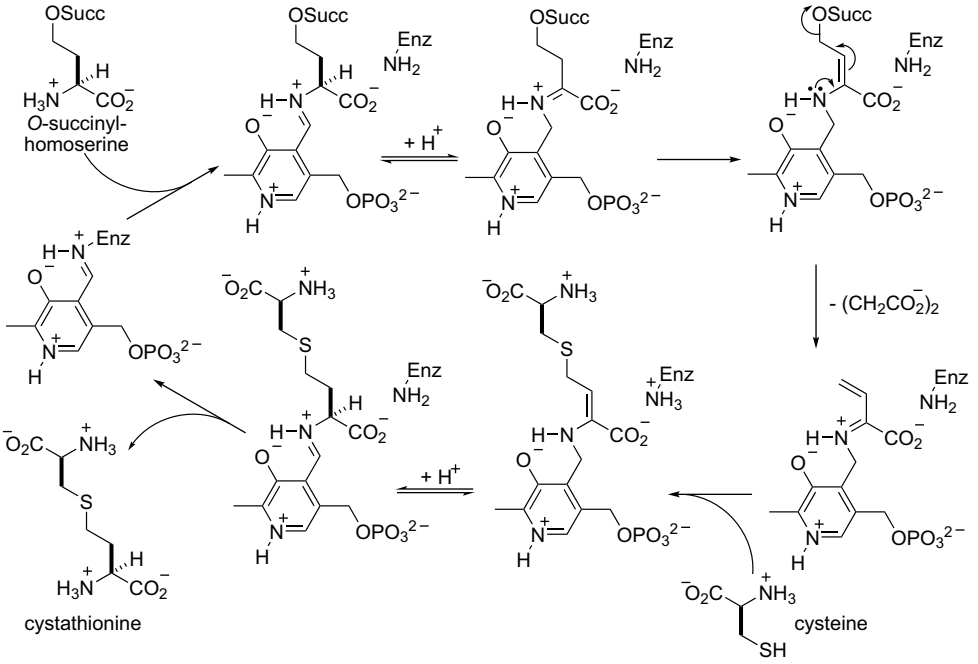

Figure 1.36 Mechanism of cystathionine-γ-synthase.

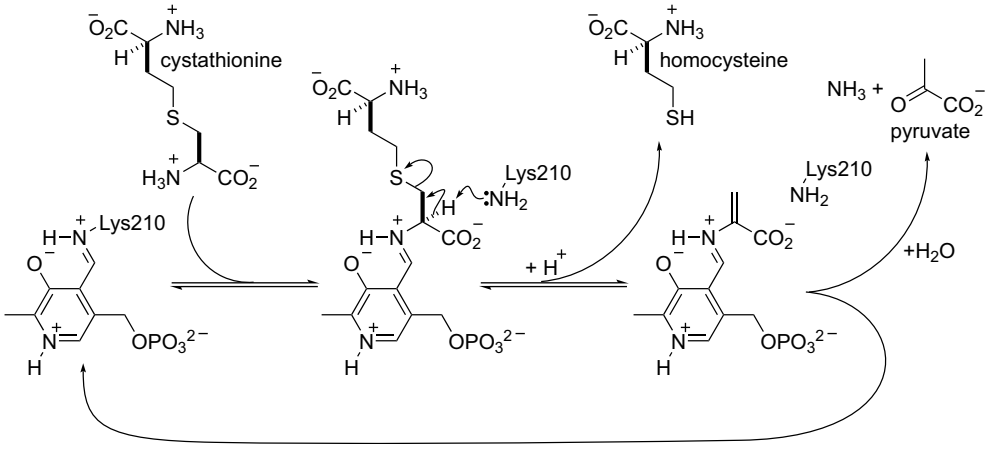

Figure 1.37 Mechanism of cystathionine-β-lyase.

1.6.2.5 **Methionine Synthase**

The biosynthesis of methionine is completed by methylation of homocysteine, catalyzed by methionine synthase (MS). The ultimate source of the methyl group is N^5-methyl-THF (Me-THF) where the methyl group can originate in the cleaved side-chain of serine (as seen in the biosynthesis of glycine). There are two distinct versions of this enzyme depending on the immediate source of the methyl group, either Me-THF or methyl cobalamin. In organisms that biosynthesize vitamin B_{12}, or obtain it from their environment, this is often carried out by a multifunctional MS that uses methyl cobalamin as the alkylating agent (Figure 1.38) [119]. After methionine synthesis, the methyl cobalamin is reconstituted by methyl transfer from Me-THF [120]. There are two MS enzymes in *E. coli* – one uses methyl cobalamin as methyl donor, whereas another uses Me-THF directly as the alkylating agent in a reaction that is dependent on a zinc ion for catalysis [121]. It is believed that homocysteine coordinates to the zinc as the thiolate and is thereby activated as a nucleophile to react with Me-THF.

1.6.3
Glutamate Family Amino Acids: Proline and Arginine

Proline and arginine are made from glutamate by routes that utilize the same chemical strategy that is seen in methionine and threonine biosynthesis. This involves activation of the γ-carboxylate and biosynthetic reduction (Figure 1.39). A bacterial pathway has been characterized: glutamate-5-kinase [122] phosphorylates the γ-carboxylate of glutamate and NADPH-dependent reduction leads to glutamate-γ-semialdehyde, which undergoes spontaneous cyclization to the corresponding imine, Δ^1-pyrroline-5-carboxylate. In plants a bifunctional enzyme mediates both of these steps and ensures efficient use of the reactive acyl phosphate intermediate [123, 124]. Two alternative pathways to this cyclic imine via oxidative deamination of ornithine have been reported [125, 126]. Reduction of the imine to proline is catalyzed

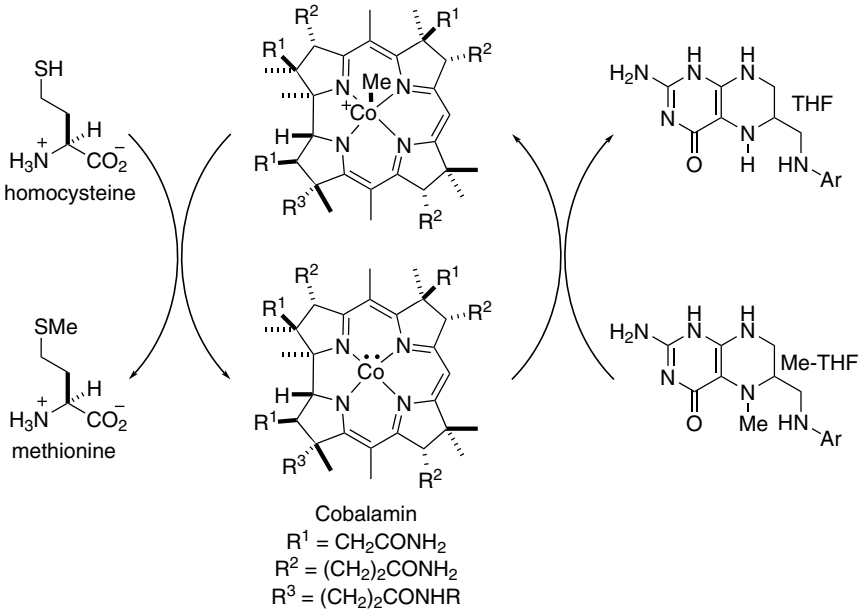

Figure 1.38 Methyl transfer chemistry of methionine synthase.

by Δ^1-pyrroline-5-carboxylate reductase and the structures of this enzyme from human pathogens (*Neisseria meningitidis* and *Streptococcus pyogenes*) have recently been characterized [127].

The chemical challenge in making the arginine precursor, ornithine, is in retaining an acyclic structure. This requires the prevention of cyclization of the α-amino group onto electrophilic functional groups in side-chain intermediates. A protecting group strategy is utilized for this purpose (Figure 1.39). The α-amino group of glutamate is first made non-nucleophilic by acetylation [128]. Phosphorylation [129, 130] and reduction [131] then produces *N*-acetylglutamate-γ-semialdehyde. In bacteria these two reactions (ArgB and ArgC) are mediated by enzymes that are homologous in structure to the corresponding enzymes, AK and ASADH, from the biosynthesis of ASA, illustrating the recurring pattern of pathway creation by gene duplication and mutation as noted above [93]. This aldehyde is converted to the corresponding amine by transamination with *N*-acetylornithine aminotransferase (Figure 1.40) [132]. This PLP-dependent enzyme utilizes glutamate as the amino donor. *N*-Acetylornithine aminotransferase has evolved an interesting multiple-substrate specificity and is also used to mediate the synthesis of *N*-succinyl-L,L-diaminopimelate in the bacterial biosynthesis of lysine [133]. This is a rare example of PLP-mediated transamination of a simple aldehyde, rather than an α-amino acid, illustrating substrate specificity divergence.

After the introduction of the γ-amino group the acetyl group is removed by hydrolysis or trans-acetylation to produce ornithine, and subsequent intermediates, *en route* to arginine (Figure 1.39) [134].

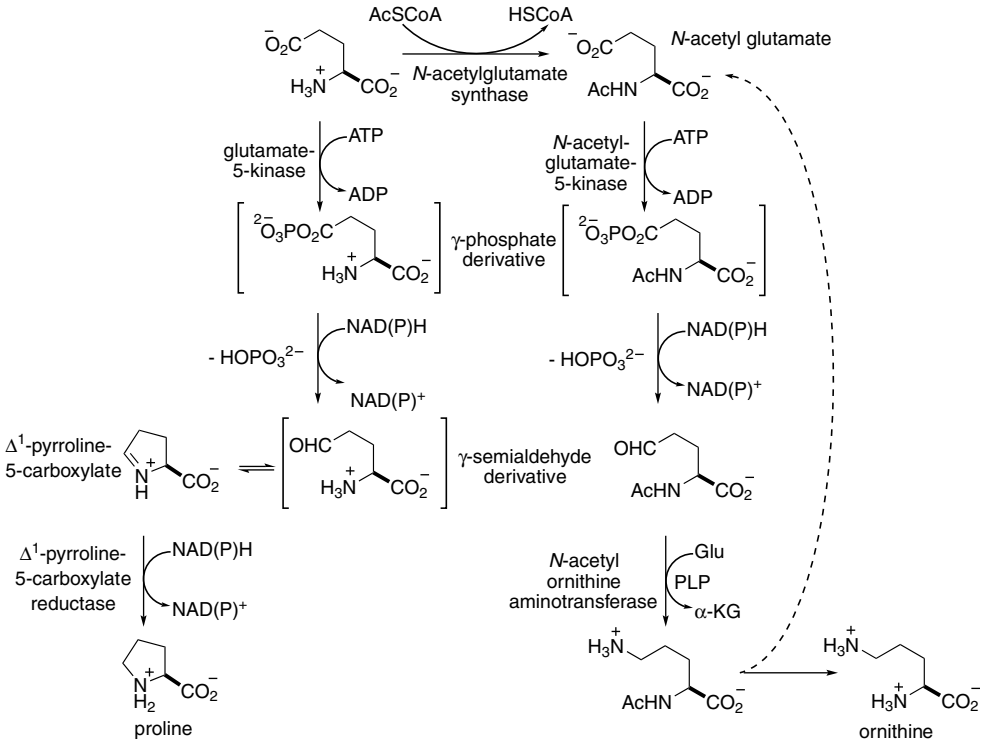

Figure 1.39 Biosynthesis of proline and ornithine.

Although the general chemical strategy for the biosynthesis of ornithine is common to many organisms, contemporary studies have revealed a diversity of detail in the pathways, associated with different acyl-transfer chemistry [135]. The first step of the biosynthesis in *E. coli*, which served as the initial exemplar for

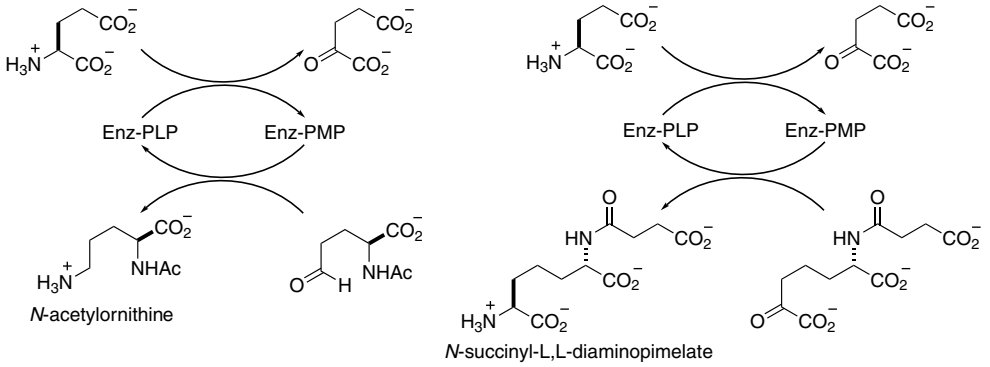

Figure 1.40 Multiple substrate specificity of *N*-acetylornithine aminotransferase.

bacterial, fungal and vertebrate pathways, is carried out by an *N*-acetylglutamate synthase [136, 137] that transfers an acetyl group directly from acetyl-CoA to glutamate. Subsequently, in other bacteria, a different family of smaller DITTOs were identified; these are sometimes fused to a second domain catalyzing the last step of arginine biosynthesis, argininosuccinate lyase – a hint of higher-level order in the biosynthetic apparatus. Other bacteria use a completely different enzyme for the acetylation chemistry: an ornithine acetyltransferase [138]. This enzyme acts via a sequential Bi Bi kinetic mechanism whereby it accepts an acetyl group from ornithine onto an active-site threonine, generating an acetyl-enzyme intermediate, and then, in a second step, transfers it to glutamate [139]. This route has the advantage of adding and removing the acetyl protecting group using a single enzyme and without paying the metabolic price of acetyl-CoA hydrolysis (although some of the ornithine acetyltransferases can be primed for acetyl donation by using acetyl-CoA as an alternative substrate) [140]. Two other biosynthetic variants have recently come to light: although ornithine is the normal product of this first section of the biosynthesis, there is evidence that some organisms only remove the *N*-acetyl group later in the pathway [141, 142]; mutation of substrate specificity, akin to that described for homoserine acyltransferases, has also underpinned the utilization of succinyl- rather than acetyltransferases in ornithine biosynthesis in *Bacteroides fragilis* [143].

The biosynthesis of arginine is completed by a three-step modification of the side-chain amino function of ornithine (Figure 1.41). Ornithine transcarbamoylase (OTCase) mediates carbamoylation with carbamoyl phosphate to produce citrulline [144]. It is one of a general class of transcarbamoylases [145] and is of clinical significance since OTCase deficiency is a relatively common genetic disease in

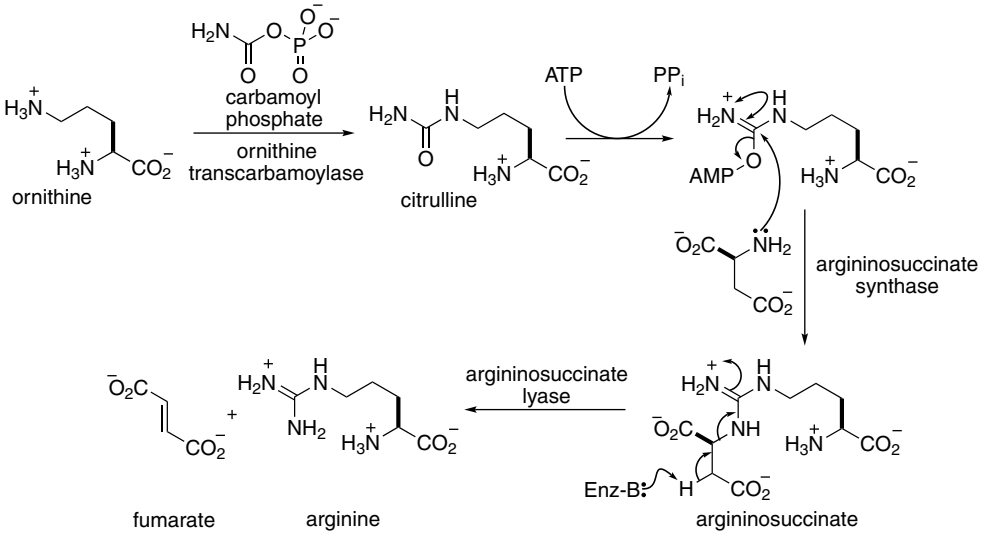

Figure 1.41 Conversion of ornithine to arginine.

humans. The enzyme mechanism is now believed to involve acid–base catalysis by the phosphate group of the substrate, carbamoyl phosphate [146].

The urea group of citrulline is converted to an amidine by the introduction of the final amino group. This transformation occurs in a two-step process that exemplifies the third general mechanism of amine transfer in metabolism (after GAT and PLP action) – ligation of the α-amino group of aspartate and then elimination of fumarate, which is recycled via the TCA cycle [147]. Argininosuccinate synthetase is homologous to asparagine synthetase [148] and uses ATP to activate the urea by adenylation [149]; nucleophilic substitution by aspartate produces argininosuccinate. Argininosuccinate lyase, the terminal enzyme of the pathway, is a member of a family of aspartase enzymes that catalyze the elimination of fumarate (which feeds into the TCA cycle) from aspartate and *N*-aspartyl derivatives [150, 151], demonstrating the generality of this two step synthetase/lyase route for the indirect transfer of ammonia – the third general process for transfer of nitrogen between metabolites.

1.7
Biosynthesis of Aliphatic Amino Acids with Modified Carbon Skeletons: Branched-Chain Amino Acids, Lysine, and Pyrrolysine

1.7.1
Overview

Four of the ubiquitous aliphatic protein amino acids, valine, leucine, isoleucine, and lysine, are made by the synthesis of new carbon skeletons. Lysine is now known to be the precursor of the 22nd ribosomally encoded amino acid, pyrrolysine. The biosynthesis of these amino acids involves parallel pathways in which a chemical strategy is duplicated and homologous or promiscuous enzymes are used for the biosynthesis of more than one amino acid. Valine and isoleucine are made from precursor α-keto acids by a common route, which also provides a key biosynthetic precursor for leucine. The carbon skeleton of leucine is made from an α-keto acid intermediate in valine biosynthesis by a pathway homologous to the biosynthesis of α-KG in the TCA cycle. This route, in turn is utilized for the biosynthesis of another amino acid, α-aminoadipic acid, which is not incorporated into proteins but is a biosynthetic precursor to lysine in one of the pathways to that amino acid. Lysine is unusual in being made in different organisms by two completely different pathways – from α-aminoadipic acid in some fungi and bacteria, and from aspartate-β-semialdehyde in plants and other bacteria.

1.7.2
Valine and Isoleucine

Three enzymes, acetohydroxyacid synthase (AHAS) [152], acetohydroxyacid isomeroreductase (AHIR) [153], and dihydroxyacid dehydratase [154], mediate the four key

steps common to the biosynthesis of all the branched-chain amino acids [155]. Being specific to branched-chain amino acid biosynthesis and not found in animals, these enzymes are key targets for herbicide research [156]. AHAS, in particular, is the target of a number of commercial herbicides. All three enzymes have relaxed substrate specificity and process metabolites on two parallel pathways to produce two α-keto acid products (Figure 1.42).

Pyruvate reacts with the anion of the thiamine pyrophosphate cofactor of AHAS (Figure 1.43). Decarboxylation of the initial adduct leads to an acetyl α-anion equivalent, illustrating the role of thiamine pyrophosphate as an umpolung reagent in biochemistry. Reaction of this nucleophile with a second α-keto acid provides a branched carbon skeleton [157]. Two α-keto acids can participate as electrophiles in the second stage of the reaction: pyruvate or α-ketobutyrate; these lead to valine and isoleucine, respectively. The α-ketobutyrate can be biosynthesized in one step from threonine (see below).

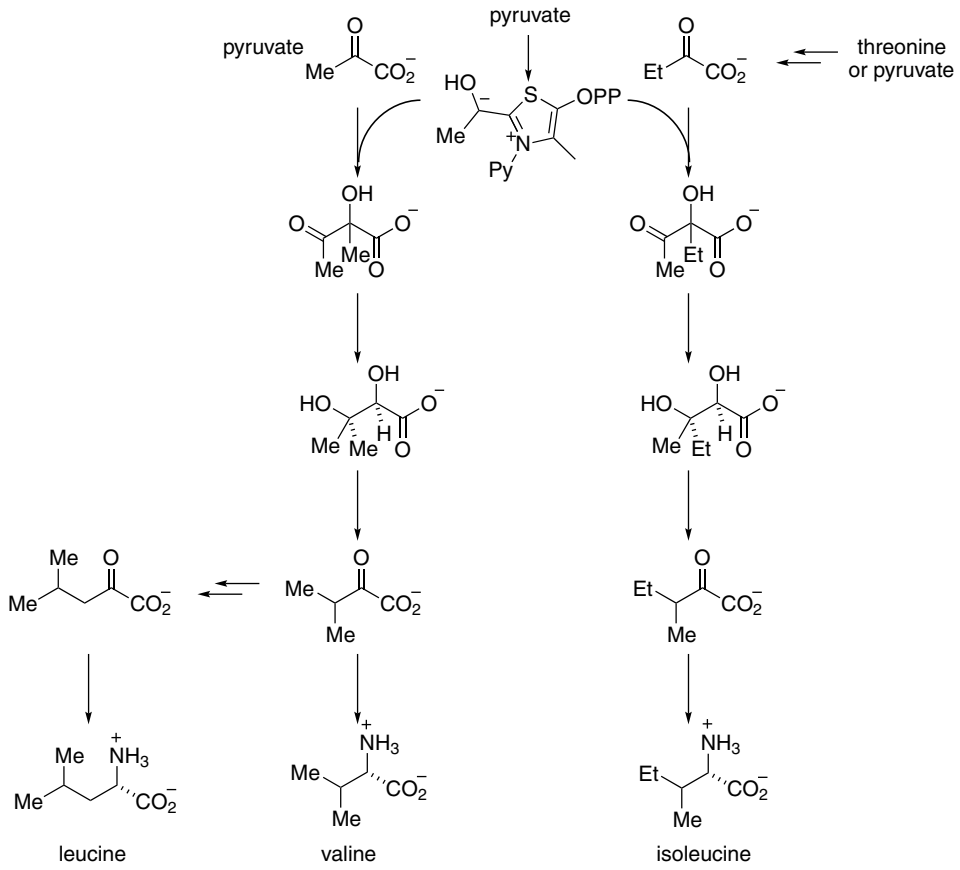

Figure 1.42 Overview of the parallel pathways to branched-chain amino acids.

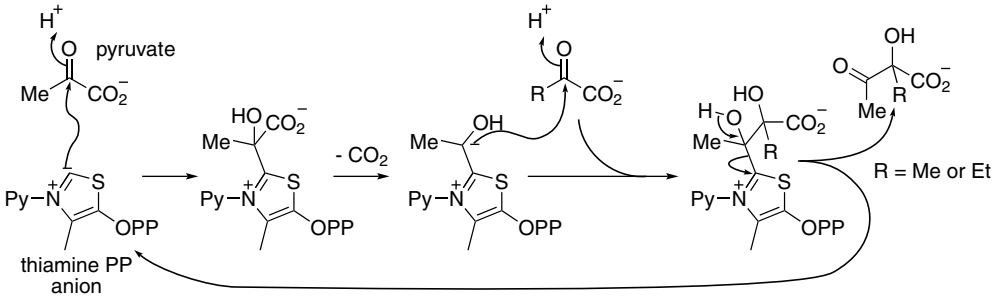

Figure 1.43 Mechanism of AHAS.

The structures of AHAS with bound sulfonylurea or imidazolinone show the mechanism of inhibition involves obstruction of the channel leading to the active site. The details of this inhibition provide an understanding of the basis of evolving herbicide resistance and will be useful in the generation of alternative herbicides [158].

Threonine deaminase (also known as threonine dehydratase) is a PLP-dependent enzyme that is the usual source of α-ketobutyrate needed for isoleucine biosynthesis [159, 160]. It is the point of commitment to isoleucine biosynthesis and the enzyme is subject to feedback regulation by isoleucine [161, 162]. Schiff base formation between threonine and the active-site PLP facilitates deprotonation at the α-center and consequent elimination of water, in a reaction characteristic of PLP-facilitated transformations of amino acids with β-leaving groups (Box 1.3). Cleavage of the link between PLP and the amino acid portion and hydrolysis chemistry produces α-ketobutyrate and ammonium ions as the product (Figure 1.44). An alternative route to α-ketobutyrate [163] based on the homologation of pyruvate is outlined later (Figure 1.48).

The two products of AHAS are processed by a bifunctional enzyme – AHIR [153]. While the enzyme acts on two different hydroxy acids, it has an absolute requirement

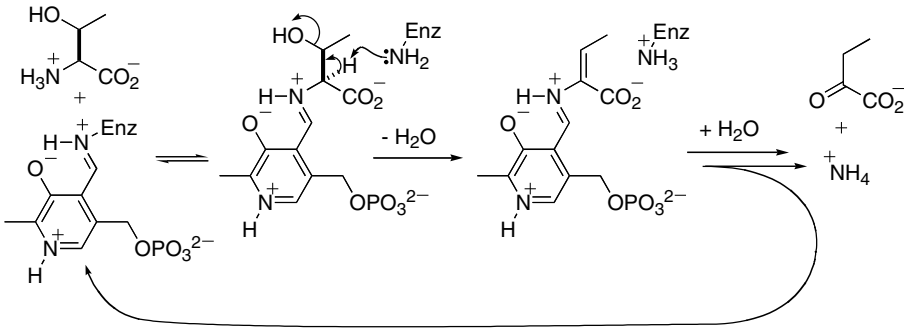

Figure 1.44 Conversion of threonine into α-ketobutyrate and ammonium ions.

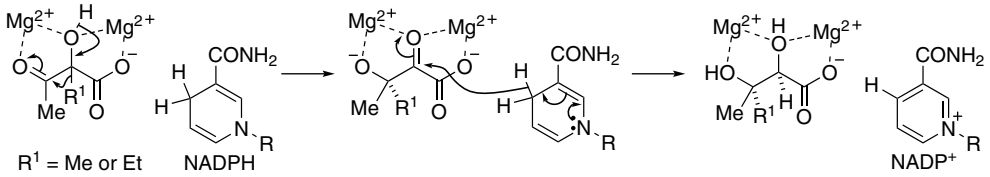

Figure 1.45 Two-stage mechanism of AHIR.

for the (*S*)-enantiomer of each substrate. Although no intermediate has been isolated, it is presumed that the reaction occurs in two stages – an alkyl migration and then a reduction step, mediated by NADPH (Figure 1.45).

The structure of plant AHIR with a herbicidal inhibitor bound [164] and, in another case, with the product and a modified cofactor bound, has allowed a mechanism to be proposed (Figure 1.45) [111]. Both steps of the reaction require Mg^{2+} for both structural and catalytic reasons. The two Mg^{2+} ions are suitably placed to polarize the starting keto group and facilitate deprotonation of the adjacent hydroxyl to facilitate push–pull catalysis of the alkyl transfer. The newly created ketone functionality is proximal to the nicotinamide cofactor and reduction traps the rearranged product.

Dehydration of the dihydroxy acid products by a dual-purpose enzyme completes the biosynthesis of the two key α-keto acids: α-ketoisovalerate and α-keto-β-methylvalerate (the precursors of valine and isoleucine, respectively). A [4Fe–4S] cluster of dihydroxyacid dehydratase catalyzes the elimination of water [154], in a mechanism believed to be analogous to that of aconitase (ACN) (Figure 1.46) [165]: coordination of the hydroxy acid to an iron center of the [4Fe–4S] cluster activates the hydroxyl as a leaving group and allows enzyme-induced elimination. Tautomerism of the resulting enol generates an α-keto acid product. The [4Fe–4S] cluster is labile to oxidation and one of the most significant antibacterial effects of nitric oxide, produced by the immune system, is now believed to be the inactivation of this enzyme [166], which leads to a diminished ability to make branched-chain amino acids [167]. The [4Fe–4S] center of dehydratases also appears to be a significant target for copper toxicity in bacteria [168].

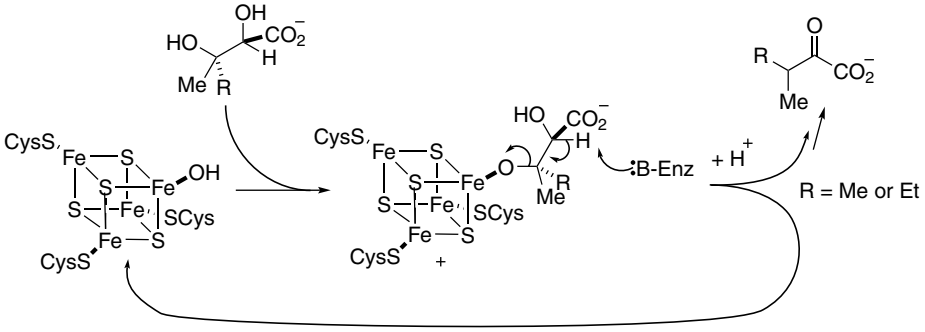

Figure 1.46 Proposed mechanism for dihydroxyacid dehydratase.

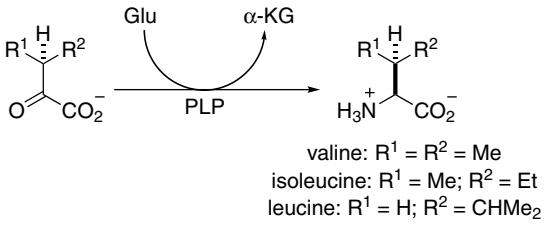

Figure 1.47 Transamination to form branched-chain amino acids.

Glutamate acts as amino donor in the transamination of α-ketoisovalerate and α-keto-β-methylvalerate catalyzed by the branched-chain aminotransferase (Figure 1.47). This produces valine and isoleucine, respectively. In addition to this fate, α-ketoisovalerate is also homologated to α-ketoisocaproate *en route* to leucine.

1.7.3
Homologation of α-Keto Acids, and the Biosynthesis of Leucine and α-Aminoadipic Acid

The aliphatic amino acids described so far provide a wide range of chemical diversity for proteins. However, there are two significant omissions that are rectified in the universal genetic code. The nonpolar amino acids, valine and isoleucine, are branched at the β-position, which causes steric congestion when multiply incorporated within α-helical structures. Homologation of valine to leucine relieves this steric crowding by placing the branching at the γ-center of the amino acid, thus increasing the opportunity for forming stable hydrophobic cores in α-helical proteins. The other omission is the lack of an amino acid with a side-chain amino substituent. Ornithine is not incorporated into proteins, possibly because the amino side-chain can cleave an adjacent peptide link via lactamization to form a six-membered ring. The only amine side-chain among the protein amino acids is that of lysine. This is a homologated version of ornithine that would produce a less favorable seven-membered ring species on lactamization. Access to a homologation pathway for α-keto acids is used to address both these issues.

In the TCA cycle, α-KG is synthesized from oxaloacetate by a three enzyme homologation process. Citrate synthase (CS) condenses oxaloacetate with acetyl-CoA. Hydrolysis of the thioester adduct ensures that the condensation reaction is favorable. Hydroxyl migration occurs via a dehydration-rehydration sequence catalyzed by an iron–sulfur-dependent enzyme, ACN, which is named in honor of the intermediate alkene, aconitate. Isocitrate dehydrogenase (IDH) catalyses the oxidation of isocitrate to a β-keto acid that spontaneously decarboxylates, in the presence of an enzymic divalent cation, to produce α-KG. Gene duplication and functional divergence has generated variants of this three-step process that are used to homologate the other two common α-keto acids of primary metabolism (pyruvate and α-KG) and a range of other α-keto acids including α-ketobutyrate (the biosynthetic precursor to

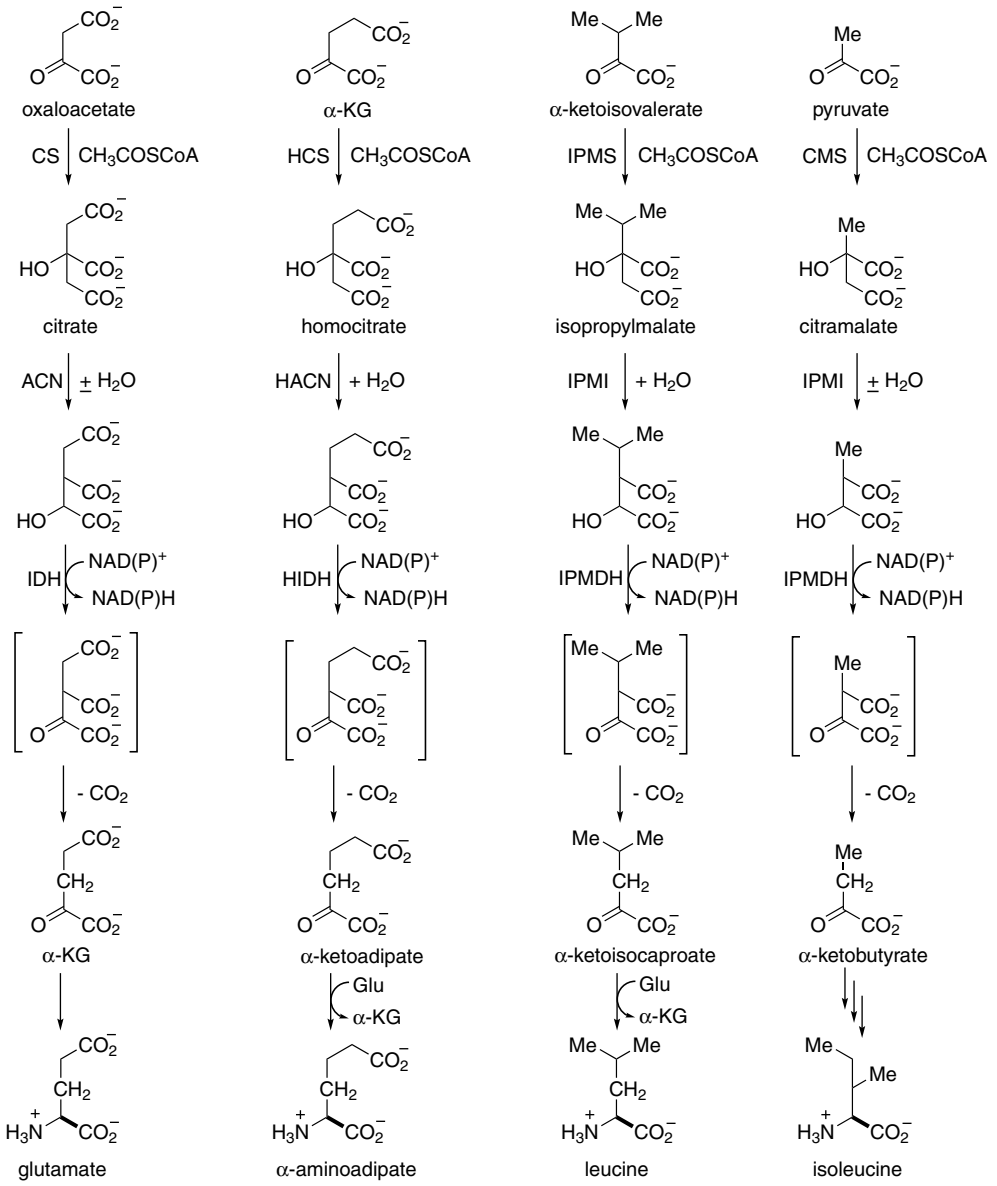

Figure 1.48 Homologation of α-keto acids to produce amino acids.

valine) (Figure 1.48) [163]. Transamination of α-ketoisovalerate and of α-ketoadipic acid makes leucine and α-aminoadipic acid, respectively [169], while the homologation of pyruvate to α-ketobutyrate provides an alternative route to the starting material for leucine biosynthesis in some Archaea and bacteria. Many of these enzymes have not been studied comprehensively and mechanistic proposals are

often drawn by analogy from the action of homologous enzymes that have been studied in more detail.

Homocitrate synthase (HCS) [170], isopropylmalate synthase (IPMS) [171], and citramalate synthase (CMS) [172] are homologous enzymes that catalyze the Claisen condensation of acetyl-CoA with α-KG, α-ketoisovalerate, and pyruvate, respectively. They are also homologous to one of the classes of CS found in anaerobic bacteria [173]. Hydrolysis of the initially formed thioester adduct makes the otherwise reversible Claisen condensation, favorable. The structure of IPMS has been determined [174] and that structure was used to shed light on the catalytic machinery of these enzymes [175]. Carbonyl groups of both substrates are polarized by the enzyme: acetyl-CoA by an arginine to facilitate enol formation and α-KG by chelation to an essential Zn^{2+}. On the basis of modeling, kinetic studies and site-directed mutagenesis, the general base for deprotonation of acetyl-CoA is believed to be a histidine, acting in concert with a glutamate as a catalytic dyad.

A variety of homologous isomerases catalyze the next step in the homologation process. These include homoaconitase (HACN) and isopropylmalate isomerase (IPMI), and are all members of the ACN superfamily [176]. As an example of the relatedness of these enzymes, in *P. horikoshii* a single enzyme, with dual substrate specificity, acts as both an IPMI and a HACN [177]. These enzymes are not fully characterized, but it is assumed that they exploit the dehydration–rehydration chemistry of a [4Fe–4S] cluster that has been characterized in ACN and was described for dihydroxyacid dehydratases above [165 (Figure 1.4–6)].

The final step in the homologation process is the oxidative decarboxylation of the β-hydroxy acids. In this step an oxidized nicotinamide cofactor ($NAD(P)^+$) accepts a hydride from the secondary alcohol center and generates a β-keto acid. This intermediate spontaneously decarboxylates, in the presence of an enzyme-bound divalent metal ion, to leave the homologated α-keto acids. This step is catalyzed by a superfamily of homologous enzymes, ICDH [178], isopropylmalate dehydrogenase (IPMDH) [179], and homoisocitrate dehydrogenase (HIDH) [180]. Dynamic X-ray crystallography has provided detailed structural information about the catalytic mechanism of ICDH which is the best characterized enzyme of the family [181]. Again, in some organisms dual substrate enzymes act in parallel pathways; for example, in both *Thermus thermophilus* [182] and *P. horikoshii* [183] a single enzyme catalyses two oxidative decarboxylation reactions producing both α-KG and α-ketoadipic acid. A loop at the active site of these enzymes appears to control specificity and mutations within this loop can modify the substrate specificity to change the pathway that an enzyme acts on. The conversion of *E. coli* ICDH to a bifunctional ICDH/IPMDH by mutagenesis has been reported by Koshland *et al.* Ser113 in the substrate recognition loop forms a hydrogen bond to the δ-carboxylate of isocitrate. Mutation of this residue to glutamate, which introduces electrostatic repulsion to the normal substrate, together with systematic mutation of two other local residues, Asp115 and Val116, produced several mutants with a preference for isopropylmalate as substrate. In *T. thermophilus* HICDH, Arg85 of the corresponding loop is involved in recognition of the δ/γ-carboxylate of isocitrate/homoisocitrate. When this residue is mutated to a large nonpolar residue, valine, the enzyme is converted to an IPMDH,

retaining some HICDH activity, but losing its ability to oxidatively decarboxylate isocitrate [182]. Other substrate specificity changes have been described for these enzymes; for example, the 100-fold preference of the *T. thermophilus* IPMDH for NAD^+ as coenzyme has been reversed to a 1000-fold preference for $NADP^+$ by mutagenesis in which seven residues involved in a β-turn were exchanged for a 13-residue sequence of α-helix and a loop modeled on the corresponding specificity determinant in *E. coli* ICDH [184].

Finally, the resulting α-keto acids are transaminated to the corresponding amino acids by appropriate aminotransferases: either the branched-chain aminotransferase described earlier (to produce leucine) or a glutamate-α-ketoadipate transaminase to generate the latter amino acid (Figure 1.48). Both enzymes utilize glutamate as nitrogen donor [185–187] and the structural basis for the multiple substrate specificity of the *T. thermophilus* aminotransferase has been studied in detail by X-ray crystallography [188].

1.7.4
Biosynthesis of Lysine: A Special Case

There are two distinct metabolic strategies for the biosynthesis of the six-carbon chain of lysine [169, 189]: the diaminopimelate pathway, which is found in plants, bacteria, and lower fungi utilizes pyruvate, and ASA (also a biosynthetic precursor to methionine and threonine as described above) as building blocks. The α-aminoadipate pathway, found in some bacteria, fungi, and euglenoids (eukaryotic single-celled flagellates), creates the carbon skeleton by a homologated version of the biosynthesis of α-KG (as found in the TCA cycle and described in the previous section). Both of these pathways are now known to occur in multiple variants [190, 191].

1.7.4.1 Diaminopimelate Pathway to Lysine

The DAP pathway produces both lysine and *meso*-DAP – an important bacterial cell wall building block (Figure 1.49). It starts with ASA, prepared by the same chemistry as the first two steps of the methionine/threonine pathway [95, 192]. As with other aspartate family amino acids, the biosynthetic enzymes are potential therapeutic and pesticide targets [193]. Dihydrodipicolinate synthase (DHDPS) forms a Schiff base with pyruvate to provide access to an enamine that condenses with ASA [194–196]. The resulting dihydrodipicolinate is reduced to tetrahydrodipicolinate [197, 198], after which the pathway diverges in different organisms.

In bacteria, *N*-acylation facilitates ring opening of tetrahydrodipicolinate; acetyl- and succinyl-CoA are used as acylating agents in different organisms. The resulting α-keto acid is transaminated, using glutamate as nitrogen donor; the dual role of this *E. coli* aminotransferase for both lysine and ornithine biosynthesis has been noted above (Figure 1.40). Removal of the *N*-acyl group gives L,L-DAP, which undergoes epimerization to *meso*-DAP catalyzed by an enzyme, DAP epimerase, that uses a pair of active-site cysteine residues to effect deprotonation and reprotonation at one of the α-amino acid centers [199, 200]. The D-amino acid

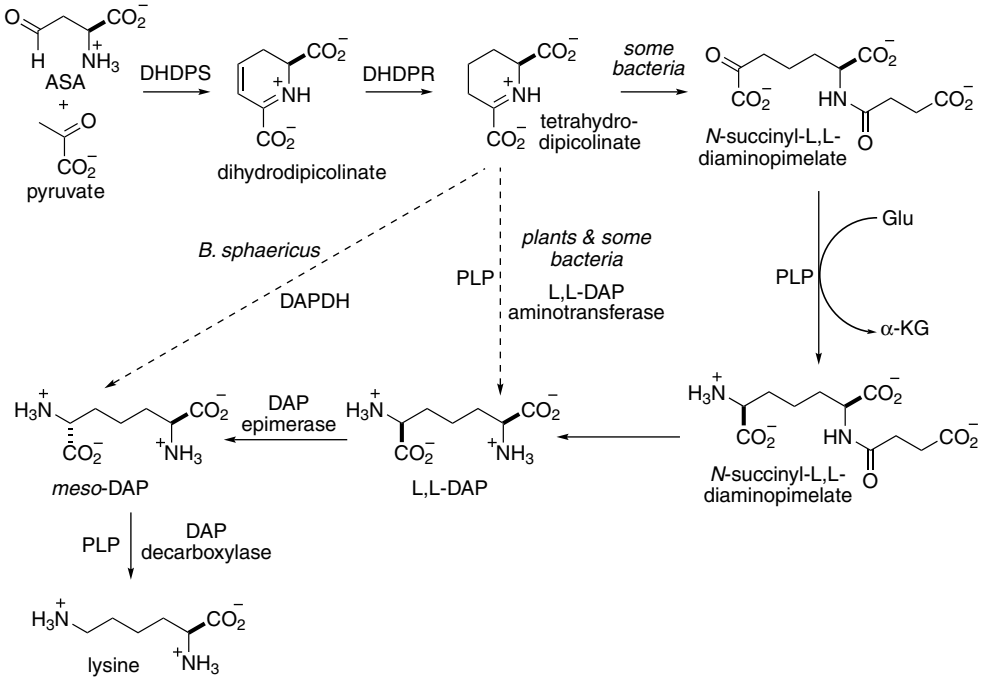

Figure 1.49 DAP pathways for the biosynthesis of lysine.

center of *meso*-DAP is decarboxylated by a PLP-dependent enzyme [201–203] to generate lysine (see Box 1.3).

In plants and some bacteria the latter stages of the DAP pathway are truncated by omission of the acylation and deacylation steps [191]; in these organisms a L,L-DAP aminotransferase converts tetrahydrodipicolinate directly to L,L-DAP [204]. *Corynebacterium glutamicum*, used in the industrial production of lysine, can run either the full or truncated pathway, depending on conditions [160]. *Bacillus sphaericus* truncates this section of the pathway still further by directly converting tetrahydrodipicolinate to *meso*-DAP using an NADPH-dependent DAP dehydrogenase [205], presumably via a reductive amination reaction on the ring-opened form of tetrahydrodipicolinate.

1.7.4.2 α-Aminoadipic Acid Pathways to Lysine

There are now known to be two separate pathways to lysine from α-aminoadipic acid (Figure 1.50). Both utilize the strategy, anticipated from the biosynthesis of aspartate and glutamate family amino acids, of activation of the δ-carboxylate, reduction to a semialdehyde, and then an amination process. Interestingly, both pathways are now believed to involve ligation to carrier proteins. The most recently discovered pathway was identified in *T. thermophilus* and *P. horikoshii* by a bioinformatic approach [190]. A cluster of three genes homologous to the central three steps of ornithine biosynthesis (phosphorylation of the side-chain carboxylate, reduction of the acyl phosphate to a

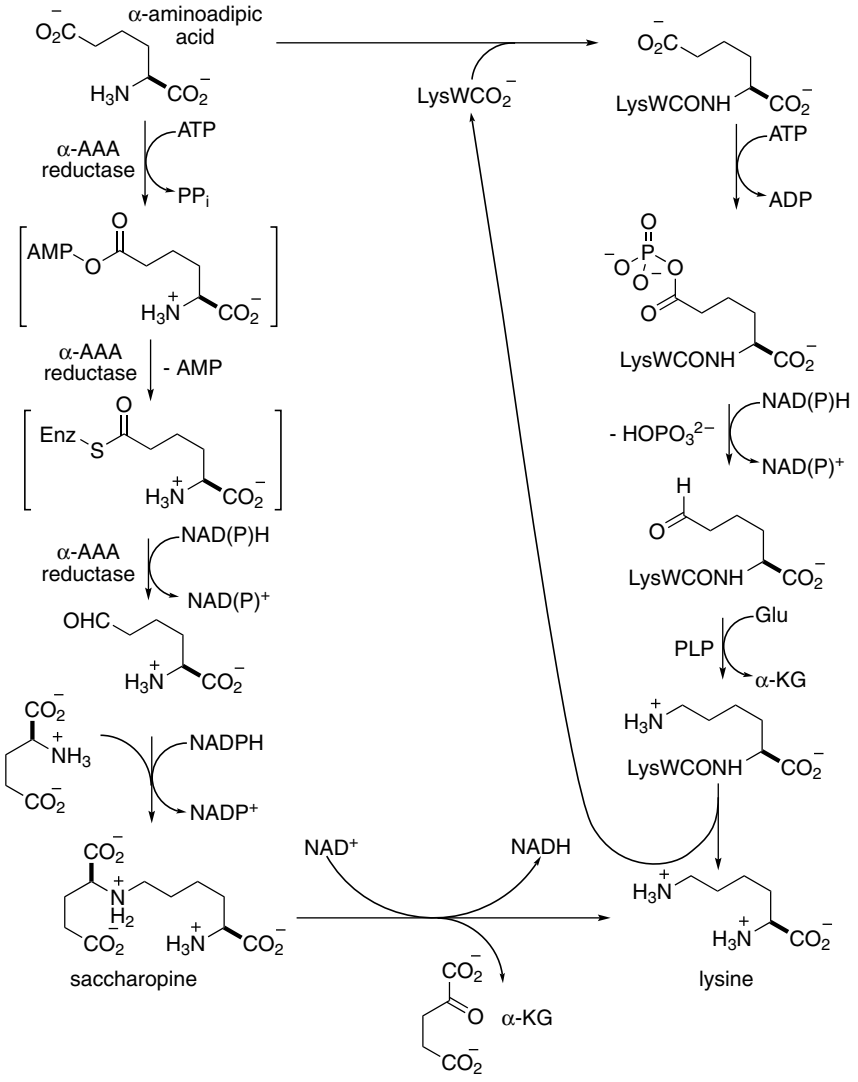

Figure 1.50 Biosynthetic routes to lysine from α-aminoadipic acid.

semialdehyde, and transamination to the amine) were identified in *T. thermophilus*. Genes for the first and last steps of arginine biosynthesis (for the protecting group chemistry of *N*-acylation and deacylation) were absent. Disruption of these putative arginine biosynthetic genes led to organisms auxotrophic for lysine. This demonstrated a biosynthetic route to lysine that is analogous to the biosynthesis of ornithine from glutamate [206]. In reconstituting the α-aminoadipic acid pathway from *T. thermophilus* it was discovered that an alternative *N*-acylation pathway operates in this bacterium. In the first step of the pathway the amino group of α-aminoadipic acid is

protected by acylation by the side-chain carboxylate of the C-terminal glutamate of a small protein, LysW. The functional group modification of the α-aminoadipic acid is mediated on the LysW adduct which acts as a carrier protein for the biosynthesis. Following completion of the side-chain manipulation, the LysW adduct is cleaved to release lysine [207].

Although the discovery of a bacterial route to lysine from α-aminoadipic acid is a recent discovery, this amino acid has been known for some time to have two metabolic roles in fungi – both as an alternative precursor to lysine [169], and as a key precursor in the biosynthesis of penicillin and cephalosporin antibiotics [208]. For penicillin biosynthesis the δ-carboxylate of α-aminoadipic acid is incorporated into a tripeptide by a nonribosomal peptide synthetase, δ-(α-L-aminoadipyl)-L-cysteinyl-D-valine synthetase [209]. The peptide bonds, including that to the side-chain of α-aminoadipic acid, are made by ligating the carboxyl group of each component to a multifunctional enzyme via thioester links to 4′-phosphopantetheine groups which then undergo successive nucleophilic substitution reactions with the amine of the adjacent component [210].

Walsh *et al*. have proposed that the activation and reduction of the δ-carboxylate of α-aminoadipic acid occurs in an analogous fashion to nonribosomal peptide synthesis (Figure 1.50). α-Aminoadipate reductase comprises two proteins – Lys2 and Lys5. Lys2 is a large (155 kDa) multidomain protein. Sequence homologies with nonribosomal peptide synthetases suggest that residues 225–808 constitute a 60-kDa adenylation domain (A) that activates α-aminoadipic acid as the aminoacyl-δ-AMP derivative [211]. Hydrolysis of the pyrophosphate side-product makes the reaction favorable. Lys5 primes the PCP domain (residues 809–924) of Lys2 by adding a 4′-phosphopantatheine unit to Ser880. The aminoacyl-δ-AMP derivative is ligated to the 4′-phosphopantatheine unit as a thioester. NADPH-dependent reduction to α-aminoadipic acid-δ-semialdehyde, mediated by the reductase domain (residues 925–1392), cleaves the link to the carrier protein.

The biosynthesis of lysine in this pathway is completed by an unusual two-step transamination process that does not involve a PLP-dependent enzyme. Typical transamination chemistry involves the reductive amination of PLP to PMP by glutamate and subsequent reductive amination of the target carbonyl compound by PMP. In this case, however, a saccharopine dehydrogenase reductively aminates α-aminoadipic acid-δ-semialdehyde with glutamate directly to produce saccharopine [212–214]. A second saccharopine dehydrogenase, structurally related to alanine dehydrogenase, mediates the NAD^+-dependent oxidative cleavage of α-KG from the adduct to leave lysine [215]. Kinetic and structural studies have led to the proposal for a proton relay mechanism for this final step of the pathway [216]. NAD^+ abstracts a hydride to generate an imine that is converted to a carbinolamine by base-catalyzed addition of water. Further acid–base chemistry leads to fragmentation of the carbinolamine and formation of the two products (Figure 1.51).

1.7.4.3 **Pyrrolysine**

Pyrrolysine is an uncommon amino acid found in some Archaea and eubacteria; only 1% of genomes thus far sequenced contain evidence for its presence. It was first

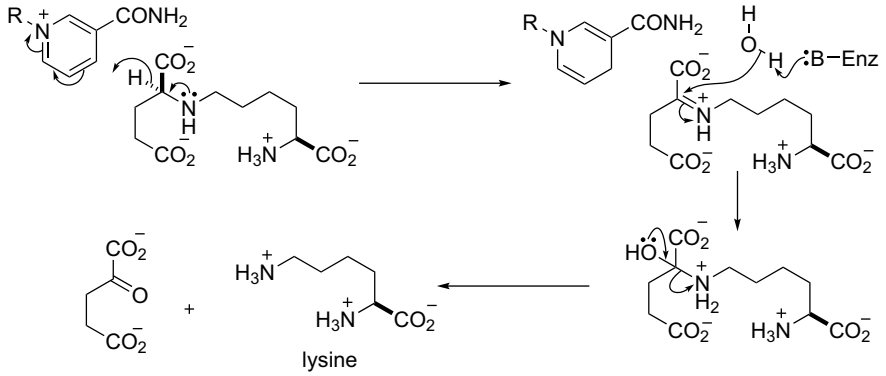

Figure 1.51 Formation of lysine by saccharopine dehydrogenase (lysine forming).

observed as an active-site residue in the crystal structure of monomethylamine methyltransferase from a methanogen, *Methanosarcina barkeri* [217], and it has now been found in other methylamine methyltransferases [218] associated with the metabolism of methylamines to methane. It is believed that the electrophilic imine of pyrrolysine is the functional group that activates methylamines for transfer of a methyl group to an adjacent cobalt corrin center [219].

In contrast to selenocysteine, this amino acid addition to the genetic code is biosynthesized from the free amino acid precursor, lysine, and then incorporated into an amber suppressor tRNA by a specific pyrrolysyl-tRNA synthetase [220–223]. The biosynthetic pathway to pyrrolysine is as yet undetermined, however a gene cluster from *Methanosarcina acetivorans pylBCD* encodes for the biosynthesis of this amino acid and recombinant *E. coli* containing these genes, together with the *pylTS* genes that encode $tRNA^{Pyl}$ and pyrrolysyl-tRNA synthetase, respectively, biosynthesize pyrrolysine and incorporate it into reading frames containing the amber codon [224]. The *pylBCD* genes show homology to genes that encode radical (*S*)-adenosylmethionine-dependent proteins, proteins forming amides and amino acid dehydrogenases, respectively; this combination of catalytic functionalities has led to the proposal of a possible biosynthetic route (Figure 1.52) [219]: manipulation of (3*R*)-3-methyl-D-glutamate, by analogy with the chemical strategy of the first stages of proline biosynthesis (reduction to the γ-aldehyde and spontaneous cyclization), could

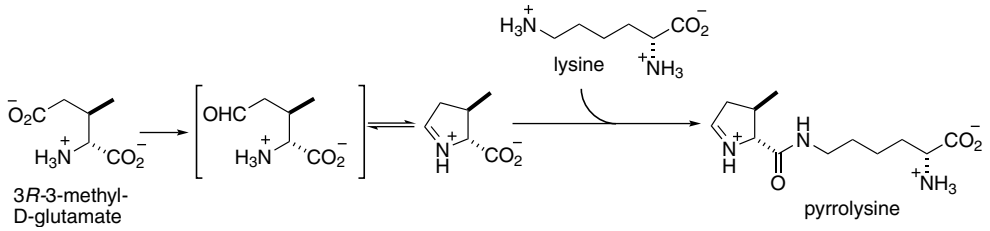

Figure 1.52 Possible biosynthetic route to pyrrolysine.

generate the required imino acid which could then be activated and used to acylate lysine to form pyrrolysine.

1.8
Biosynthesis of the Aromatic Amino Acids

1.8.1
Shikimate Pathway

The biosynthesis of the aromatic amino acids tryptophan, phenylalanine, and tyrosine begins with the shikimate pathway (Figure 1.53). This pathway consists of seven enzyme-catalyzed reactions, which convert erythrose 4-phosphate (E4P) and phosphoenol pyruvate (PEP), both originally derived from glucose, into the prearomatic compound chorismate [225, 226]. From chorismate, the pathway branches to produce tryptophan, or phenylalanine and tyrosine. Chorismate is also the precursor for other important aromatic compounds.

The first step of the shikimate pathway is catalyzed by 3-deoxy-D-*arabino*-heptulosonate-phosphate (DAH7P) synthase. Feedback regulation of this enzyme by

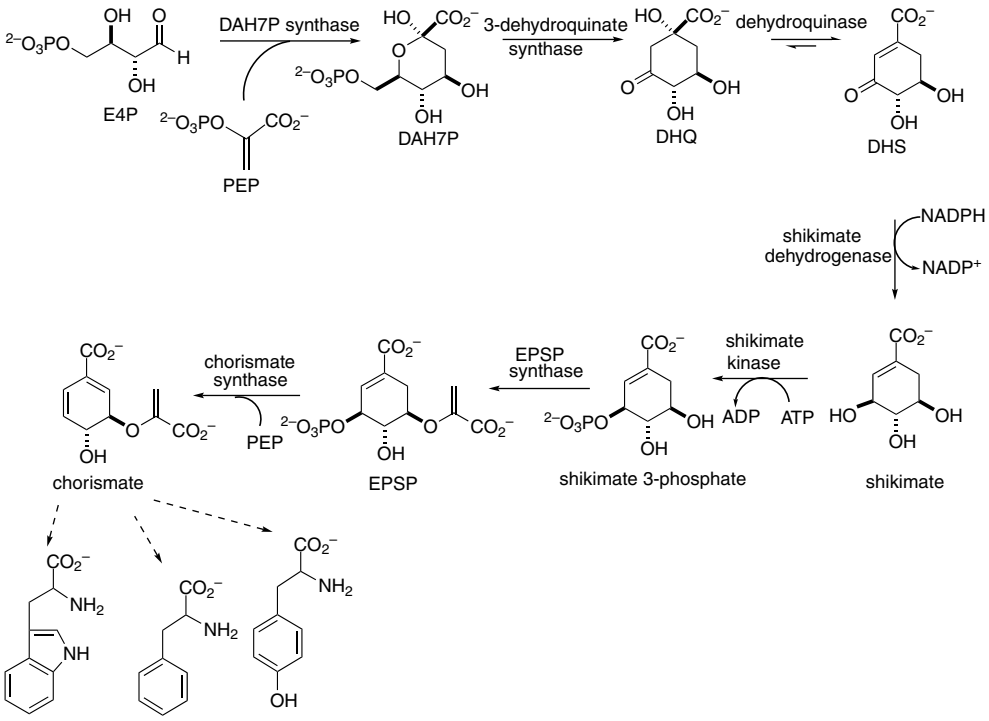

Figure 1.53 Shikimate pathway.

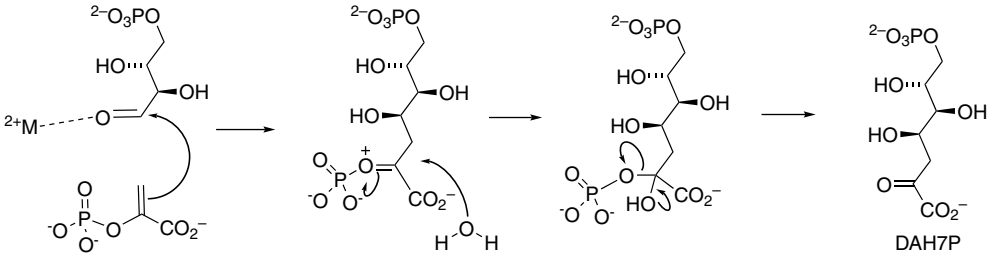

Figure 1.54 Proposed mechanism for DAH7P synthase.

aromatic amino acids is an important mechanism for control of flux through the shikimate pathway. DAH7P synthase catalyses an aldol-like reaction in which the three-carbon unit PEP condenses with the four-carbon aldehyde, E4P. It has been shown that the C–O bond of PEP is cleaved during the reaction, requiring water to act as a nucleophile on C2 of PEP, generating a phosphorylated hemiacetal intermediate (Figure 1.54). This intermediate then loses phosphate to produce the linear form of DAH7P. All DAH7P synthases have been shown to require a divalent metal ion for activity [227]. It is likely that the metal ion plays a role in activating the aldehydic carbon to nucleophilic attack (Figure 1.54) [228].

Directed evolution experiments have been used to replace DAH7P synthase with a pyruvate-utilizing aldolase, 2-keto-3-deoxy-6-phosphogalactonate (KDPGal) synthase (Figure 1.55) [229, 230]. Frost *et al.* showed that both the *E. coli* enzyme and that from *Klebsiella pneumoniae* could support biosynthesis of aromatic metabolites in a cell line lacking all isozymes of DAH7P synthase. Gene shuffling and modifications of the

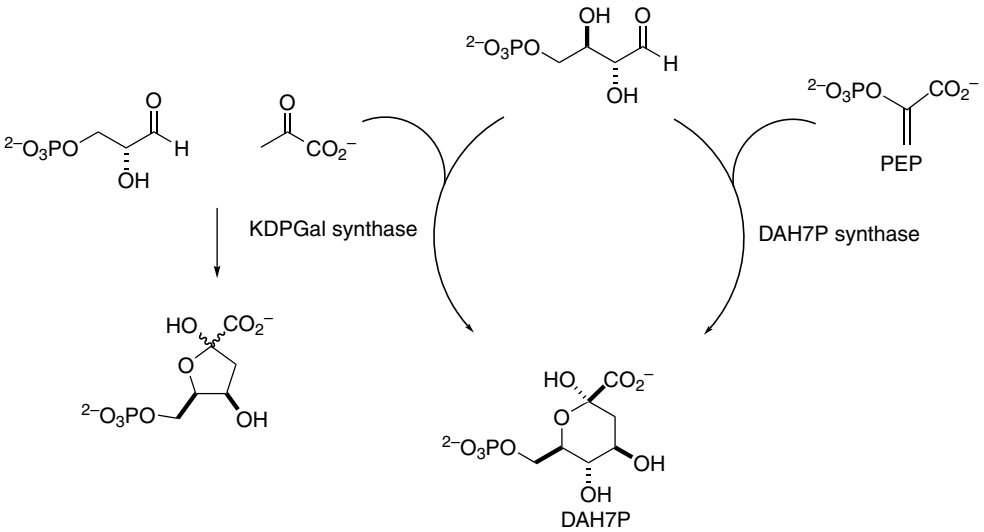

Figure 1.55 Directed evolution of the pyruvate-utilizing aldolase KDPGal synthase to replace DAH7P synthase.

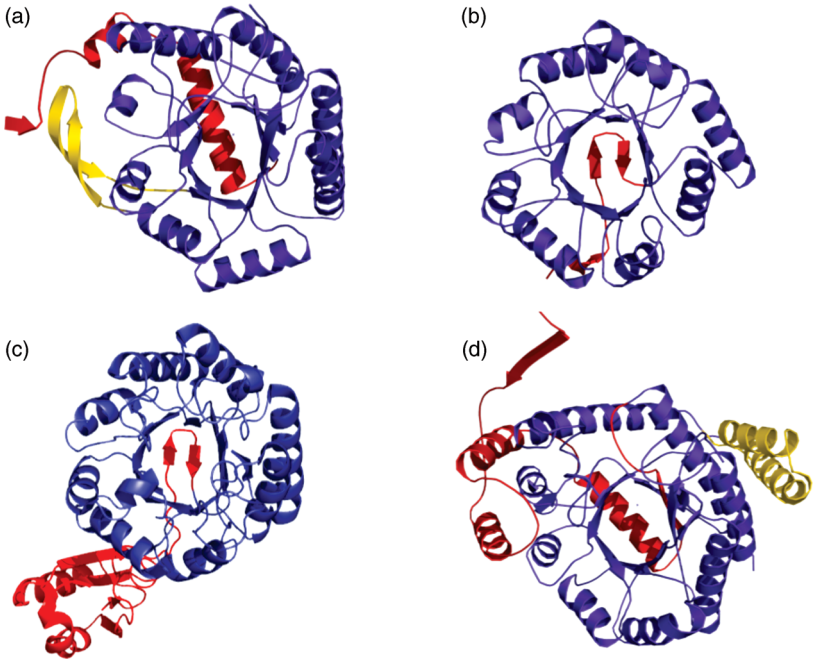

Figure 1.56 Different forms of DAH7P synthase showing basic catalytic barrel in blue, and N-terminal and loop extensions in red and yellow, respectively, from (a) *E. coli* type Iα (Phe sensitive), (b) *P. furiosus* type Iβ (unregulated), (c) *T. maritima* Iβ (Phe, Tyr inhibited) [235], and (d) *M. tuberculosis* (Phe + Tyr inhibited) [231].

E. coli enzyme by site directed mutagenesis produced mutant forms of the aldolase that exhibited a 60-fold increase of k_{cat}/K_m over wild-type activity.

One of the most interesting aspects of DAH7P synthase is the variation in structures and regulation patterns that have been observed for this enzyme [231]. Structures of DAH7P synthases have been determined from a variety of sources including *E. coli*, *Pyrococcus furiosus*, *S. cerevisiae*, *Thermotoga maritima*, and *M. tuberculosis* (Figure 1.56) [231–234]. Despite large primary sequence variation, the core catalytic unit for each of these proteins is a standard $(\beta\alpha)_8$ barrel. Variable accessory domains have been shown to augment this barrel structure and different quaternary structures are observed for enzymes from different species. The variable extra-barrel elements are associated with feedback regulation. *E. coli* expresses three DAH7P synthase isozymes each with a binding site for a single aromatic amino acid. On the other hand, the *M. tuberculosis* genome encodes a single DAH7P synthase. This enzyme shows synergistic inhibition by a combination of tryptophan and phenylalanine, with both amino acids binding simultaneously to independent allosteric sites formed extra-barrel subdomains.

3-Dehydroquinate (DHQ) synthase, which catalyzes the second step of the shikimate pathway, is responsible for production of the first carbocycle of the pathway. This enzyme has attracted a great deal of attention due to the number of

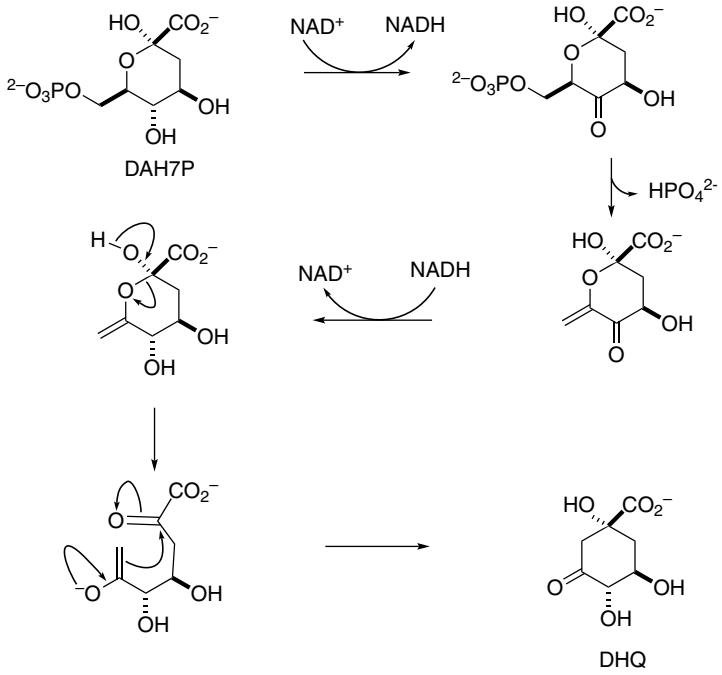

Figure 1.57 Reaction mechanism for dehydroquinate synthase.

different chemical steps catalyzed by a single enzyme (Figure 1.57) [236–238]. DHQ synthase uses the pyranose form of DAH7P. In the first step it undergoes temporary oxidation at C5 to facilitate *syn* elimination by an $E1_{cb}$ mechanism to produce an enol pyranose intermediate. The C5 keto group of the product is then reduced. These redox steps use NAD^+/NADH as a cofactor to accept and deliver the hydride. Following reduction, the enol pyranose intermediate ring opens and cyclizes via an intramolecular aldol reaction. There has been some debate about the role of the enzyme in these final two steps, as the enol pyranose intermediate, released *in situ* via photolysis of an *o*-nitrobenzyl protected form, was able to form dehydroquinate without assistance from the enzyme (Figure 1.58). However, as some epimer is produced in the nonenzymatic reaction (produced by the enol attacking the wrong

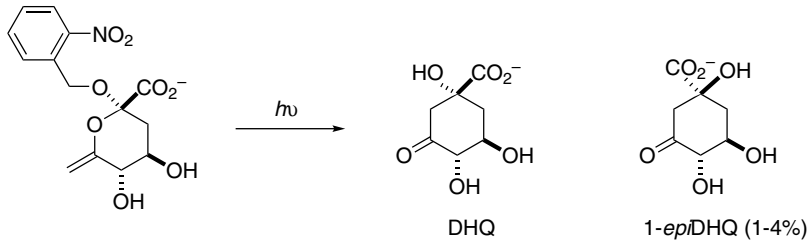

Figure 1.58 Nonenzymatic generation of DHQ.

face of the carbonyl), the enzyme appears to be required at least as a template to ensure the correct stereochemistry of the final product dehydroquinate is generated (Figure 1.58). DHQ synthase is one of a handful of enzymes that use transient oxidation to achieve its overall chemistry [239].

1.8.2
Case Study: Alternative Synthesis of Dehydroquinate in Archaea

Euryarchaea have a different strategy for the biosynthesis of dehydroquinate (Figure 1.59) [240, 241]. Recent work on *Methanocaldococcus jannaschii* has shown that dehydroquinate production occurs through two alternative enzyme-catalyzed

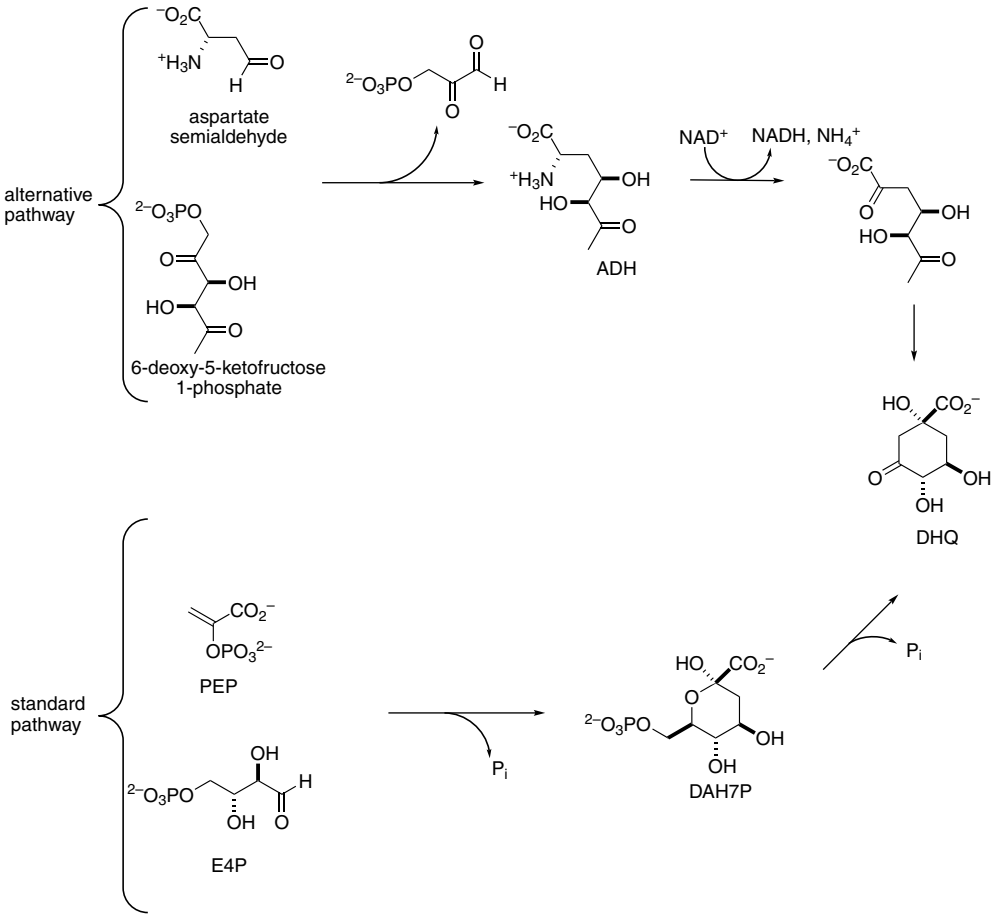

Figure 1.59 Alternative routes for aromatic amino acid biosynthesis. Dehydroquinate synthase II catalyzes the oxidative deamination of ADH and its cyclization to form DHQ, which then feeds into the standard shikimate pathway.

steps. The first of these is catalyzed by a lysine-dependent, Schiff base-utilizing, type I aldolase. This enzyme, 2-amino-3,7-dideoxy-D-*threo*-hept-6-ulosonic acid (ADH) synthase, catalyses a transaldolase reaction between 6-deoxy-5-ketofructose 1-phosphate and ASA (a biosynthetic precursor to threonine, methionine, and lysine). The structure of this enzyme has revealed the likely active site residues and allowed the mechanism of this reaction to be predicted [242].

Following the production of ADH, the DHQ is produced in an oxidative deamination reaction that requires NAD^+. In contrast to DHQ synthase where oxidation is transient, an equivalent of NAD^+ is required in this transformation. Analogous to the DHQ synthase reaction that takes place as part of the canonical shikimate pathway, stereospecific intramolecular cyclization is required to produce DHQ. The discovery of this alternate route to DHQ in these organisms highlights how different strategies can be employed and different chemistries can evolve to achieve the same overall solution.

The third step in the pathway towards chorismate is catalyzed by dehydroquinase. There are two distinct types of dehydroquinase that operate in shikimate pathway metabolism that have evolved convergently and utilize different mechanisms for the dehydration reaction [243]. Whereas the type I enzyme catalyzes a reaction with overall *syn* elimination, the type II enzymes catalyze *anti* elimination in which the more acidic hydrogen is lost (Figure 1.60) [244]. Type I enzymes proceed via a Schiff base mechanism [245, 246]. The covalent attachment of substrate to the enzymes enables conformational change promoting the *syn* elimination to occur by increasing the acidity of the *pro*-(*S*) hydrogen. The reaction catalyzed by the type II enzyme proceeds via a standard $E1_{cb}$ mechanism, with the loss of the more acidic *pro*-(*R*) hydrogen. Type II enzymes operate in the shikimate pathway of some significant human pathogens and there has been considerable attention on the development of inhibitors. Several inhibitors with nanomolar inhibition constants have been described [247].

The fourth step of the shikimate pathway is the NADPH-mediated reduction of dehydroshikimate catalyzed by shikimate dehydrogenase [248, 249]. Structures of several shikimate dehydrogenases have been determined with the ternary shikimate/NADPH/enzyme complex of the shikimate dehydrogenase from *Staphylococcus epidermidis* revealing clearly the interaction of substrates with the enzyme, and

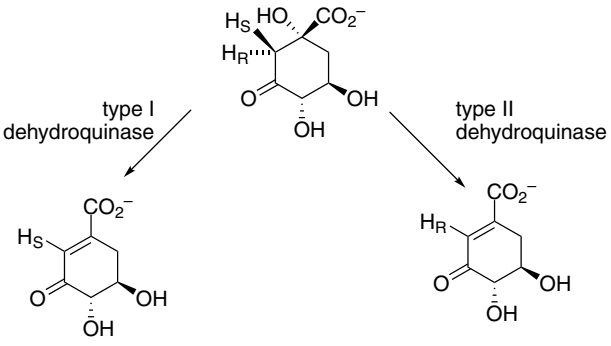

Figure 1.60 Opposite stereochemical pathways catalyzed by the two types of dehydroquinase.

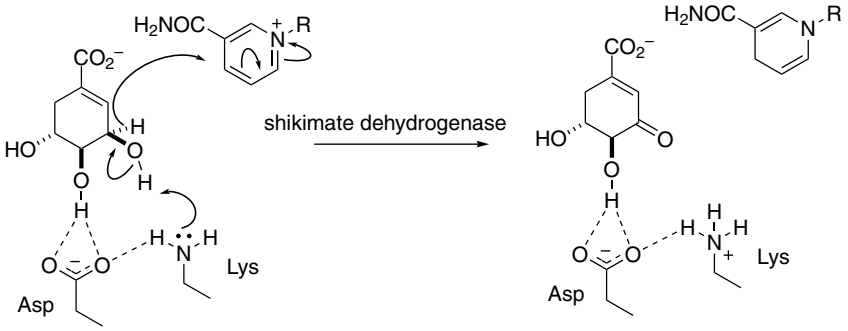

Figure 1.61 Reaction catalyzed by shikimate dehydrogenase.

identifying active-site lysine and aspartate residues as a key catalytic diad (Figure 1.61) [250–252].

In the fifth step of the pathway, shikimate becomes selectively phosphorylated on the C3 hydroxyl group to give shikimate 3-phosphate. This phosphoryl transfer reaction uses ATP as a cosubstrate and is catalyzed by shikimate kinase. Some organisms such as *E. coli* express two shikimate kinases that have quite different substrate affinities, while other organisms such as *M. tuberculosis* and *Helicobacter pylori* have a single enzyme responsible for catalyzing this transformation [253, 254].

The penultimate step of the pathway, catalyzed by enolpyruvylshikimate 3-phosphate synthase (EPSP synthase), has attracted a large amount of interest, as this enzyme is the target of the herbicide glyphosate [*N*-(phosphonomethyl)glycine] (Figure 1.62). The mechanism of the reaction, a stereospecific addition–elimination,

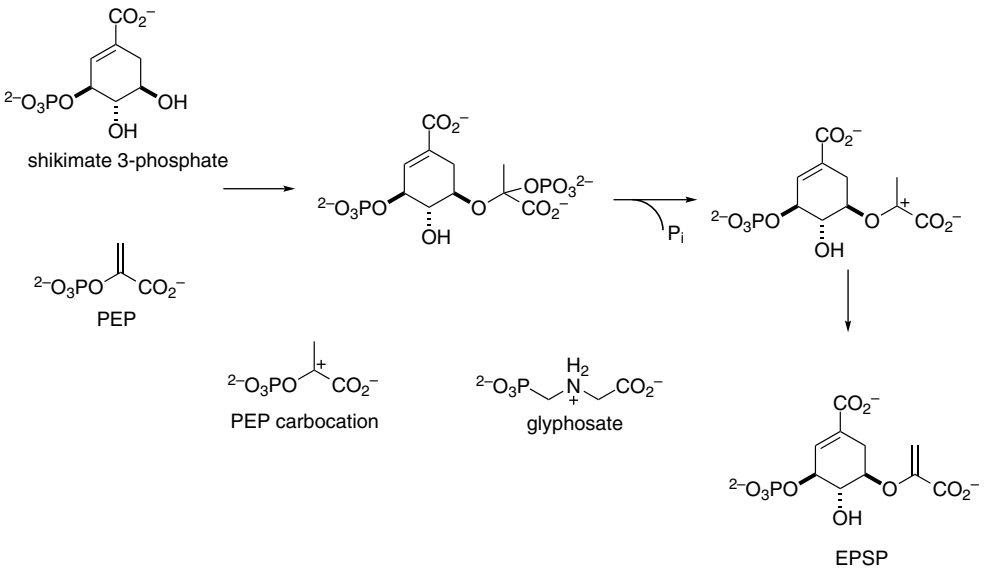

Figure 1.62 Reaction catalyzed by EPSP synthase.

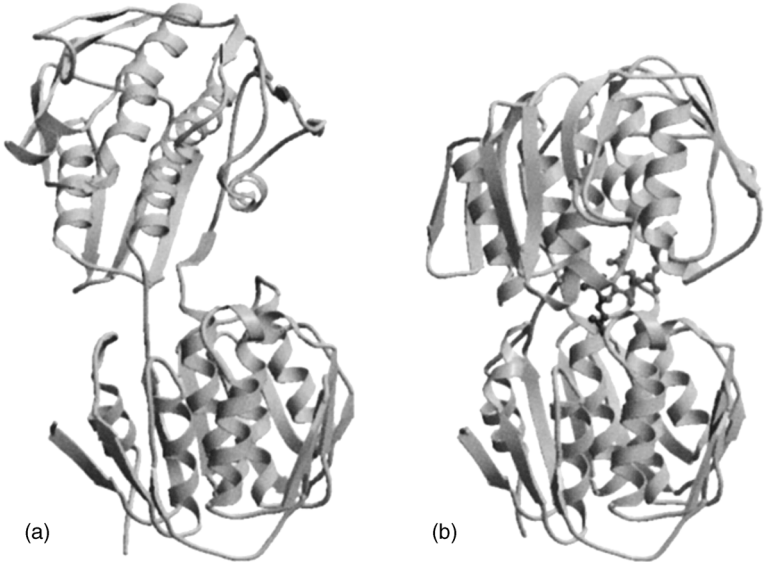

Figure 1.63 EPSP synthase in open (unliganded, PDB ID: 1EPS) and closed forms (liganded). (From [257].)

has been well studied [255, 256]. The active site is found in a cleft between two domains and during the catalytic cycle there is extensive domain movement (Figure 1.63). Glyphosate inhibits by mimicking the cationic transition state associated with the protonated PEP substrate (Figure 1.64) [257]. Transition state analogs that include both PEP and shikimate 3-phosphate functionality are particularly

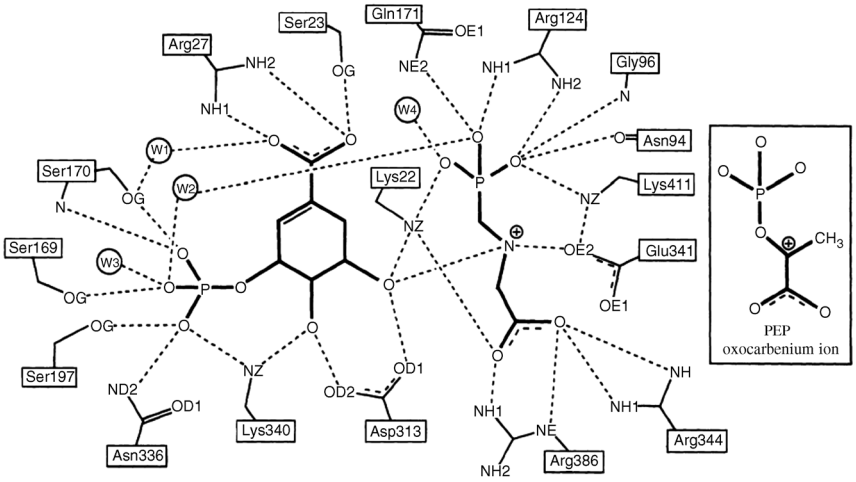

Figure 1.64 Interactions of the glyphosate and shikimate 3-phosphate with EPSP synthase. (From [257].)

potent, but intriguingly show different abilities to inhibit enzymes that are glyphosate-tolerant to those which are sensitive to this inhibitor [256].

Chorismate synthase catalyzes the *anti* 1,4-elimination of phosphate and the C6 *pro*-(*R*) hydrogen, in the last step of the shikimate pathway. The mechanism of this reaction is intriguing, as the reaction, which is overall redox neutral, requires a reduced flavin mononucleotide – a cofactor associated with redox chemistry [258–260]. Some enzymes such as the chorismate synthases from *Neurospora crassa* and *S. cerevisiae* are bifunctional with both chorismate synthase and flavin reductase activity. The reduced flavin is predicted to help catalyze the reaction by a transient transfer of an electron, and by acting as a base to remove the *pro*-(*R*) hydrogen from EPSP (Figure 1.65). Various active site residues, notably histidine, are available to support this role [261, 262].

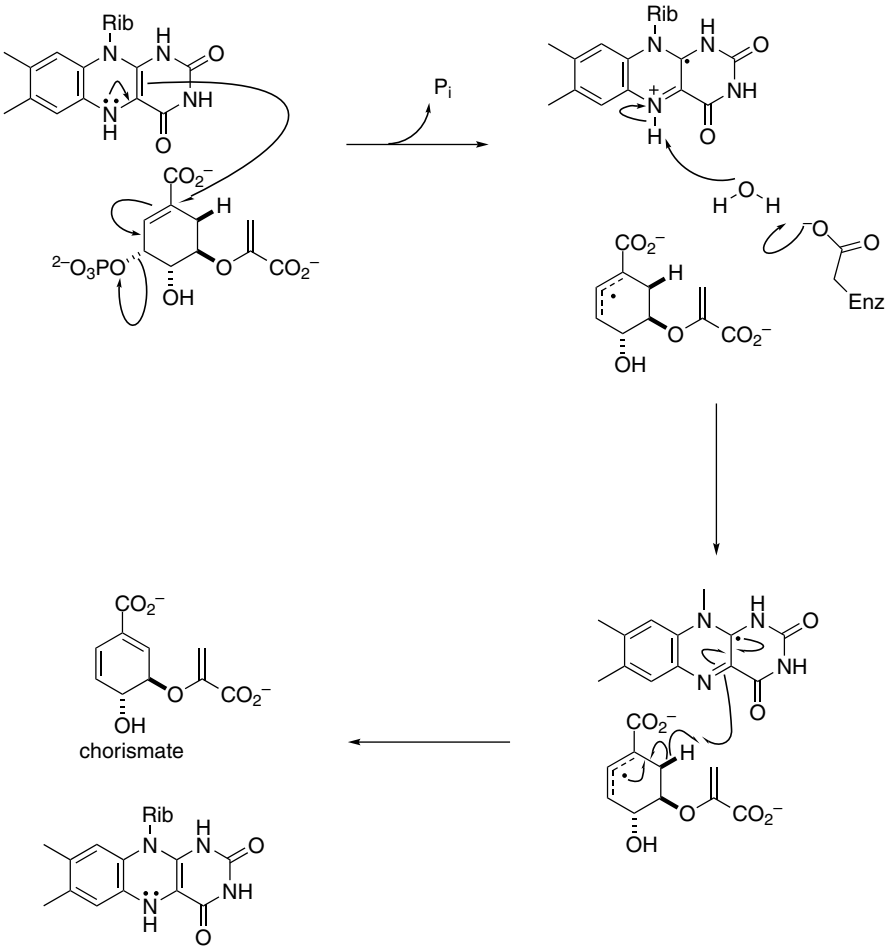

Figure 1.65 Proposed reaction mechanism for chorismate synthase.

1.8.3
Biosynthesis of Tryptophan, Phenylalanine, and Tyrosine from Chorismate

From chorismate the pathway for the synthesis of aromatic amino acids branches to produce either anthranilate for tryptophan biosynthesis or prephenate, the precursor to both phenylalanine and tyrosine. Chorismate is also the precursor to a range of other aromatic metabolites (Figure 1.66).

1.8.3.1 Tryptophan Biosynthesis

Anthranilate synthase catalyses the first committed step in the biosynthesis of tryptophan from chorismate [263–265]. This enzyme is one of a group of chorismate utilizing enzymes that are predicted to share many mechanistic features and are likely to have common evolutionary origins (Figure 1.67) [266–268]. The first step is 1,4-nucleophilic substitution by ammonia. This is followed by elimination of pyruvate. The ammonia used in this reaction is generated *in situ* by a glutamine amidotransferase.

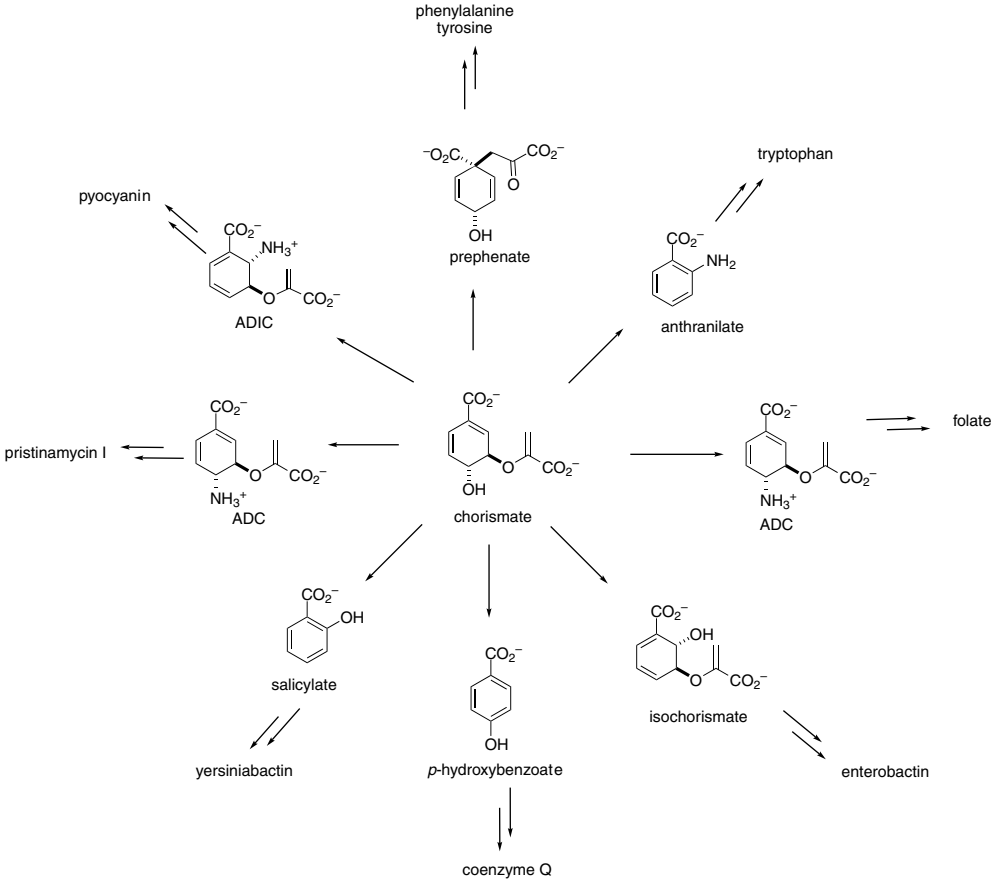

Figure 1.66 Multiple end-products generated from chorismate.

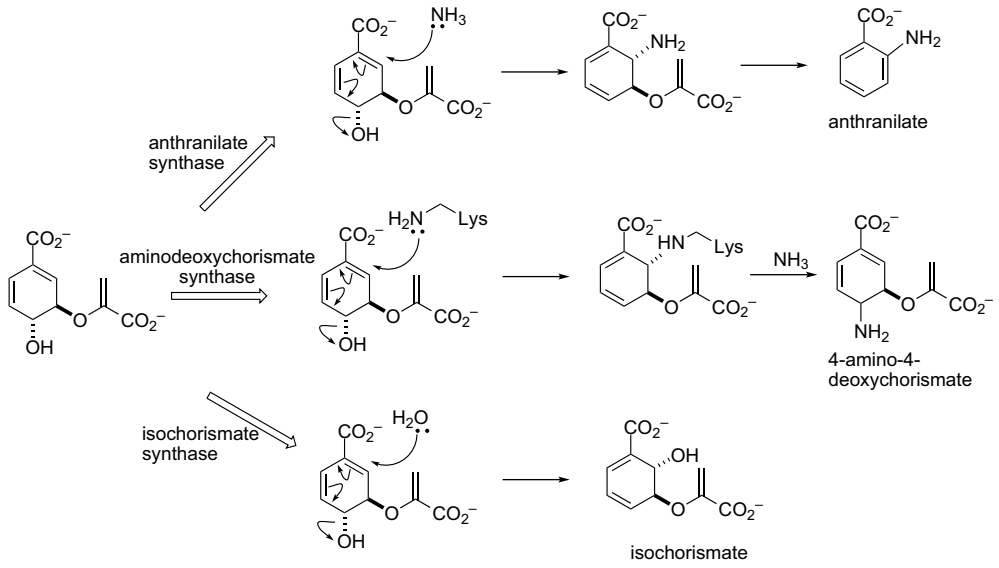

Figure 1.67 Related enzymatic reactions using chorismate as a substrate.

The indole ring of tryptophan is created by the next three steps of the pathway (Figure 1.68). A ribose moiety is first tethered to anthranilate, in a reaction catalyzed by phosphoribosyl anthranilate synthase [269, 270]. Following isomerization of phosphoribosyl anthranilate involving an Amadori rearrangement (Figure 1.69), the indole ring is constructed by intramolecular electrophilic substitution. This reaction chemistry is analogous to that observed for histidine biosynthesis, as described below [271, 272].

The final step in tryptophan production is catalyzed by the tryptophan synthase complex [273]. This enzyme has attracted a great deal of attention and been extensively reviewed as the one of the first enzymes to be discovered that catalyzes two distinct reactions at independent active sites (in the α- and β-domains) that are connected via an internal tunnel [274]. This was the first well-documented example of substrate channeling in amino acid biosynthesis. The reaction chemistry is relatively straightforward; glyceraldehyde 3-phosphate is eliminated in the α-tryptophan synthase reaction, producing indole, which is channeled to the second active site (Figure 1.70). In the PLP-dependent β-reaction, serine undergoes nucleophilic displacement of water by indole via an elimination–addition mechanism typical of β-substitution reactions of PLP (Box 1.3). The nett result is the generation of tryptophan (Figure 1.68).

1.8.3.2 **Phenylalanine and Tyrosine Biosynthesis**

Prephenate is formed by the reaction catalyzed by chorimate mutase (Figure 1.71) [275]. This is the only known example of a Claisen rearrangement

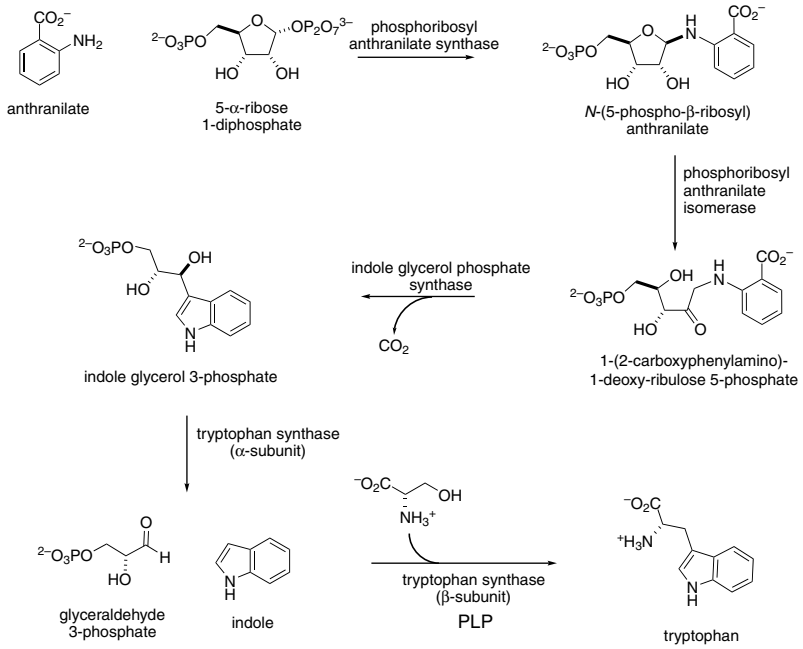

Figure 1.68 Biosynthesis of tryptophan from anthranilate.

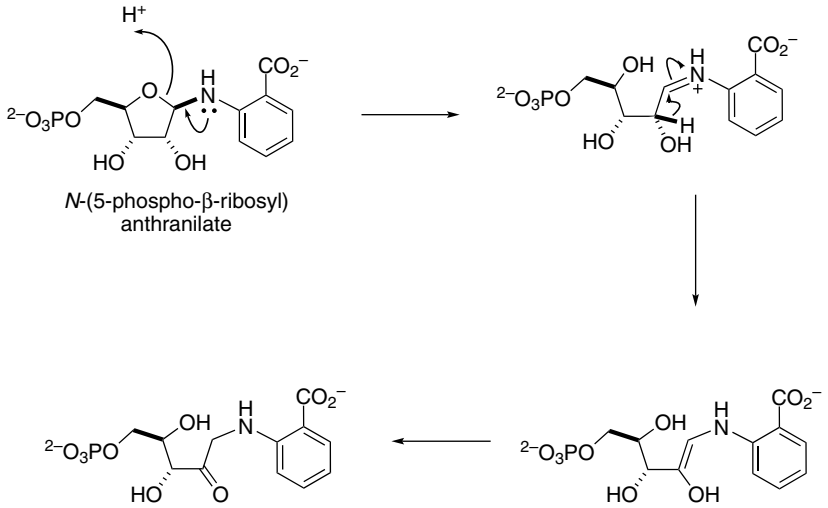

Figure 1.69 Amadori rearrangement catalyzed by indole glycerol phosphate synthase.

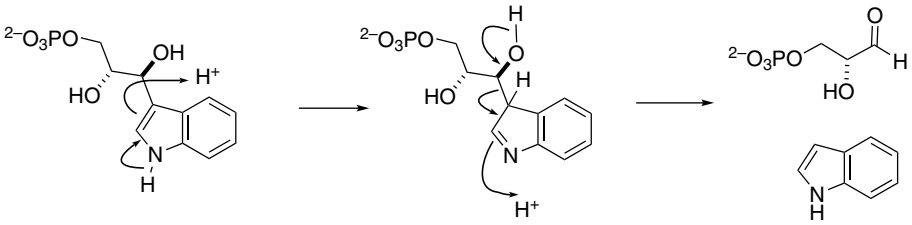

Figure 1.70 Generation of indole via a retro-aldol reaction catalyzed by the α-subunit of tryptophan synthase.

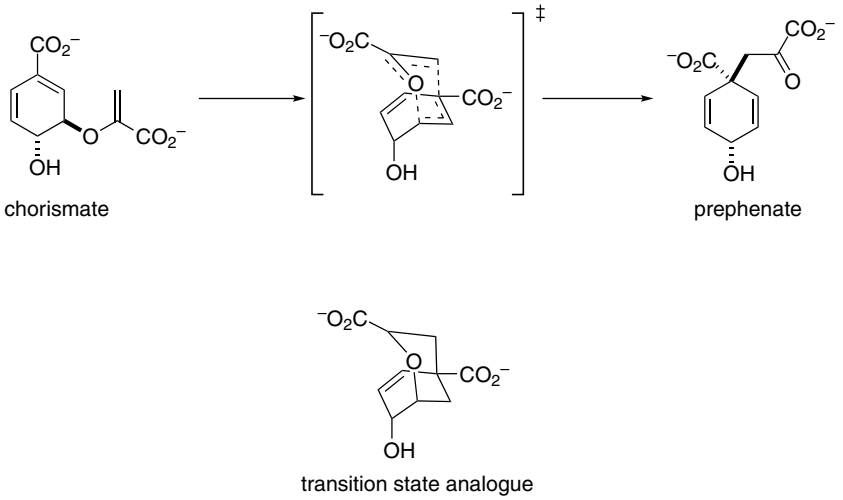

Figure 1.71 Reaction catalyzed by chorismate mutase.

reaction in primary metabolism and one of the few enzyme-catalyzed pericyclic reactions. Chorismate mutase can be effectively inhibited with a transition state inhibitor, and the activity of the enzyme is often subject to inhibition by tyrosine and/or phenylalanine as part of regulation of the pathway.

From prephenate there are a number of alternative pathways to aromatic metabolites (Figure 1.72). Tyrosine is produced by a combination of oxidation and transamination reactions, whereas phenylalanine is produced by dehydration and transamination. As the order of these reactions can vary there are usually two pathways for tyrosine and phenylalanine generation [276–279].

1.8.4
Histidine Biosynthesis

Histidine is synthesized in eight steps from precursors phosphoribosyl pyrophosphate (PRPP) and ATP [280, 281]. The reaction chemistry for the formation of

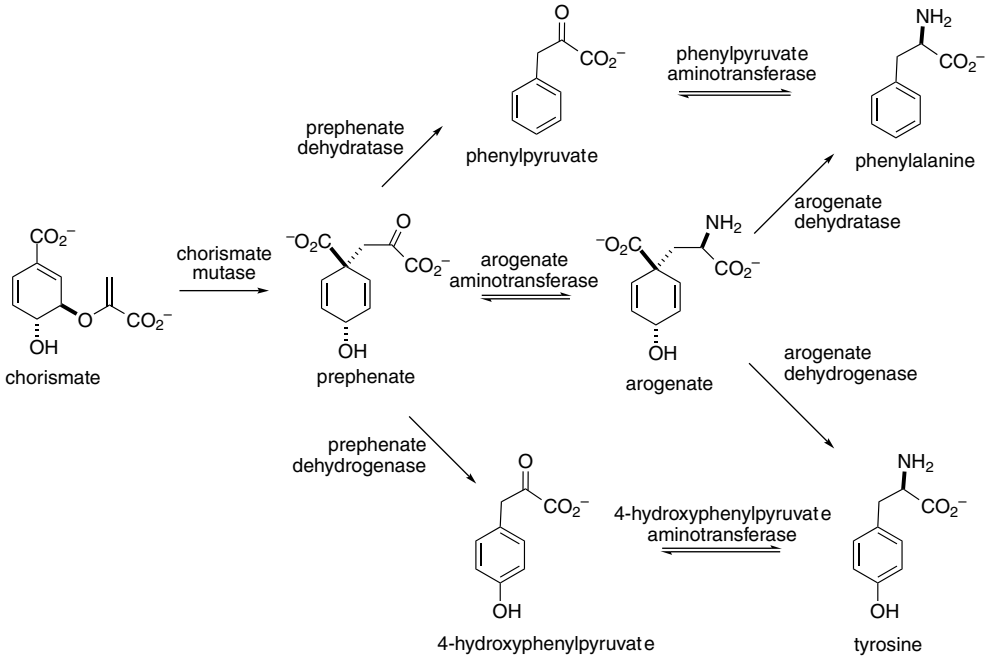

Figure 1.72 Pathways to phenylalanine and tyrosine.

histidine has distinct parallels with that of tryptophan biosynthesis. This relationship is apparent from the first step of the pathway with the reaction catalyzed by ATP-PRPP transferase (Figure 1.73) being analogous to the first step in tryptophan biosynthesis.

In many organisms the next two steps of the pathway – loss of diphosphate and hydrolysis of the adenine ring – are catalyzed by a single bifunctional protein, HisI

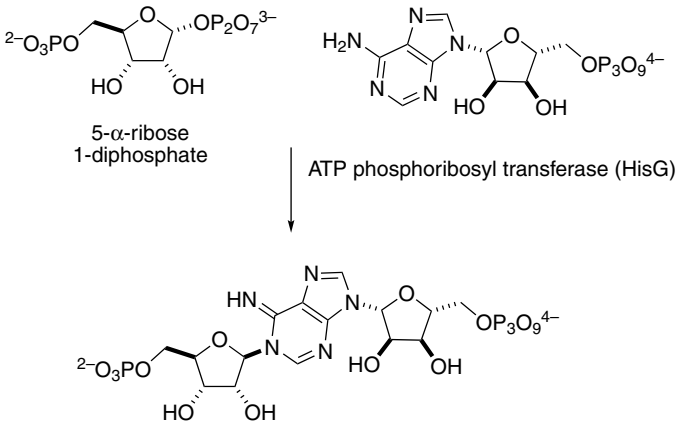

Figure 1.73 First step of histidine biosynthesis.

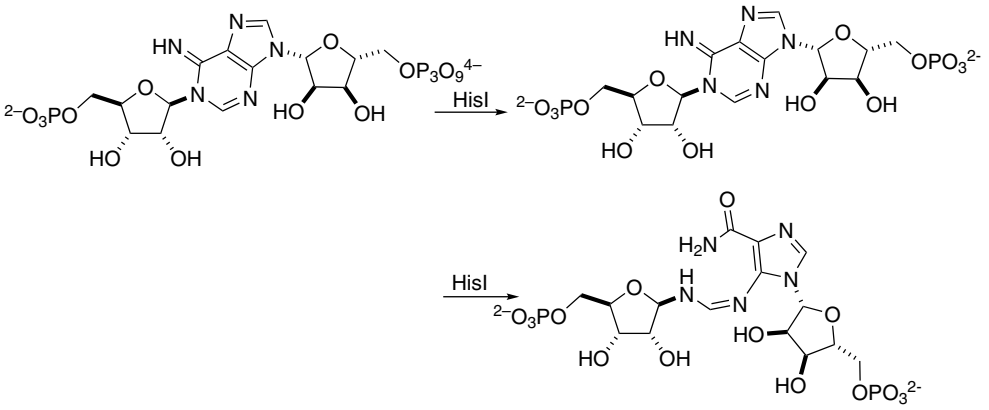

Figure 1.74 Two sequential reactions catalyzed by HisI.

(Figure 1.74). However, there are cases in Archaea and proteobacteria where there are two distinct proteins responsible for these transformations. It has been speculated that the genes giving rise to these enzyme activities were originally separate entities and gene fusion was part of their evolution [282–285].

Following hydrolysis of the adenine ring, the ribofuranose ring is opened by way of the Amadori rearrangement (Figure 1.75), again in a step analogous to the reaction catalyzed by phosphoribosyl anthranilate isomerase as part of tryptophan biosynthesis [286–288]. The overlap between these reactions of tryptophan and histidine biosynthesis is more than just common reaction chemistry. Gene complementation studies in *Streptomyces coelicolor* have shown that a single isomerase operates in both tryptophan and histidine pathways, with dual substrate specificity.

Following the Amadori rearrangement the indole ring is formed [289, 290]. This step also is particularly interesting from a molecular evolution perspective. Ammonia is required for this transformation and this is provided by the glutaminase, HisF. This step also leads to the generation of the purine intermediate aminoimidazole carboxamide ribonucleotide.

The final steps of histidine biosynthesis involve transformation of the glycerol phosphate tail of the intermediate imidazole glycerol 3-phosphate (Figure 1.76). The first step is a dehydration reaction catalyzed by imidazole glycerol phosphate dehydratase (HisB) [291, 292]. As with other enzyme activities in this pathway, this reaction is catalyzed by an enzyme that forms one part of a bifunctional enzyme in many organisms. The other function of the protein is to catalyze the dephosphorylation reaction in a later step in the pathway. Biochemical studies indicate that these two enzyme activities operate independently and therefore that the bifunctional protein is likely to have arisen by gene fusion [285].

The intervening step between dehydration and dephosphorylation of the glycerol phosphate side-chain is catalyzed by the PLP-dependent histidinol phosphate aminotransferase, HisC [293–295]. The final steps for histidine biosynthesis are the oxidation of the primary alcohol functionality to the carboxylate, in two sequential NAD^+-dependent oxidations.

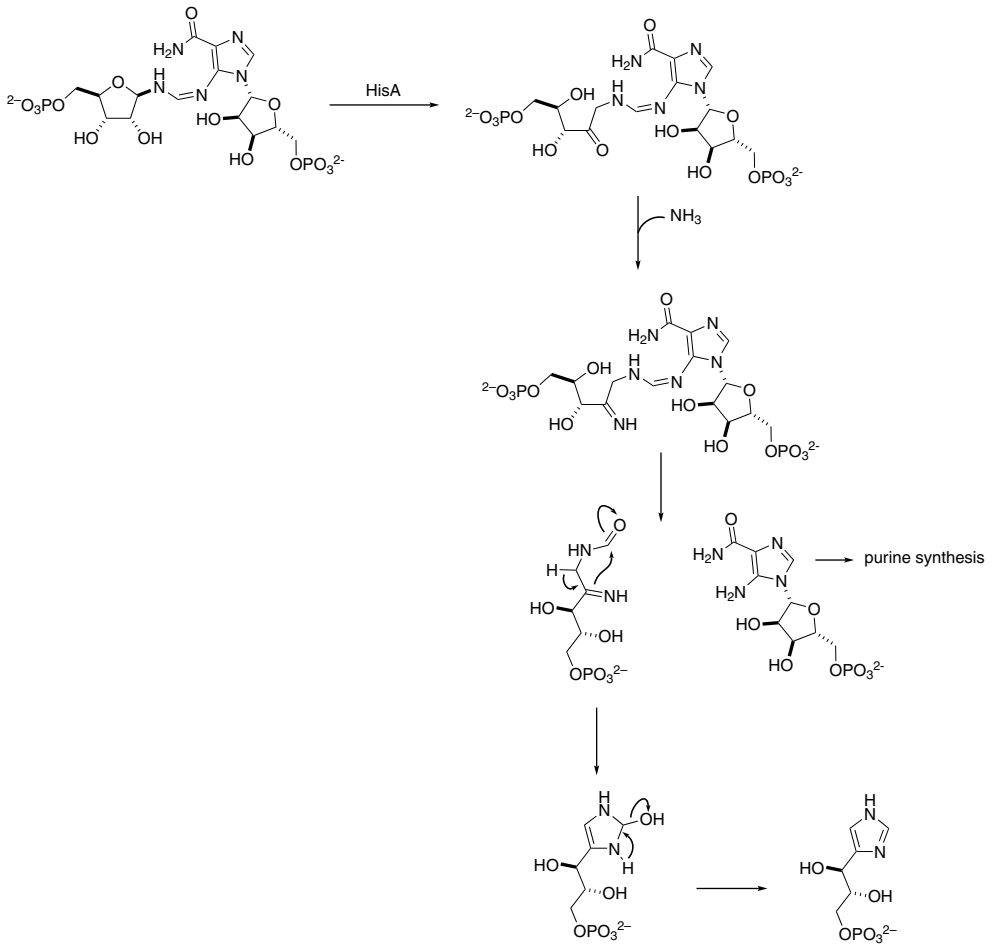

Figure 1.75 Amadori rearrangement and indole ring formation (catalyzed by HisA) reactions of histidine biosynthesis. This step requires ammonia generated by glutaminase, HisF.

1.9 Conclusions

This is an exciting time for research on amino acid biosynthesis. Genome projects and bioinformatics are providing rich details on metabolic diversity and the tailoring of metabolism to particular contexts. Structural biology is providing ever more three-dimensional detail on biosynthetic enzymes that underpins continued insights into enzyme catalysis and provides critical information for the design of synthetic inhibitors of critical biosynthetic enzymes of target organisms. Furthermore, evolutionary studies are providing new catalysts for interesting chemical transforma-

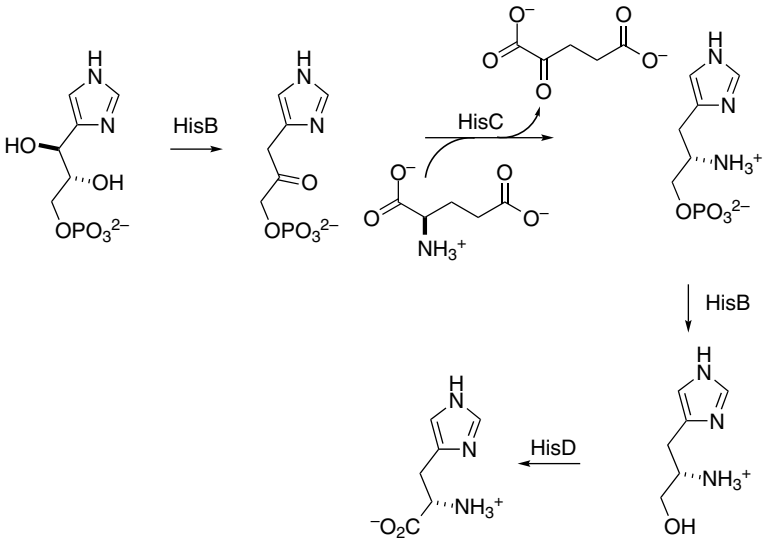

Figure 1.76 Final steps in the synthesis of histidine.

tions as well as new insights into the origins and development of this fascinating area of metabolism.

References

1 Garavelli, J.S. (2004) The RESID database of protein modifications as a resource and annotation tool. *Proteomics*, **4**, 1527–1533.

2 Copley, R.R. and Bork, P. (2000) Homology among (beta alpha)$_8$ barrels: implications for the evolution of metabolic pathways. *Journal of Molecular Biology*, **303**, 627–640.

3 Woese, C.R., Kandler, O., and Wheelis, M.L. (1990) Towards a natural system of organisms: proposal for the domains Archaea, Bacteria, and Eucarya. *Proceedings of the National Academy of Sciences of the United States of America*, **87**, 4576–4579.

4 Nishida, H. (2001) Evolution of amino acid biosynthesis and enzymes with broad substrate specificity. *Bioinformatics*, **17**, 1224–1225.

5 Shinivasan, V., Morowitz, H., and Smith, E. (2008) Essential amino acids, from LUCA to LUCY. *Complexity*, **13**, 8–9.

6 Hudson, R.C. and Daniel, R.M. (1993) l-Glutamate dehydrogenases – distribution, properties and mechanism. *Comparative Biochemistry and Physiology B*, **106**, 767–792.

7 Smith, T.J., Peterson, P.E., Schmidt, T., Fang, J., and Stanley, C.A. (2001) Structures of bovine glutamate dehydrogenase complexes elucidate the mechanism of purine regulation. *Journal of Molecular Biology*, **307**, 707–720.

8 Helling, R.B. (1994) Why does *Escherichia coli* have two primary pathways for synthesis of glutamate. *Journal of Bacteriology*, **176**, 4664–4668.

9 Woods, D.R. and Reid, S.J. (1993) Recent developments on the regulation and structure of glutamine-synthetase enzymes from selected bacterial groups. *FEMS Microbiology Reviews*, **11**, 273–283.

10 Stadtman, E.R. (2001) The story of glutamine synthetase regulation. *The*

Journal of Biological Chemistry, **276**, 44357–44364.

11 Reitzer, L. (2003) Nitrogen assimilation and global regulation in *Escherichia coli*. *Annual Review of Microbiology*, **57**, 155–176.

12 Liaw, S.H., Pan, C., and Eisenberg, D. (1993) Feedback inhibition of fully unadenylylated glutamine-synthetase from *Salmonella typhimurium* by glycine, alanine, and serine. *Proceedings of the National Academy of Sciences of the United States of America*, **90**, 4996–5000.

13 Zalkin, H. and Smith, J.L. (1998) Enzymes utilizing glutamine as an amide donor. *Advances in Enzymology*, **72**, 87–144.

14 van den Heuvel, R.H.H., Curti, B., Vanoni, M.A., and Mattevi, A. (2004) Glutamate synthase: a fascinating pathway from L-glutamine to L-glutamate. *Cellular and Molecular Life Sciences*, **61**, 669–681.

15 Lea, P.J. and Miflin, B.J. (2003) Glutamate synthase and the synthesis of glutamate in plants. *Plant Physiology and Biochemistry*, **41**, 555–564.

16 Vanoni, M.A. and Curti, B. (1999) Glutamate synthase: a complex iron–sulfur flavoprotein. *Cellular and Molecular Life Sciences*, **55**, 617–638.

17 Stabile, H., Curti, B., and Vanoni, M.A. (2000) Functional properties of recombinant *Azospirillum brasilense* glutamate synthase, a complex iron–sulfur flavoprotein. *European Journal of Biochemistry*, **267**, 2720–2730.

18 Massiere, F. and Badet-Denisot, M.-A. (1998) The mechanism of glutamine-dependent amidotransferases. *Cellular and Molecular Life Sciences*, **54**, 205–222.

19 Binda, C., Bossi, R.T., Wakatsuki, S., Arzt, S., Coda, A., Curti, B., Vanoni, M.A., and Mattevi, A. (2000) Cross-talk and ammonia channeling between active centers in the unexpected domain arrangement of glutamate synthase. *Structure*, **8**, 1299–1308.

20 Raushel, F.M., Thoden, J.B., and Holden, H.M. (2003) Enzymes with molecular tunnels. *Accounts of Chemical Research*, **36**, 539–548.

21 van den Heuvel, R.H.H., Ferrari, D., Bossi, R.T., Ravasio, S., Curti, B., Vanoni, M.A., Florencio, F.J., and Mattevi, A. (2002) Structural studies on the synchronization of catalytic centers in glutamate synthase. *The Journal of Biological Chemistry*, **277**, 24579–24583.

22 Dossena, L., Curti, B., and Vanoni, M.A. (2007) Activation and coupling of the glutaminase and synthase reaction of glutamate synthase is mediated by E1013 of the ferredoxin-dependent enzyme, belonging to loop 4 of the synthase domain. *Biochemistry*, **46**, 4473–4485.

23 Christen, P. and Mehta, P.K. (2001) From cofactor to enzymes. The molecular evolution of pyridoxal-5′-phosphate-dependent enzymes. *Chemical Record*, **1**, 436–447.

24 Hayashi, H. (1995) Pyridoxal enzymes: mechanistic diversity and uniformity. *Journal of Biochemistry*, **118**, 463–473.

25 John, R.A. (1995) Pyridoxal phosphate-dependent enzymes. *Biochimica et Biophysica Acta – Protein Structure and Molecular Enzymology*, **1248**, 81–96.

26 Jansonius, J.N. (1998) Structure, evolution and action of vitamin B_6-dependent enzymes. *Current Opinion in Structural Biology*, **8**, 759–769.

27 Schneider, G., Käck, H., and Lindqvist, Y. (2000) The manifold of vitamin B6 dependent enzymes. *Structure*, **8**, R1–R6.

28 Ford, G.C., Eichele, G., and Jansonius, J.N. (1980) Three-dimensional structure of a pyridoxal-phosphate-dependent enzyme, mitochondrial aspartate-aminotransferase. *Proceedings of the National Academy of Sciences of the United States of America*, **77**, 2559–2563.

29 Borisov, V.V., Borisova, S.N., Sosfenov, N.I., and Vainshtein, B.K. (1980) Electron density map of chicken heart cytosol aspartate transaminase at 3.5 Å resolution. *Nature*, **284**, 189–190.

30 Kirsch, J.F., Eichele, G., Ford, G.C., Vincent, M.G., Jansonius, J.N., Gehring, H., and Christen, P. (1984) Mechanism of action of aspartate-aminotransferase proposed on the basis of its spatial structure. *Journal of Molecular Biology*, **174**, 497–525.

31 Kochhar, S., Finlayson, W.L., Kirsch, J.F., and Christen, P. (1987) The stereospecific labilization of the C-4′ pro-*S* hydrogen of pyridoxamine 5′-phosphate is abolished

in (Lys258Ala) aspartate-aminotransferase. *The Journal of Biological Chemistry*, **262**, 11446–11448.

32 Dunathan, H.C. (1966) Conformation and reaction specificity in pyridoxal phosphate enzymes. *Proceedings of the National Academy of Sciences of the United States of America*, **55**, 712–716.

33 Matthews, R.G. and Drummond, J.T. (1990) Providing one-carbon units for biological methylations: mechanistic studies on serine hydroxymethyltransferase, methylenetetrahydrofolate reductase, and methyltetrahydrofolate-homocysteine methyltransferase. *Chemical Reviews*, **90**, 1275–1290.

34 Cronin, C.N. and Kirsch, J.F. (1988) Role of arginine-292 in the substrate-specificity of aspartate-aminotransferase as examined by site-directed mutagenesis. *Biochemistry*, **27**, 4572–4579.

35 Eliot, A.C. and Kirsch, J.F. (2004) Pyridoxal phosphate enzymes: Mechanistic, structural, and evolutionary considerations. *Annual Review of Biochemistry*, **73**, 383–415.

36 Okamoto, A., Nakai, Y., Hayashi, H., Hirotsu, K., and Kagamiyama, H. (1998) Crystal structures of *Paracoccus denitrificans* aromatic amino acid aminotransferase: a substrate recognition site constructed by rearrangement of hydrogen bond network. *Journal of Molecular Biology*, **280**, 443–461.

37 Okamoto, A., Ishii, S., Hirotsu, K., and Kagamiyama, H. (1999) The active site of *Paracoccus denitrificans* aromatic amino acid aminotransferase has contrary properties: flexibility and rigidity. *Biochemistry*, **38**, 1176–1184.

38 Onuffer, J.J. and Kirsch, J.F. (1995) Redesign of the substrate specificity of *Escherichia coli* aspartate aminotransferase to that of *Escherichia coli* tyrosine aminotransferase by homology modeling and site-directed mutagenesis. *Protein Science*, **4**, 1750–1757.

39 Malashkevich, V.N., Onuffer, J.J., Kirsch, J.F., and Jansonius, J.N. (1995) Alternating arginine-modulated substrate specificity in an engineered tyrosine aminotransferase. *Nature Structural Biology*, **2**, 548–553.

40 Penning, T.M. and Jez, J.M. (2001) Enzyme redesign. *Chemical Reviews*, **101**, 3027–3046.

41 Jäckel, C., Kast, P., and Hilvert, D. (2008) Protein design by directed evolution. *Annual Review of Biophysics*, **37**, 153–173.

42 Rothman, S.C. and Kirsch, J.F. (2003) How does an enzyme evolved *in vitro* compare to naturally occurring homologs possessing the targeted function? Tyrosine aminotransferase from aspartate aminotransferase. *Journal of Molecular Biology*, **327**, 593–608.

43 Yano, T., Oue, S., and Kagamiyama, H. (1998) Directed evolution of an aspartate aminotransferase with new substrate specificities. *Proceedings of the National Academy of Sciences of the United States of America*, **95**, 5511–5515.

44 Oue, S., Okamoto, A., Yano, T., and Kagamiyama, H. (1999) Redesigning the substrate specificity of an enzyme by cumulative effects of the mutations of non-active site residues. *The Journal of Biological Chemistry*, **274**, 2344–2349.

45 Oue, S., Okamoto, A., Yano, T., and Kagamiyama, H. (2000) Cocrystallization of a mutant aspartate aminotransferase with a C5-dicarboxylic substrate analog: structural comparison with the enzyme–C4-dicarboxylic analog complex. *Journal of Biochemistry*, **127**, 337–343.

46 Ura, H., Harata, K., Matsui, I., and Kuramitsu, S. (2001) Temperature dependence of the enzyme–substrate recognition mechanism. *Journal of Biochemistry*, **129**, 173–178.

47 Matsui, I., Matsui, E., Sakai, Y., Kikuchi, H., Kawarabayasi, Y., Ura, H., Kawaguchi, S., Kuramitsu, S., and Harata, K. (2000) The molecular structure of hyperthermostable aromatic aminotransferase with novel substrate specificity from *Pyrococcus horikoshii*. *The Journal of Biological Chemistry*, **275**, 4871–4879.

48 Goto, M., Miyahara, I., Hayashi, H., Kagamiyama, H., and Hirotsu, K. (2003) Crystal structures of branched-chain amino acid aminotransferase complexed with glutamate and glutarate: true reaction intermediate and double substrate recognition of the enzyme. *Biochemistry*, **42**, 3725–3733.

49 Schlösser, T., Gätgens, C., Weber, U., and Stahmann, K.-P. (2004) Alanine: glyoxylate aminotransferase of *Saccharomyces cerevisiae*-encoding gene AGX1 and metabolic significance. *Yeast*, **21**, 63–73.

50 Takada, Y. and Noguchi, T. (1985) Characteristics of alanine glyoxylate aminotransferase from *Saccharomyces cerevisiae*, a regulatory enzyme in the glyoxylate pathway of glycine and serine biosynthesis from tricarboxylic acid-cycle intermediates. *Biochemical Journal*, **231**, 157–163.

51 Monschau, N., Stahmann, K.-P., Sahm, H., McNeil, J.B., and Bognar, A.L. (1997) Identification of *Saccharomyces cerevisiae* GLY1 as a threonine aldolase: a key enzyme in glycine biosynthesis. *FEMS Microbiology Letters*, **150**, 55–60.

52 Liu, J.-Q., Nagata, S., Dairi, T., Misono, H., Shimizu, S., and Yamada, H. (1997) The GLY1 gene of *Saccharomyces cerevisiae* encodes a low-specific L-threonine aldolase that catalyzes cleavage of L-allo-threonine and L-threonine to glycine. *European Journal of Biochemistry*, **245**, 289–293.

53 Melendez-Hevia, E., de Paz-Lugo, P., Cornish-Bowden, A., and Cardenas, M.L. (2009) A weak link in metabolism: the metabolic capacity for glycine biosynthesis does not satisfy the need for collagen synthesis. *Journal of Biosciences*, **34**, 853–872.

54 Renwick, S.B., Snell, K., and Baumann, U. (1998) The crystal structure of human cytosolic serine hydroxymethyltransferase: a target for cancer chemotherapy. *Structure*, **6**, 1105–1116.

55 Rajaram, V., Bhavan, B.S., Kaul, P., Prakash, V., Rao, N.A., Savithri, H.S., and Murthyl, M.R.N. (2007) Structure determination and biochemical studies on *Bacillus stearothermophilus* E53Q serine hydroxymethyltransferase and its complexes provide insights on function and enzyme memory. *FEBS Journal*, **274**, 4148–4160.

56 Bhavani, S., Trivedi, V., Jala, V.R., Subramanya, H.S., Kaul, P., Prakash, V., Rao, N.A., and Savithri, H.S. (2005) Role of Lys-226 in the catalytic mechanism of *Bacillus stearothermophilus* serine hydroxymethyltransferase – crystal structure and kinetic studies. *Biochemistry*, **44**, 6929–6937.

57 Szebenyi, D.M.E., Musayev, F.N., di Salvo, M.L., Safo, M.K., and Schirch, V. (2004) Serine hydroxymethyltransferase: role of Glu75 and evidence that serine is cleaved by a retroaldol mechanism. *Biochemistry*, **43**, 6865–6876.

58 Trivedi, V., Gupta, A., Jala, V.R., Saravanan, P., Rao, G.S.J., Rao, N.A., Savithri, H.S., and Subramanya, H.S. (2002) Crystal structure of binary and ternary complexes of serine hydroxymethyltransferase from *Bacillus stearothermophilus* – insights into the catalytic mechanism. *The Journal of Biological Chemistry*, **277**, 17161–17169.

59 Stauffer, G.V. (1996) Biosynthesis of serine, glycine, and one-carbon unit, in *Escherichia coli and Salmonella: Cellular and Molecular Biology*, vol. I (eds F.C. Neidhardt, R. CurtissIII, J.L. Ingraham, E.C.C. Lin, K.B. Low, B. Magasanik, W.S. Reznikoff, M. Riley, M. Schaechter, and H.E. Umbarger), 2nd edn, American Society for Microbiology, Washington, DC, pp. 506–513.

60 Burton, R.L., Chen, S., Xu, X.L., and Grant, G.A. (2009) Transient kinetic analysis of the interaction of L-serine with *Escherichia coli*D-3-phosphoglycerate dehydrogenase reveals the mechanism of V-type regulation and the order of effector binding. *Biochemistry*, **48**, 12242–12251.

61 Wang, W., Cho, H.S., Kim, R., Jancarik, J., Yokota, H., Nguyen, H.H., Grigoriev, I.V., Wemmer, D.E., and Kim, S.-H. (2002) Structural characterization of the reaction pathway in phosphoserine phosphatase: crystallographic "snapshots" of intermediate states. *Journal of Molecular Biology*, **319**, 421–431.

62 Singh, S.K., Yang, K., Karthikeyan, S., Huynh, T., Zhang, X.J., Phillips, M.A., and Zhang, H. (2004) The *thrH* gene product of *Pseudomonas aeruginosa* is a dual activity enzyme with a novel phosphoserine: homoserine phosphotransferase activity. *The Journal of Biological Chemistry*, **279**, 13166–13173.

63 Feldman-Salit, A., Wirtz, M., Hell, R., and Wade, R.C. (2009) A mechanistic model of

the cysteine synthase complex. *Journal of Molecular Biology*, **386**, 37–59.

64 Mino, K. and Ishikawa, K. (2003) Characterization of a novel thermostable *O*-acetylserine sulfhydrylase from *Aeropyrum pernix* K1. *Journal of Bacteriology*, **185**, 2277–2284.

65 Rabeh, W.M. and Cook, P.F. (2004) Structure and mechanism of *O*-acetylserine sulfhydrylase. *The Journal of Biological Chemistry*, **279**, 26803–26806.

66 Tai, C.-H. and Cook, P.F. (2001) Pyridoxal 5′-phosphate-dependent α,β-elimination reactions: mechanism of *O*-acetylserine sulfhydrylase. *Accounts of Chemical Research*, **34**, 49–59.

67 Su, D., Hohn, M.J., Palioura, S., Sherrer, R.L., Yuan, J., Söll, D., and O'Donoghue, P. (2009) How an obscure archaeal gene inspired the discovery of selenocysteine biosynthesis in humans. *IUBMB Life*, **61**, 35–39.

68 Cole, S.T., Brosch, R., Parkhill, J., Garnier, T., Churcher, C., Harris, D., Gordon, S.V., Eiglmeier, K., Gas, S., Barry, C.E., Tekaia, F., Badcock, K., Basham, D., Brown, D., Chillingworth, T., Connor, R., Davies, R., Devlin, K., Feltwell, T., Gentles, S., Hamlin, N., Holroyd, S., Hornsby, T., Jagels, K., Krogh, A., McLean, J., Moule, S., Murphy, L., Oliver, K., Osborne, J., Quail, M.A., Rajandream, M.-A., Rogers, J., Rutter, S., Seeger, K., Skelton, J., Squares, R., Squares, S., Sulston, J.E., Taylor, K., Whitehead, S., and Barrell, B.G. (1998) Deciphering the biology of *Mycobacterium tuberculosis* from the complete genome sequence. *Nature*, **393** 537–544.

69 Schnell, R., Oehlmann, W., Singh, M., and Schneider, G. (2007) Structural insights into catalysis and inhibition of *O*-acetylserine sulfhydrylase from *Mycobacterium tuberculosis*:crystal structures of the enzyme α-aminoacrylate intermediate and an enzyme–inhibitor complex. *The Journal of Biological Chemistry*, **282**, 23473–23481.

70 Park, J.-H., Dorrestein, P.C., Zhai, H., Kinsland, C., McLafferty, F.W., and Begley, T.P. (2003) Biosynthesis of the thiazole moiety of thiamin pyrophosphate (vitamin B_1). *Biochemistry*, **42**, 12430–12438.

71 Burns, K.E., Baumgart, S., Dorrestein, P.C., Zhai, H., McLafferty, F.W., and Begley, T.P. (2005) Reconstitution of a new cysteine biosynthetic pathway in *Mycobacterium tuberculosis*. *Journal of the American Chemical Society*, **127**, 11602–11603.

72 Ågren, D., Schnell, R., Oehlmann, W., Singh, M., and Schneider, G. (2008) Cysteine synthase (CysM) of *Mycobacterium tuberculosis* is an *O*-phosphoserine sulfhydrylase: evidence for an alternative cysteine biosynthesis pathway in Mycobacteria. *The Journal of Biological Chemistry*, **283**, 31567–31574.

73 Sauerwald, A., Zhu, W.H., Major, T.A., Roy, H., Palioura, S., Jahn, D., Whitman, W.B., Yates, J.R., Ibba, M., and Söll, D. (2005) RNA-dependent cysteine biosynthesis in archaea. *Science*, **307**, 1969–1972.

74 Cone, J.E., Del Rio, M.R., Davis, J.N., and Stadtman, T.C. (1976) Chemical characterization of selenoprotein component of clostridial glycine reductase: identification of selenocysteine as the organoselenium moiety. *Proceedings of the National Academy of Sciences of the United States of America*, **73**, 2659–2663.

75 Leinfelder, W., Zehelein, E., Mandrandberthelot, M.A., and Bock, A. (1988) Gene for a novel transfer-RNA species that accepts L-serine and cotranslationally inserts selenocysteine. *Nature*, **331**, 723–725.

76 Mullins, L.S., Hong, S.-B., Gibson, G.E., Walker, H., Stadtman, T.C., and Raushel, F.M. (1997) Identification of a phosphorylated enzyme intermediate in the catalytic mechanism for selenophosphate synthetase. *Journal of the American Chemical Society*, **119**, 6684–6685.

77 Midelfort, C.F. and Rose, I.A. (1976) A stereochemical method for detection of ATP terminal phosphate transfer in enzymatic reactions. Glutamine synthetase. *The Journal of Biological Chemistry*, **251**, 5881–5887.

78 Forchhammer, K. and Böck, A. (1991) Selenocysteine synthase from *Escherichia coli*. Analysis of the reaction sequence. *The Journal of Biological Chemistry*, **266**, 6324–6328.

79 Kernebeck, T., Lohse, A.W., and Grötzinger, J. (2001) A bioinformatical approach suggests the function of the autoimmune hepatitis target antigen soluble liver antigen/liver pancreas. *Hepatology*, **34**, 230–233.

80 Ganichkin, O.M., Xu, X.-M., Carlson, B.A., Mix, H., Hatfield, D.L., Gladyshev, V.N., and Wahl, M.C. (2008) Structure and catalytic mechanism of eukaryotic selenocysteine synthase. *The Journal of Biological Chemistry*, **283**, 5849–5865.

81 Araiso, Y., Palioura, S., Ishitani, R., Sherrer, R.L., O'Donoghue, P., Yuan, J., Oshikane, H., Domae, N., DeFranco, J., Söll, D., and Nureki, O. (2008) Structural insights into RNA-dependent eukaryal and archaeal selenocysteine formation. *Nucleic Acids Research*, **36**, 1187–1199.

82 Xu, X.-M., Carlson, B.A., Mix, H., Zhang, Y., Saira, K., Glass, R.S., Berry, M.J., Gladyshev, V.N., and Hatfield, D.L. (2007) Biosynthesis of selenocysteine on its tRNA in eukaryotes. *PLoS Biology*, **5**, 96–105.

83 Yuan, J., Palioura, S., Salazar, J.C., Su, D., O'Donoghue, P., Hohn, M.J., Cardoso, A.M., Whitman, W.B., and Söll, D. (2006) RNA-dependent conversion of phosphoserine forms selenocysteine in eukaryotes and archaea. *Proceedings of the National Academy of Sciences of the United States of America*, **103**, 18923–18927.

84 Schmitt, E., Panvert, M., Blanquet, S., and Mechulam, Y. (1998) Crystal structure of methionyl-$tRNA_f^{Met}$ transformylase complexed with the initiator formylmethionyl-$tRNA_f^{Met}$. *The EMBO Journal*, **17**, 6819–6826.

85 Curnow, A.W., Hong, K.-W., Yuan, R., Kim, S.-I., Martins, O., Winkler, W., Henkin, T.M., and Söll, D. (1997) Glu-$tRNA^{Gln}$ amidotransferase: a novel heterotrimeric enzyme required for correct decoding of glutamine codons during translation. *Proceedings of the National Academy of Sciences of the United States of America*, **94**, 11819–11826.

86 Ibba, M. and Soll, D. (2000) Aminoacyl-tRNA synthesis. *Annual Review of Biochemistry*, **69**, 617–650.

87 Humbert, R. and Simoni, R.D. (1980) Genetic and biochemical studies demonstrating a second gene coding for asparagine synthetase in *Escherichia coli*. *Journal of Bacteriology*, **142**, 212–220.

88 Cedar, H. and Schwartz, J.H. (1969) Asparagine synthetase of *Escherichia coli* I. Biosynthetic role of the enzyme, purification, and characterization of the reaction products. *The Journal of Biological Chemistry*, **244**, 4112–4121.

89 Tesson, A.R., Soper, T.S., Ciustea, M., and Richards, N.G.J. (2003) Revisiting the steady state kinetic mechanism of glutamine-dependent asparagine synthetase from *Escherichia coli*. *Archives of Biochemistry and Biophysics*, **413**, 23–31.

90 Larsen, T.M., Boehlein, S.K., Schuster, S.M., Richards, N.G.J., Thoden, J.B., Holden, H.M., and Rayment, I. (1999) Three-dimensional structure of *Escherichia coli* asparagine synthetase B: a short journey from substrate to product. *Biochemistry*, **38**, 16146–16157.

91 Richards, N.G.J. and Kilberg, M.S. (2006) Asparagine synthetase chemotherapy. *Annual Review of Biochemistry*, **75**, 629–654.

92 Koizumi, M., Hiratake, J., Nakatsu, T., Kato, H., and Oda, J. (1999) A potent transition-state analogue inhibitor of *Escherichia coli* asparagine synthetase A. *Journal of the American Chemical Society*, **121**, 5799–5800.

93 Zhang, Y., Thiele, I., Weekes, D., Li, Z., Jaroszewski, L., Ginalski, K., Deacon, A.M., Wooley, J., Lesley, S.A., Wilson, I.A., Palsson, B., Osterman, A., and Godzik, A. (2009) Three-dimensional structural view of the central metabolic network of *Thermotoga maritima*. *Science*, **325**, 1544–1549.

94 Curien, G., Biou, V., Mas-Droux, C., Robert-Genthon, M., Ferrer, J.-L., and Dumas, R. (2008) Amino acid biosynthesis: new architectures in allosteric enzymes. *Plant Physiology and Biochemistry*, **46**, 325–339.

95 Azevedo, R.A., Lancien, M., and Lea, P.J. (2006) The aspartic acid metabolic pathway, an exciting and essential

pathway in plants. *Amino Acids*, **30**, 143–162.

96 Liu, X., Pavlovsky, A.G., and Viola, R.E. (2008) The structural basis for allosteric inhibition of a threonine-sensitive aspartokinase. *The Journal of Biological Chemistry*, **283**, 16216–16225.

97 Hadfield, A., Shammas, C., Kryger, G., Ringe, D., Petsko, G.A., Ouyang, J., and Viola, R.E. (2001) Active site analysis of the potential antimicrobial target aspartate semialdehyde dehydrogenase. *Biochemistry*, **40**, 14475–14483.

98 Blanco, J., Moore, R.A., and Viola, R.E. (2003) Capture of an intermediate in the catalytic cycle of L-aspartate-β-semialdehyde dehydrogenase. *Proceedings of the National Academy of Sciences of the United States of America*, **100**, 12613–12617.

99 Blanco, J., Moore, R.A., Kabaleeswaran, V., and Viola, R.E. (2003) A structural basis for the mechanism of aspartate-β-semialdehyde dehydrogenase from *Vibrio cholerae*. *Protein Science*, **12**, 27–33.

100 Holland, M.J. and Westhead, E.W. (1973) Purification and characterization of aspartic beta-semialdehyde dehydrogenase from yeast and purification of an isoenzyme of glyceraldehyde-3-phosphate dehydrogenase. *Biochemistry*, **12**, 2264–2270.

101 Geck, M.K. and Kirsch, J.F. (1999) A novel, definitive test for substrate channeling illustrated with the aspartate aminotransferase/malate dehydrogenase system. *Biochemistry*, **38**, 8032–8037.

102 James, C.L. and Viola, R.E. (2002) Production and characterization of bifunctional enzymes. Substrate channeling in the aspartate pathway. *Biochemistry*, **41**, 3726–3731.

103 DeLaBarre, B., Thompson, P.R., Wright, G.D., and Berghuis, A.M. (2000) Crystal structures of homoserine dehydrogenase suggest a novel catalytic mechanism for oxidoreductases. *Nature Structural Biology*, **7**, 238–244.

104 Jacques, S.L., Ejim, L.J., and Wright, G.D. (2001) Homoserine dehydrogenase from *Saccharomyces cerevisiae*: kinetic mechanism and stereochemistry of hydride transfer. *Biochimica et Biophysica Acta – Protein Structure and Molecular Enzymology*, **1544**, 42–54.

105 Huo, X. and Viola, R.E. (1996) Substrate specificity and identification of functional groups of homoserine kinase from *Escherichia coli*. *Biochemistry*, **35**, 16180–16185.

106 Mirza, I.A., Nazi, I., Korczynska, M., Wright, G.D., and Berghuis, A.M. (2005) Crystal structure of homoserine transacetylase from *Haemophilus influenzae* reveals a new family of α/β-hydrolases. *Biochemistry*, **44**, 15768–15773.

107 Zubieta, C., Arkus, K.A.J., Cahoon, R.E., and Jez, J.M. (2008) A single amino acid change is responsible for evolution of acyltransferase specificity in bacterial methionine biosynthesis. *The Journal of Biological Chemistry*, **283**, 7561–7567.

108 Laber, B., Gerbling, K.-P., Harde, C., Neff, K.-H., Nordhoff, E., and Pohlenz, H.-D. (1994) Mechanisms of interaction of *Escherichia coli* threonine synthase with substrates and inhibitors. *Biochemistry*, **33**, 3413–3423.

109 Laber, B., Maurer, W., Hanke, C., Gräfe, S., Ehlert, S., Messerschmidt, A., and Clausen, T. (1999) Characterization of recombinant *Arabidopsis thaliana* threonine synthase. *European Journal of Biochemistry*, **263**, 212–221.

110 Curien, G., Job, D., Douce, R., and Dumas, R. (1998) Allosteric activation of *Arabidopsis* threonine synthase by *S*-adenosylmethionine. *Biochemistry*, **37**, 13212–13221.

111 Thomazeau, K., Curien, G., Dumas, R., and Biou, V. (2001) Crystal structure of threonine synthase from *Arabidopsis thaliana*. *Protein Science*, **10**, 638–648.

112 Omi, R., Goto, M., Miyahara, I., Mizuguchi, H., Hayashi, H., Kagamiyama, H., and Hirotsu, K. (2003) Crystal structures of threonine synthase from *Thermus thermophilus* HB8 – conformational change, substrate recognition, and mechanism. *The Journal of Biological Chemistry*, **278**, 46035–46045.

113 Garrido-Franco, M., Ehlert, S., Messerschmidt, A., Marinkovic, S., Huber, R., Laber, B., Bourenkov, G.P., and

Clausen, T. (2002) Structure and function of threonine synthase from yeast. *The Journal of Biological Chemistry*, **277**, 12396–12405.

114 Sassetti, C.M. and Rubin, E.J. (2003) Genetic requirements for mycobacterial survival during infection. *Proceedings of the National Academy of Sciences of the United States of America*, **100**, 12989–12994.

115 Covarrubias, A.S., Högbom, M., Bergfors, T., Carroll, P., Mannerstedt, K., Oscarson, S., Parish, T., Jones, T.A., and Mowbray, S.L. (2008) Structural, biochemical, and *in vivo* investigations of the threonine synthase from *Mycobacterium tuberculosis*. *Journal of Molecular Biology*, **381**, 622–633.

116 Clausen, T., Huber, R., Prade, L., Wahl, M.C., and Messerschmidt, A. (1998) Crystal structure of *Escherichia coli* cystathionine γ-synthase at 1.5 Å resolution. *The EMBO Journal*, **17**, 6827–6838.

117 Kong, Y., Wu, D., Bai, H., Han, C., Chen, J., Chen, L., Hu, L., Jiang, H., and Shen, X. (2008) Enzymatic characterization and inhibitor discovery of a new cystathionine γ-synthase from *Helicobacter pylori*. *Journal of Biochemistry*, **143**, 59–68.

118 Clausen, T., Huber, R., Laber, B., Pohlenz, H.-D., and Messerschmidt, A. (1996) Crystal structure of the pyridoxal-5′-phosphate dependent cystathionine β-lyase from *Escherichia coli* at 1.83 Å. *Journal of Molecular Biology*, **262**, 202–224.

119 Goulding, C.W., Postigo, D., and Matthews, R.G. (1997) Cobalamin-dependent methionine synthase is a modular protein with distinct regions for binding homocysteine, methyltetrahydrofolate, cobalamin, and adenosylmethionine. *Biochemistry*, **36**, 8082–8091.

120 Matthews, R.G., Koutmos, M., and Datta, S. (2008) Cobalamin-dependent and cobamide-dependent methyltransferases. *Current Opinion in Structural Biology*, **18**, 658–666.

121 Gonzalez, J.C., Peariso, K., PennerHahn, J.E., and Matthews, R.G. (1996) Cobalamin-independent methionine synthase from *Escherichia coli*: a zinc metalloenzyme. *Biochemistry*, **35**, 12228–12234.

122 Marco-Marin, C., Gil-Ortiz, F., Perez-Arellano, I., Cervera, J., Fita, I., and Rubio, V. (2007) A novel two-domain architecture within the amino acid kinase enzyme family revealed by the crystal structure of *Escherichia coli* glutamate 5-kinase. *Journal of Molecular Biology*, **367**, 1431–1446.

123 Hu, C.A., Delauney, A.J., and Verma, D.P. (1992) A bifunctional enzyme (δ-1-pyrroline-5-carboxylate synthetase) catalyzes the first two steps in proline biosynthesis in plants. *Proceedings of the National Academy of Sciences of the United States of America*, **89**, 9354–9358.

124 Turchetto-Zolet, A.C., Margis-Pinheiro, M., and Margis, R. (2009) The evolution of pyrroline-5-carboxylate synthase in plants: a key enzyme in proline synthesis. *Molecular Genetics and Genomics*, **281**, 87–97.

125 Costilow, R.N. and Laycock, L. (1971) Ornithine cyclase (deaminating) – purification of a protein that converts ornithine to proline and definition of optimal assay conditions. *The Journal of Biological Chemistry*, **246**, 6655–6660.

126 Graupner, M. and White, R.H. (2001) Methanococcus *jannaschii* generates L-proline by cyclization of L-ornithine. *Journal of Bacteriology*, **183**, 5203–5205.

127 Nocek, B., Chang, C., Li, H., Lezondra, L., Holzle, D., Collart, F., and Joachimiak, A. (2005) Crystal structures of δ-1-pyrroline-5-carboxylate reductase from human pathogens *Neisseria meningitides* and *Streptococcus pyogenes*. *Journal of Molecular Biology*, **354**, 91–106.

128 Caldovic, L. and Tuchman, M. (2003) N-Acetylglutamate and its changing role through evolution. *Biochemical Journal*, **372**, 279–290.

129 Fernandez-Murga, M.L., Gil-Ortiz, F., Llacer, J.L., and Rubio, V. (2004) Arginine biosynthesis in *Thermotoga maritima*: characterization of the arginine-sensitive *N*-acetyl-L-glutamate kinase. *Journal of Bacteriology*, **186**, 6142–6149.

130 Ramon-Maiques, S., Marina, A., Gil-Ortiz, F., Fita, I., and Rubio, V. (2002) Structure of acetylglutamate kinase, a key enzyme for arginine biosynthesis and a prototype for the amino acid kinase enzyme family, during catalysis. *Structure*, **10**, 329–342.

131 Cherney, L.T., Cherney, M.M., Garen, C.R., Niu, C., Moradian, F., and James, M.N.G. (2007) Crystal structure of *N*-acetyl-γ-glutamyl-phosphate reductase from *Mycobacterium tuberculosis* in complex with $NADP^+$. *Journal of Molecular Biology*, **367**, 1357–1369.

132 Rajaram, V., Prasuna, P.R., Savithri, H.S., and Murthy, M.R.N. (2008) Structure of biosynthetic *N*-acetylornithine aminotransferase from *Salmonella typhimurium*: studies on substrate specificity and inhibitor binding. *Proteins – Structure Function and Bioinformatics*, **70**, 429–441.

133 Ledwidge, R. and Blanchard, J.S. (1999) The dual biosynthetic capability of *N*-acetylornithine aminotransferase in arginine and lysine biosynthesis. *Biochemistry*, **38**, 3019–3024.

134 Slocum, R.D. (2005) Genes, enzymes and regulation of arginine biosynthesis in plants. *Plant Physiology and Biochemistry*, **43**, 729–745.

135 Xu, Y., Labedan, B., and Glansdorff, N. (2007) Surprising arginine biosynthesis: a reappraisal of the enzymology and evolution of the pathway in microorganisms. *Microbiology and Molecular Biology Reviews*, **71**, 36–47.

136 Bachmann, C., Krähenbühl, S., and Colombo, J.P. (1982) Purification and properties of acetyl-CoA: L-glutamate *N*-acetyltransferase from human liver. *Biochemical Journal*, **205**, 123–127.

137 Shi, D., Sagar, V., Jin, Z.M., Yu, X.L., Caldovic, L., Morizono, H., Allewell, N.M., and Tuchman, M. (2008) The crystal structure of *N*-acetyl-L-glutamate synthase from *Neisseria gonorrhoeae* provides insights into mechanisms of catalysis and regulation. *The Journal of Biological Chemistry*, **283**, 7176–7184.

138 Alonso, E. and Rubio, V. (1989) Participation of ornithine aminotransferase in the synthesis and catabolism of ornithine in mice. Studies using gabaculine and arginine deprivation. *Biochemical Journal*, **259**, 131–138.

139 Lqbal, A., Clifton, I.J., Bagonis, M., Kershaw, N.J., Domene, C., Claridge, T.D.W., Wharton, C.W., and Schofield, C.J. (2009) Anatomy of a simple acyl intermediate in enzyme catalysis: combined biophysical and modeling studies on ornithine acetyl transferase. *Journal of the American Chemical Society*, **131**, 749–757.

140 Marc, F., Weigel, P., Legrain, C., Almeras, Y., Santrot, M., Glansdorff, N., and Sakanyan, V. (2000) Characterization and kinetic mechanism of mono- and bifunctional ornithine acetyltransferases from thermophilic microorganisms. *European Journal of Biochemistry*, **267**, 5217–5226.

141 Shi, D., Yu, X., Roth, L., Morizono, H., Hathout, Y., Allewell, N.M., and Tuchman, M. (2005) Expression, purification, crystallization and preliminary X-ray crystallographic studies of a novel acetylcitrulline deacetylase from *Xanthomonas campestris*. *Acta Crystallographica F*, **61**, 676–679.

142 Shi, D., Morizono, H., Yu, X., Roth, L., Caldovic, L., Allewell, N.M., Malamy, M.H., and Tuchman, M. (2005) Crystal structure of *N*-acetylornithine transcarbamylase from *Xanthomonas campestris*: a novel enzyme in a new arginine biosynthetic pathway found in several eubacteria. *The Journal of Biological Chemistry*, **280**, 14366–14369.

143 Shi, D., Morizono, H., Cabrera-Luque, J., Yu, X.L., Roth, L., Malamy, M.H., Allewell, N.M., and Tuchman, M. (2006) Structure and catalytic mechanism of a novel *N*-succinyl-L-ornithine transcarbamylase in arginine biosynthesis of *Bacteroides fragilis*. *The Journal of Biological Chemistry*, **281**, 20623–20631.

144 Allewell, N.M., Shi, D., Morizono, H., and Tuchman, M. (1999) Molecular recognition by ornithine and aspartate transcarbamylases. *Accounts of Chemical Research*, **32**, 885–894.

145 Labedan, B., Boyen, A., Baetens, M., Charlier, D., Chen, P., Cunin, R., Durbeco, V., Glansdorff, N., Herve, G., Legrain, C., Liang, Z., Purcarea, C., Roovers, M., Sanchez, R., Toong, T.-L., Van de Casteele, M., van Vliet, F., Xu, Y., and Zhang, Y.-F. (1999) The evolutionary history of carbamoyltransferases: a complex set of paralogous genes was already present in the last universal

common ancestor. *Journal of Molecular Evolution*, **49**, 461–473.

146 Sankaranarayanan, R., Cherney, M.M., Cherney, L.T., Garen, C.R., Moradian, F., and James, M.N.G. (2008) The crystal structures of ornithine carbamoyltransferase from *Mycobacterium tuberculosis* and its ternary complex with carbamoyl phosphate and L-norvaline reveal the enzyme's catalytic mechanism. *Journal of Molecular Biology*, **375**, 1052–1063.

147 Yu, Y., Terada, K., Nagasaki, A., Takiguchi, M., and Mori, M. (1995) Preparation of recombinant argininosuccinate synthetase and argininosuccinate lyase – expression of the enzymes in rat tissues. *Journal of Biochemistry*, **117**, 952–957.

148 Bork, P. and Koonin, E.V. (1994) A P-loop-like motif in a widespread ATP pyrophosphatase domain: implications for the evolution of sequence motifs and enzyme activity. *Proteins – Structure Function and Genetics*, **20**, 347–355.

149 Goto, M., Omi, R., Miyahara, I., Sugahara, M., and Hirotsu, K. (2003) Structures of argininosuccinate synthetase in enzyme-ATP substrates and enzyme-AMP product forms: stereochemistry of the catalytic reaction. *The Journal of Biological Chemistry*, **278**, 22964–22971.

150 Tsai, M., Koo, J., and Howell, P.L. (2005) Recovery of argininosuccinate lyase activity in duck δ1 crystallin. *Biochemistry*, **44**, 9034–9044.

151 Fujii, T., Sakai, H., Kawata, Y., and Hata, Y. (2003) Crystal structure of thermostable aspartase from *Bacillus* sp YM55-1: structure-based exploration of functional sites in the aspartase family. *Journal of Molecular Biology*, **328**, 635–654.

152 Dailey, F.E. and Cronan, J.E. (1986) Acetohydroxy acid synthase I, a required enzyme for isoleucine and valine biosynthesis in *Escherichia coli* K-12 during growth on acetate as the sole carbon source. *Journal of Bacteriology*, **165**, 453–460.

153 Dumas, R., Biou, V., Halgand, F., Douce, R., and Duggleby, R.G. (2001) Enzymology, structure, and dynamics of acetohydroxy acid isomeroreductase. *Accounts of Chemical Research*, **34**, 399–408.

154 Flint, D.H., Emptage, M.H., Finnegan, M.G., Fu, W., and Johnson, M.K. (1993) The role and properties of the iron–sulfur cluster in *Escherichia coli* dihydroxy-acid dehydratase. *The Journal of Biological Chemistry*, **268**, 14732–14742.

155 Chipman, D., Barak, Z., and Schloss, J.V. (1998) Biosynthesis of 2-aceto-2-hydroxy acids: acetolactate synthases and acetohydroxyacid synthases. *Biochimica et Biophysica Acta – Protein Structure and Molecular Enzymology*, **1385**, 401–419.

156 Kishore, G.M. and Shah, D.M. (1988) Amino acid biosynthesis inhibitors as herbicides. *Annual Review of Biochemistry*, **57**, 627–663.

157 Engel, S., Vyazmensky, M., Vinogradov, M., Berkovich, D., Bar-Ilan, A., Qimron, U., Rosiansky, Y., Barak, Z., and Chipman, D.M. (2004) Role of a conserved arginine in the mechanism of acetohydroxyacid synthase: catalysis of condensation with a specific ketoacid substrate. *The Journal of Biological Chemistry*, **279**, 24803–24812.

158 McCourt, J.A., Pang, S.S., King-Scott, J., Guddat, L.W., and Duggleby, R.G. (2006) Herbicide-binding sites revealed in the structure of plant acetohydroxyacid synthase. *Proceedings of the National Academy of Sciences of the United States of America*, **103**, 569–573.

159 Scarselli, M., Padula, M.G., Bernini, A., Spiga, O., Ciutti, A., Leoncini, R., Vannoni, D., Marinello, E., and Niccolai, N. (2003) Structure and function correlations between the rat liver threonine deaminase and aminotransferases. *Biochimica et Biophysica Acta – Proteins and Proteomics*, **1645**, 40–48.

160 Eikmanns, B.J., Eggeling, L., and Sahm, H. (1993) Molecular aspects of lysine, threonine, and isoleucine biosynthesis in *Corynebacterium glutamicum*. *Antonie Van Leeuwenhoek International Journal of General and Molecular Microbiology*, **64**, 145–163.

161 Shulman, A., Zalyapin, E., Vyazmensky, M., Yifrach, O., Barak, Z., and Chipman, D.M. (2008) Allosteric regulation of *Bacillus subtilis* threonine deaminase, a biosynthetic threonine deaminase with a single regulatory domain. *Biochemistry*, **47**, 11783–11792.

162 Eisenstein, E. (1991) Cloning, expression, purification, and characterization of biosynthetic threonine deaminase from *Escherichia coli*. *The Journal of Biological Chemistry*, **266**, 5801–5807.

163 Drevland, R.M., Waheed, A., and Graham, D.E. (2007) Enzymology and evolution of the pyruvate pathway to 2-oxobutyrate in *Methanocaldococcus jannaschii*. *Journal of Bacteriology*, **189**, 4391–4400.

164 Biou, V., Dumas, R., CohenAddad, C., Douce, R., Job, D., and PebayPeyroula, E. (1997) The crystal structure of plant acetohydroxy acid isomeroreductase complexed with NADPH, two magnesium ions and a herbicidal transition state analog determined at 1.65 Å resolution. *The EMBO Journal*, **16**, 3405–3415.

165 Beinert, H., Kennedy, M.C., and Stout, C.D. (1996) Aconitase as iron–sulfur protein, enzyme, and iron-regulatory protein. *Chemical Reviews*, **96**, 2335–2374.

166 Duan, X., Yang, J., Ren, B., Tan, G., and Ding, H. (2009) Reactivity of nitric oxide with the [4Fe–4S] cluster of dihydroxyacid dehydratase from *Escherichia coli*. *Biochemical Journal*, **417**, 783–789.

167 Hyduke, D.R., Jarboe, L.R., Tran, L.M., Chou, K.J.Y., and Liao, J.C. (2007) Integrated network analysis identifies nitric oxide response networks and dihydroxyacid dehydratase as a crucial target in *Escherichia coli*. *Proceedings of the National Academy of Sciences of the United States of America*, **104**, 8484–8489.

168 Macomber, L. and Imlay, J.A. (2009) The iron–sulfur clusters of dehydratases are primary intracellular targets of copper toxicity. *Proceedings of the National Academy of Sciences of the United States of America*, **106**, 8344–8349.

169 Xu, H., Andi, B., Qian, J., West, A.H., and Cook, P.F. (2006) The α-aminoadipate pathway for lysine biosynthesis in fungi. *Cell Biochemistry and Biophysics*, **46**, 43–64.

170 Wulandari, A.P., Miyazaki, J., Kobashi, N., Nishiyama, M., Hoshino, T., and Yamane, H. (2002) Characterization of bacterial homocitrate synthase involved in lysine biosynthesis. *FEBS Letters*, **522**, 35–40.

171 de Carvalho, L.P.S. and Blanchard, J.S. (2006) Kinetic and chemical mechanism of alpha-isopropylmalate synthase from *Mycobacterium tuberculosis*. *Biochemistry*, **45**, 8988–8999.

172 Howell, D.M., Xu, H.M., and White, R.H. (1999) (*R*)-Citramalate synthase in methanogenic archaea. *Journal of Bacteriology*, **181**, 331–333.

173 Li, F., Hagemeier, C.H., Seedorf, H., Gottschalk, G., and Thauer, R.K. (2007) Re-citrate synthase from *Clostridium kluyveri* is phylogenetically related to homocitrate synthase and isopropylmalate synthase rather than to *Si*-citrate synthase. *Journal of Bacteriology*, **189**, 4299–4304.

174 Koon, N., Squire, C.J., and Baker, E.N. (2004) Crystal structure of LeuA from *Mycobacterium tuberculosis*, a key enzyme in leucine biosynthesis. *Proceedings of the National Academy of Sciences of the United States of America*, **101**, 8295–8300.

175 Qian, J., Khandogin, J., West, A.H., and Cook, P.F. (2008) Evidence for a catalytic dyad in the active site of homocitrate synthase from *Saccharomyces cerevisiae*. *Biochemistry*, **47**, 6851–6858.

176 Gruer, M.J., Artymiuk, P.J., and Guest, J.R. (1997) The aconitase family: three structural variations on a common theme. *Trends in Biochemical Sciences*, **22**, 3–6.

177 Yasutake, Y., Yao, M., Sakai, N., Kirita, T., and Tanaka, I. (2004) Crystal structure of the *Pyrococcus horikoshii* isopropylmalate isomerase small subunit provides insight into the dual substrate specificity of the enzyme. *Journal of Molecular Biology*, **344**, 325–333.

178 Hurley, J.H., Thorsness, P.E., Ramalingam, V., Helmers, N.H., Koshland, D.E., and Stroud, R.M. (1989) Structure of a bacterial enzyme regulated by phosphorylation, isocitrate dehydrogenase. *Proceedings of the National Academy of Sciences of the United States of America*, **86**, 8635–8639.

179 Imada, K., Sato, M., Tanaka, N., Katsube, Y., Matsuura, Y., and Oshima, T. (1991) 3-Dimensional structure of a highly thermostable enzyme, 3-isopropylmalate dehydrogenase of *Thermus thermophilus* at 2.2 Å resolution. *Journal of Molecular Biology*, **222**, 725–738.

180 Howell, D.M., Graupner, M., Xu, H., and White, R.H. (2000) Identification of enzymes homologous to isocitrate

dehydrogenase that are involved in coenzyme B and leucine biosynthesis in methanoarchaea. *Journal of Bacteriology*, **182**, 5013–5016.

181 Bolduc, J.M., Dyer, D.H., Scott, W.G., Singer, P., Sweet, R.M., Koshland, D.E., and Stoddard, B.L. (1995) Mutagenesis and Laue structures of enzyme intermediates: isocitrate dehydrogenase. *Science*, **268**, 1312–1318.

182 Miyazaki, J., Kobashi, N., Nishiyama, M., and Yamane, H. (2003) Characterization of homoisocitrate dehydrogenase involved in lysine biosynthesis of an extremely thermophilic bacterium, *Thermus thermophilus* HB27, and evolutionary implication of beta-decarboxylating dehydrogenase. *The Journal of Biological Chemistry*, **278**, 1864–1871.

183 Miyazaki, K. (2005) Bifunctional isocitrate-homoisocitrate dehydrogenase: a missing link in the evolution of β-decarboxylating dehydrogenase. *Biochemical and Biophysical Research Communications*, **331**, 341–346.

184 Chen, R., Greer, A., and Dean, A.M. (1996) Redesigning secondary structure to invert coenzyme specificity in isopropylmalate dehydrogenase. *Proceedings of the National Academy of Sciences of the United States of America*, **93**, 12171–12176.

185 Miyazaki, T., Miyazaki, J., Yamane, H., and Nishiyama, M. (2004) α-Aminoadipate aminotransferase from an extremely thermophilic bacterium, *Thermus thermophilus*. *Microbiology*, **150**, 2327–2334.

186 Matsuda, M. and Ogur, M. (1969) Enzymatic and physiological properties of yeast glutamate-α-ketoadipate transaminase. *The Journal of Biological Chemistry*, **244**, 5153–5158.

187 Matsuda, M. and Ogur, M. (1969) Separation and specificity of yeast glutamate-α-ketoadipate transaminase. *The Journal of Biological Chemistry*, **244**, 3352–3358.

188 Tomita, T., Miyagawa, T., Miyazaki, T., Fushinobu, S., Kuzuyama, T., and Nishiyama, M. (2009) Mechanism for multiple-substrates recognition of α-aminoadipate aminotransferase from *Thermus thermophilus*. *Proteins – Structure Function and Bioinformatics*, **75**, 348–359.

189 Velasco, A.M., Leguina, J.I., and Lazcano, A. (2002) Molecular evolution of the lysine biosynthetic pathways. *Journal of Molecular Evolution*, **55**, 445–449.

190 Nishida, H., Nishiyama, M., Kobashi, N., Kosuge, T., Hoshino, T., and Yamane, H. (1999) A prokaryotic gene cluster involved in synthesis of lysine through the amino adipate pathway: a key to the evolution of amino acid biosynthesis. *Genome Research*, **9**, 1175–1183.

191 Hudson, A.O., Gilvarg, C., and Leustek, T. (2008) Biochemical and phylogenetic characterization of a novel diaminopimelate biosynthesis pathway in prokaryotes identifies a diverged form of LL-diaminopimelate aminotransferase. *Journal of Bacteriology*, **190**, 3256–3263.

192 Viola, R.E. (2001) The central enzymes of the aspartate family of amino acid biosynthesis. *Accounts of Chemical Research*, **34**, 339–349.

193 Coulter, C.V., Gerrard, J.A., Kraunsoe, J.A.E., and Pratt, A.J. (1999) Escherichia *coli* dihydrodipicolinate synthase and dihydrodipicolinate reductase: kinetic and inhibition studies of two putative herbicide targets. *Pesticide Science*, **55**, 887–895.

194 Dobson, R.C.J., Valegard, K., and Gerrard, J.A. (2004) The crystal structure of three site-directed mutants of *Escherichia coli* dihydrodipicolinate synthase: further evidence for a catalytic triad. *Journal of Molecular Biology*, **338**, 329–339.

195 Devenish, S.R.A., Huisman, F.H.A., Parker, E.J., Hadfield, A.T., and Gerrard, J.A. (2009) Cloning and characterisation of dihydrodipicolinate synthase from the pathogen *Neisseria meningitidis*. *Biochimica et Biophysica Acta – Proteins and Proteomics*, **1794**, 1168–1174.

196 Dobson, R.C.J., Griffin, M.D.W., Devenish, S.R.A., Pearce, F.G., Hutton, C.A., Gerrard, J.A., Jameson, G.B., and Perugini, M.A. (2008) Conserved main-chain peptide distortions: a proposed role for Ile203 in catalysis by dihydrodipicolinate synthase. *Protein Science*, **17**, 2080–2090.

197 Ge, X., Olson, A., Cai, S., and Sem, D.S. (2008) Binding synergy and cooperativity in dihydrodipicolinate reductase: implications for mechanism and the design of biligand inhibitors. *Biochemistry*, **47**, 9966–9980.

198 Pearce, F.G., Sprissler, C., and Gerrard, J.A. (2008) Characterization of dihydrodipicolinate reductase from *Thermotoga maritima* reveals evolution of substrate binding kinetics. *Journal of Biochemistry*, **143**, 617–623.

199 Pillai, B., Moorthie, V.A., van Belkum, M.J., Marcus, S.L., Cherney, M.M., Diaper, C.M., Vederas, J.C., and James, M.N.G. (2009) Crystal structure of diaminopimelate epimerase from *Arabidopsis thaliana*, an amino acid racemase critical for L-lysine biosynthesis. *Journal of Molecular Biology*, **385**, 580–594.

200 Usha, V., Dover, L.G., Roper, D.L., and Besra, G.S. (2008) Characterization of *Mycobacterium tuberculosis* diaminopimelic acid epimerase: paired cysteine residues are crucial for racemization. *FEMS Microbiology Letters*, **280**, 57–63.

201 Hu, T., Wu, D., Chen, J., Ding, J., Jiang, H., and Shen, X. (2008) The catalytic intermediate stabilized by a "Down" active site loop for diaminopimelate decarboxylase from *Helicobacter pylori*: enzymatic characterization with crystal structure analysis. *The Journal of Biological Chemistry*, **283**, 21284–21293.

202 Lee, J., Michael, A.J., Martynowski, D., Goldsmith, E.J., and Phillips, M.A. (2007) Phylogenetic diversity and the structural basis of substrate specificity in the β/α-barrel fold basic amino acid decarboxylases. *The Journal of Biological Chemistry*, **282**, 27115–27125.

203 Gokulan, K., Rupp, B., Pavelka, M.S., Jacobs, W.R., and Sacchettini, J.C. (2003) Crystal structure of *Mycobacterium tuberculosis* diaminopimelate decarboxylase, an essential enzyme in bacterial lysine biosynthesis. *The Journal of Biological Chemistry*, **278**, 18588–18596.

204 Watanabe, N., Cherney, M.M., van Belkum, M.J., Marcus, S.L., Flegel, M.D., Clay, M.D., Deyholos, M.K., Vederas, J.C., and James, M.N.G. (2007) Crystal structure of LL-diaminopimelate aminotransferase from *Arabidopsis thaliana*: a recently discovered enzyme in the biosynthesis of L-lysine by plants and *Chlamydia*. *Journal of Molecular Biology*, **371**, 685–702.

205 White, P.J. (1983) The essential role of diaminopimelate dehydrogenase in the biosynthesis of lysine by *Bacillus sphaericus*. *Journal of General Microbiology*, **129**, 739–749.

206 Miyazaki, J., Kobashi, N., Nishiyama, M., and Yamane, H. (2001) Functional and evolutionary relationship between arginine biosynthesis and prokaryotic lysine biosynthesis through alpha-aminoadipate. *Journal of Bacteriology*, **183**, 5067–5073.

207 Horie, A., Tomita, T., Saiki, A., Kono, H., Taka, H., Mineki, R., Fujimura, T., Nishiyama, C., Kuzuyama, T., and Nishiyama, M. (2009) Discovery of proteinaceous N-modification in lysine biosynthesis of *Thermus thermophilus*. *Nature Chemical Biology*, **5**, 673–679.

208 Baldwin, J.E., Shiau, C.Y., Byford, M.F., and Schofield, C.J. (1994) Substrate-specificity of L-δ-(α-aminoadipoyl)-L-cysteinyl-D-valine synthetase from *Cephalosporium acremonium*: demonstration of the structure of several unnatural tripeptide products. *Biochemical Journal*, **301**, 367–372.

209 Aharonowitz, Y., Bergmeyer, J., Cantoral, J.M., Cohen, G., Demain, A.L., Fink, U., Kinghorn, J., Kleinkauf, H., MacCabe, A., Palissa, H., Pfeifer, E., Schwecke, T., Vanliempt, H., Vondohren, H., Wolfe, S., and Zhang, J.Y. (1993) δ-(L-α-Aminoadipyl)-L-cysteinyl-D-valine synthetase, the multienzyme integrating the four primary reactions in β-lactam biosynthesis, as a model peptide synthetase. *Bio/Technology*, **11**, 807–810.

210 Byford, M.F., Baldwin, J.E., Shiau, C.-Y., and Schofield, C.J. (1997) The mechanism of ACV synthetase. *Chemical Reviews*, **97**, 2631–2650.

211 An, K.-D., Nishida, H., Miura, Y., and Yokota, A. (2003) Molecular evolution of adenylating domain of aminoadipate reductase. *BMC Evolutionary Biology*, **3**, 9.

212 Storts, D.R. and Bhattacharjee, J.K. (1987) Purification and properties of saccharopine dehydrogenase (glutamate

forming) in the *Saccharomyces cerevisiae* lysine biosynthetic pathway. *Journal of Bacteriology*, **169**, 416–418.

213 Johansson, E., Steffens, J.J., Lindqvist, Y., and Schneider, G. (2000) Crystal structure of saccharopine reductase from *Magnaporthe grisea*, an enzyme of the alpha-aminoadipate pathway of lysine biosynthesis. *Structure*, **8**, 1037–1047.

214 Andi, B., Cook, P.F., and West, A.H. (2006) Crystal structure of the His-tagged saccharopine reductase from *Saccharomyces cerevisiae* at 1.7 Å resolution. *Cell Biochemistry and Biophysics*, **46**, 17–26.

215 Burk, D.L., Hwang, J., Kwok, E., Marrone, L., Goodfellow, V., Dmitrienko, G.I., and Berghuis, A.M. (2007) Structural studies of the final enzyme in the α-aminoadipate pathway – saccharopine dehydrogenase from *Saccharomyces cerevisiae*. *Journal of Molecular Biology*, **373**, 745–754.

216 Xu, H.Y., Alguindigue, S.S., West, A.H., and Cook, P.F. (2007) A proposed proton shuttle mechanism for saccharopine dehydrogenase from *Saccharomyces cerevisiae*. *Biochemistry*, **46**, 871–882.

217 Hao, B., Gong, W., Ferguson, T.K., James, C.M., Krzycki, J.A., and Chan, M.K. (2002) A new UAG-encoded residue in the structure of a methanogen methyltransferase. *Science*, **296**, 1462–1466.

218 Soares, J.A., Zhang, L., Pitsch, R.L., Kleinholz, N.M., Jones, R.B., Wolff, J.J., Amster, J., Green-Church, K.B., and Krzycki, J.A. (2005) The residue mass of L-pyrrolysine in three distinct methylamine methyltransferases. *The Journal of Biological Chemistry*, **280**, 36962–36969.

219 Krzycki, J.A. (2004) Function of genetically encoded pyrrolysine in corrinoid-dependent methylamine methyltransferases. *Current Opinion in Chemical Biology*, **8**, 484–491.

220 Blight, S.K., Larue, R.C., Mahapatra, A., Longstaff, D.G., Chang, E., Zhao, G., Kang, P.T., Green-Church, K.B., Chan, M.K., and Krzycki, J.A. (2004) Direct charging of $tRNA^{CUA}$ with pyrrolysine *in vitro* and *in vivo*. *Nature*, **431**, 333–335.

221 Polycarpo, C., Ambrogelly, A., Berube, A., Winbush, S.A.M., McCloskey, J.A., Crain, P.F., Wood, J.L., and Soll, D. (2004) An aminoacyl-tRNA synthetase that specifically activates pyrrolysine. *Proceedings of the National Academy of Sciences of the United States of America*, **101**, 12450–12454.

222 Yuan, J., O'Donoghue, P., Ambrogelly, A., Gundllapalli, S., Sherrer, R.L., Palioura, S., Simonovic, M., and Söll, D. (2010) Distinct genetic code expansion strategies for selenocysteine and pyrrolysine are reflected in different aminoacyl-tRNA formation systems. *FEBS Letters*, **584**, 342–349.

223 Kavran, J.M., Gundlliapalli, S., O'Donoghue, P., Englert, M., Söll, D., and Steitz, T.A. (2007) Structure of pyrrolysyl-tRNA synthetase, an archaeal enzyme for genetic code innovation. *Proceedings of the National Academy of Sciences of the United States of America*, **104**, 11268–11273.

224 Longstaff, D.G., Larue, R.C., Faust, J.E., Mahapatra, A., Zhang, L., Green-Church, K.B., and Krzycki, J.A. (2007) A natural genetic code expansion cassette enables transmissible biosynthesis and genetic encoding of pyrrolysine. *Proceedings of the National Academy of Sciences of the United States of America*, **104**, 1021–1026.

225 Abell, C. (1999) Enzymology and molecular biology of the shikimate pathway. *Comprehensive Natural Products Chemistry*, **1**, 573–607.

226 Herrmann, K.M. and Weaver, L.M. (1999) The shikimate pathway. *Annual Review of Plant Physiology and Plant Molecular Biology*, **50**, 473–503.

227 Stephens, C.M. and Bauerle, R. (1991) Analysis of the metal requirement of 3-deoxy-D-*arabino*-heptulosonate-7-phosphate synthase from *Escherichia coli*. *The Journal of Biological Chemistry*, **266**, 20810–20817.

228 Shumilin, I.A., Bauerle, R., Wu, J., Woodard, R.W., and Kretsinger, R.H. (2004) Crystal structure of the reaction complex of 3-deoxy-D-*arabino*-heptulosonate-7-phosphate synthase from *Thermotoga maritima* refines the catalytic mechanism and indicates a new mechanism of allosteric regulation. *Journal of Molecular Biology*, **341**, 455–466.

229 Ran, N., Draths, K.M., and Frost, J.W. (2004) Creation of a shikimate pathway

variant. *Journal of the American Chemical Society*, **126**, 6856–6857.

230 Ran, N. and Frost, J.W. (2007) Directed evolution of 2-keto-3-deoxy-6-phosphogalactonate aldolase to replace 3-deoxy-D-*arabino*-heptulosonic acid 7-phosphate synthase. *Journal of the American Chemical Society*, **129**, 6130–6139.

231 Webby, C.J., Baker, H.M., Lott, J.S., Baker, E.N., and Parker, E.J. (2005) The structure of 3-deoxy-D-*arabino*-heptulosonate 7-phosphate synthase from *Mycobacterium tuberculosis* reveals a common catalytic scaffold and ancestry for type I and type II enzymes. *Journal of Molecular Biology*, **354**, 927–939.

232 Wagner, T., Shumilin, I.A., Bauerle, R., and Kretsinger, R.H. (2000) Structure of 3-deoxy-D-*arabino*-heptulosonate-7-phosphate synthase from *Escherichia coli*: Comparison of the Mn^{2+}*2-phosphoglycolate and the Pb^{2+}*2-phosphoenolpyruvate complexes and implications for catalysis. *Journal of Molecular Biology*, **301**, 389–399.

233 Schofield, L.R., Anderson, B.F., Patchett, M.L., Norris, G.E., Jameson, G.B., and Parker, E.J. (2005) Substrate ambiguity and structure of *Pyrococcus furiosus* 3-deoxy-D-*arabino*-heptulosonate-7-phosphate synthase: an ancestral 3-deoxyald-2-ulosonate phosphate synthase? *Biochemistry*, **44**, 11950–11962.

234 König, V., Pfeil, A., Braus, G.H., and Schneider, T.R. (2004) Substrate and metal complexes of 3-deoxy-D-*arabino*-heptulosonate-7-phosphate synthase from *Saccharomyces cerevisiae* provide new insights into the catalytic mechanism. *Journal of Molecular Biology*, **337**, 675–690.

235 Wu, J., Howe, D.L., and Woodard, R.W. (2003) Thermotoga *maritima* 3-deoxy-D-*arabino*-heptulosonate 7-phosphate (DAHP) synthase: the ancestral eubacterial DAHP synthase? *The Journal of Biological Chemistry*, **278**, 27525–31.

236 Widlanski, T., Bender, S.L., and Knowles, J.R. (1989) Dehydroquinate synthase: a sheep in wolf's clothing? *Journal of the American Chemical Society*, **111**, 2299–2300.

237 Carpenter, E.P., Hawkins, A.R., Frost, J.W., and Brown, K.A. (1998) Structure of dehydroquinate synthase reveals an active site capable of multistep catalysis. *Nature*, **394**, 299–302.

238 Bartlett, P.A. and Satake, K. (1988) Does dehydroquinate synthase synthesize dehydroquinate? *Journal of the American Chemical Society*, **110**, 1628–1630.

239 Tanner, M.E. (2008) Transient oxidation as a mechanistic strategy in enzymatic catalysis. *Current Opinion in Chemical Biology*, **12**, 532–538.

240 Porat, I., Sieprawska-Lupa, M., Teng, Q., Bohanon, F.J., White, R.H., and Whitman, W.B. (2006) Biochemical and genetic characterization of an early step in a novel pathway for the biosynthesis of aromatic amino acids and *p*-aminobenzoic acid in the archaeon *Methanococcus maripaludis*. *Molecular Microbiology*, **62**, 1117–1131.

241 White, R.H. (2004) l-Aspartate semialdehyde and a 6-deoxy-5-ketohexose 1-phosphate are the precursors to the aromatic amino acids in *Methanocaldococcus jannaschii*. *Biochemistry*, **43**, 7618–7627.

242 Morar, M., White, R.H., and Ealick, S.E. (2007) Structure of 2-amino-3,7-dideoxy-D-threo-hept-6-ulosonic acid synthase, a catalyst in the archaeal pathway for the biosynthesis of aromatic amino acids. *Biochemistry*, **46**, 10562–10571.

243 Gourley, D.G., Shrive, A.K., Polikarpov, I., Krell, T., Coggins, J.R., Hawkins, A.R., Isaacs, N.W., and Sawyer, L. (1999) The two types of 3-dehydroquinase have distinct structures but catalyze the same overall reaction. *Nature Structural Biology*, **6**, 521–525.

244 Shneier, A., Harris, J., Kleanthous, C., Coggins, J.R., Hawkins, A.R., and Abell, C. (1993) Evidence for opposite stereochemical courses for the reactions catalyzed by type I and type II dehydroquinases. *Bioorganic & Medicinal Chemistry Letters*, **3**, 1399–402.

245 Shneier, A., Kleanthous, C., Deka, R., Coggins, J.R., and Abell, C. (1991) Observation of an imine intermediate on dehydroquinase by electrospray mass spectrometry. *Journal of the American Chemical Society*, **113**, 9416–9418.

246 Kleanthous, C., Reilly, M., Cooper, A., Kelly, S., Price, N.C., and Coggins, J.R.

(1991) Stabilization of the shikimate pathway enzyme dehydroquinase by covalently bound ligand. *The Journal of Biological Chemistry*, **266**, 10893–10898.

247 Gonzalez-Bello, C. and Castedo, L. (2007) Progress in type II dehydroquinase inhibitors: from concept to practice. *Medicinal Research Reviews*, **27**, 177–208.

248 Chaudhuri, S. and Coggins, J.R. (1985) The purification of shikimate dehydrogenase from *Escherichia coli*. *Biochemical Journal*, **226**, 217–223.

249 Chaudhuri, S., Anton, I.A., and Coggins, J.R. (1987) Shikimate dehydrogenase from *Escherichia coli*. *Methods in Enzymology*, **142**, 315–320.

250 Han, C., Hu, T., Wu, D., Qu, S., Zhou, J., Ding, J., Shen, X., Qu, D., and Jiang, H. (2009) X-ray crystallographic and enzymatic analyses of shikimate dehydrogenase from *Staphylococcus epidermidis*. *FEBS Journal*, **276**, 1125–1139.

251 Singh, S., Korolev, S., Koroleva, O., Zarembinski, T., Collart, F., Joachimiak, A., and Christendat, D. (2005) Crystal structure of a novel shikimate dehydrogenase from *Haemophilus influenzae*. *The Journal of Biological Chemistry*, **280**, 17101–17108.

252 Michel, G., Roszak, A.W., Sauve, V., Maclean, J., Matte, A., Coggins, J.R., Cygler, M., and Lapthorn, A.J. (2003) Structures of shikimate dehydrogenase AroE and its paralog YdiB: a common structural framework for different activities. *The Journal of Biological Chemistry*, **278**, 19463–19472.

253 Segura-Cabrera, A. and Rodriguez-Perez, M.A. (2008) Structure-based prediction of *Mycobacterium tuberculosis* shikimate kinase inhibitors by high-throughput virtual screening. *Bioorganic & Medicinal Chemistry Letters*, **18**, 3152–3157.

254 Pauli, I., Caceres, R.A., and Filgueira de Azevedo, W. (2008) Molecular modeling and dynamics studies of shikimate kinase from *Bacillus anthracis*. *Bioorganic and Medicinal Chemistry*, **16**, 8098–8108.

255 Berti, P.J. and Chindemi, P. (2009) Catalytic residues and an electrostatic sandwich that promote enolpyruvyl shikimate 3-phosphate synthase (AroA) catalysis. *Biochemistry*, **48**, 3699–3707.

256 Funke, T., Healy-Fried, M.L., Han, H., Alberg, D.G., Bartlett, P.A., and Schönbrunn, E. (2007) Differential inhibition of class I and class II 5-enolpyruvylshikimate-3-phosphate synthases by tetrahedral reaction intermediate analogues. *Biochemistry*, **46**, 13344–13351.

257 Schonbrunn, E., Eschenburg, S., Shuttleworth, W.A., Schloss, J.V., Amrhein, N., Evans, J.N.S., and Kabsch, W. (2001) Interaction of the herbicide glyphosate with its target enzyme 5-enolpyruvylshikimate 3-phosphate synthase in atomic detail. *Proceedings of the National Academy of Sciences of the United States of America*, **98**, 1376–1380.

258 Fernandes, C.L., Breda, A., Santos, D.S., Basso, L.A., and de Souza, O.N. (2007) A structural model for chorismate synthase from *Mycobacterium tuberculosis* in complex with coenzyme and substrate. *Computers in Biology and Medicine*, **37**, 149–158.

259 Bornemann, S., Balasubramanian, S., Coggins, J.R., Abell, C., Lowe, D.J., and Thorneley, R.N. (1995) Escherichia *coli* chorismate synthase: a deuterium kinetic-isotope effect under single-turnover and steady-state conditions shows that a flavin intermediate forms before the C-(6*proR*)-H bond is cleaved. *Biochemical Journal*, **305**, 707–710.

260 Balasubramanian, S., Coggins, J.R., and Abell, C. (1995) Observation of a secondary tritium isotope effect in the chorismate synthase reaction. *Biochemistry*, **34**, 341–348.

261 Rauch, G., Ehammer, H., Bornemann, S., and Macheroux, P. (2008) Replacement of two invariant serine residues in chorismate synthase provides evidence that a proton relay system is essential for intermediate formation and catalytic activity. *FEBS Journal*, **275**, 1464–1473.

262 Rauch, G., Ehammer, H., Bornemann, S., and Macheroux, P. (2007) Mutagenic analysis of an invariant aspartate residue in chorismate synthase supports its role as an active site base. *Biochemistry*, **46**, 3768–74.

263 Lin, X., Xu, S., Yang, Y., Wu, J., Wang, H., Shen, H., and Wang, H. (2009) Purification and characterization of

anthranilate synthase component I (TrpE) from *Mycobacterium tuberculosis* H37Rv. *Protein Expression and Purification*, **64**, 8–15.

264 Morollo, A.A. and Eck, M.J. (2001) Structure of the cooperative allosteric anthranilate synthase from *Salmonella typhimurium*. *Nature Structural Biology*, **8**, 243–247.

265 Tang, X.-F., Ezaki, S., Atomi, H., and Imanaka, T. (2001) Anthranilate synthase without an LLES motif from a hyperthermophilic archaeon is inhibited by tryptophan. *Biochemical and Biophysical Research Communications*, **281**, 858–865.

266 Bulloch, E.M.M., Jones, M.A., Parker, E.J., Osborne, A.P., Stephens, E., Davies, G.M., Coggins, J.R., and Abell, C. (2004) Identification of 4-amino-4-deoxychorismate synthase as the molecular target for the antimicrobial action of (6*S*)-6-fluoroshikimate. *Journal of the American Chemical Society*, **126**, 9912–9913.

267 He, Z., Lavoie, K.D.S., Bartlett, P.A., and Toney, M.D. (2004) Conservation of mechanism in three chorismate-utilizing enzymes. *Journal of the American Chemical Society*, **126**, 2378–2385.

268 He, Z. and Toney, M.D. (2006) Direct detection and kinetic analysis of covalent intermediate formation in the 4-amino-4-deoxychorismate synthase catalyzed reaction. *Biochemistry*, **45**, 5019–5028.

269 Kim, C., Xuong, N.-H., Edwards, S., Madhusudan; Yee, M.-C., Spraggon, G., and Mills, S.E. (2002) The crystal structure of anthranilate phosphoribosyltransferase from the enterobacterium *Pectobacterium carotovorum*. *FEBS Letters*, **523**, 239–246.

270 Schlee, S., Deuss, M., Bruning, M., Ivens, A., Schwab, T., Hellmann, N., Mayans, O., and Sterner, R. (2009) Activation of anthranilate phosphoribosyltransferase from *Sulfolobus solfataricus* by removal of magnesium inhibition and acceleration of product release. *Biochemistry*, **48**, 5199–5209.

271 Sterner, R., Merz, A., Thoma, R., and Kirschner, K. (2001) Phosphoribosylanthranilate isomerase and indoleglycerol-phosphate synthase: tryptophan biosynthetic enzymes from *Thermotoga maritima*. *Methods in Enzymology*, **331**, 270–280.

272 Sterner, R., Dahm, A., Darimont, B., Ivens, A., Liebl, W., and Kirschner, K. (1995) $(\beta\alpha)_8$-Barrel proteins of tryptophan biosynthesis in the hyperthermophile *Thermotoga maritima*. *The EMBO Journal*, **14**, 4395–4402.

273 Raboni, S., Bettati, S., and Mozzarelli, A. (2009) Tryptophan synthase: a mine for enzymologists. *Cellular and Molecular Life Sciences*, **66**, 2391–2403.

274 Leopoldseder, S., Hettwer, S., and Sterner, R. (2006) Evolution of multi-enzyme complexes: the case of tryptophan synthase. *Biochemistry*, **45**, 14111–14119.

275 Sasso, S., Ökvist, M., Roderer, K., Gamper, M., Codoni, G., Krengel, U., and Kast, P. (2009) Structure and function of a complex between chorismate mutase and DAHP synthase: efficiency boost for the junior partner. *The EMBO Journal*, **28**, 2128–2142.

276 Song, J., Bonner, C.A., Wolinsky, M., and Jensen, R.A. (2005) The TyrA family of aromatic-pathway dehydrogenases in phylogenetic context. *BMC Biology*, **3**, 13.

277 Bonner, C.A., Jensen, R.A., Gander, J.E., and Keyhani, N.O. (2004) A core catalytic domain of the TyrA protein family: arogenate dehydrogenase from *Synechocystis*. *The Biochemical Journal*, **382**, 2792–91.

278 Bonner, C.A., Disz, T., Hwang, K., Song, J., Vonstein, V., Overbeek, R., and Jensen, R.A. (2008) Cohesion group approach for evolutionary analysis of TyrA, a protein family with wide-ranging substrate specificities. *Microbiology and Molecular Biology Reviews*, **72**, 13–53.

279 Sun, W., Shahinas, D., Bonvin, J., Hou, W., Kimber, M.S., Turnbull, J., and Christendat, D. (2009) The crystal structure of *Aquifex aeolicus* prephenate dehydrogenase reveals the mode of tyrosine inhibition. *The Journal of Biological Chemistry*, **284**, 13223–13232.

280 Alifano, P., Fani, R., Lio, P., Lazcano, A., Bazzicalupo, M., Carlomagno, M.S., and Bruni, C.B. (1996) Histidine biosynthetic pathway and genes: structure, regulation, and evolution. *Microbiological Reviews*, **60**, 44–69.

281 Martin, R.G., Berberich, M.A., Ames, B.N., Davis, W.W., Goldberger, R.F., and Yourno, J.D. (1971) Enzymes and intermediates of histidine biosynthesis in *Salmonella typhimurium*. *Methods in Enzymology*, **17**, 3–44.

282 Papaleo, M.C., Russo, E., Fondi, M., Emiliani, G., Frandi, A., Brilli, M., Pastorelli, R., and Fani, R. (2009) Structural, evolutionary and genetic analysis of the histidine biosynthetic "core" in the genus *Burkholderia*. *Gene*, **448**, 16–28.

283 Fondi, M., Emiliani, G., Lio, P., Gribaldo, S., and Fani, R. (2009) The evolution of histidine biosynthesis in archaea: insights into the his genes structure and organization in LUCA. *Journal of Molecular Evolution*, **69**, 512–526.

284 Jung, S., Chun, J.-Y., Yim, S.-H., Cheon, C.-I., Song, E., Lee, S.-S., and Lee, M.-S. (2009) Organization and analysis of the histidine biosynthetic genes from *Corynebacterium Glutamicum*. *Genes Genomics*, **31**, 315–323.

285 Fani, R., Brilli, M., Fondi, M., and Lio, P. (2007) The role of gene fusions in the evolution of metabolic pathways: the histidine biosynthesis case. *BMC Evolutionary Biology*, **7** (Suppl. 2), S12.

286 Henn-Sax, M., Thoma, R., Schmidt, S., Hennig, M., Kirschner, K., and Sterner, R. (2002) Two $(\beta\alpha)_8$-barrel enzymes of histidine and tryptophan biosynthesis have similar reaction mechanisms and common strategies for protecting their labile substrates. *Biochemistry*, **41**, 12032–12042.

287 Leopoldseder, S., Claren, J., Juergens, C., and Sterner, R. (2004) Interconverting the catalytic activities of (beta alpha)8-barrel enzymes from different metabolic pathways: sequence requirements and molecular analysis. *Journal of Molecular Biology*, **337**, 871–879.

288 Mayans, O., Ivens, A., Nissen, L.J., Kirschner, K., and Wilmanns, M. (2002) Structural analysis of two enzymes catalysing reverse metabolic reactions implies common ancestry. *The EMBO Journal*, **21**, 3245–54.

289 Lipchock, J.M. and Loria, J.P. (2008) 1H, 15N and ^{13}C resonance assignment of imidazole glycerol phosphate (IGP) synthase protein HisF from *Thermotoga maritima*. *Biomolecular NMR Assignments*, **2**, 219–221.

290 Chaudhuri, B.N., Lange, S.C., Myers, R.S., Davisson, V.J., and Smith, J.L. (2003) Toward understanding the mechanism of the complex cyclization reaction catalyzed by imidazole glycerolphosphate synthase: crystal structures of a ternary complex and the free enzyme. *Biochemistry*, **42**, 7003–7012.

291 Glynn, S.E., Baker, P.J., Sedelnikova, S.E., Davies, C.L., Eadsforth, T.C., Levy, C.W., Rodgers, H.F., Blackburn, G.M., Hawkes, T.R., Viner, R., and Rice, D.W. (2005) Structure and mechanism of imidazoleglycerol-phosphate dehydratase. *Structure*, **13**, 1809–1817.

292 Sinha, S.C., Chaudhuri, B.N., Burgner, J.W., Yakovleva, G., Davisson, V.J., and Smith, J.L. (2004) Crystal structure of imidazole glycerol-phosphate dehydratase: duplication of an unusual fold. *The Journal of Biological Chemistry*, **279**, 15491–15498.

293 Marineo, S., Cusimano, M.G., Limauro, D., Coticchio, G., and Puglia, A.M. (2008) The histidinol phosphate phosphatase involved in histidine biosynthetic pathway is encoded by SCO5208 (hisN) in *Streptomyces coelicolor* $A3_2$. *Current Microbiology*, **56**, 6–13.

294 Fernandez, F.J., Vega, M.C., Lehmann, F., Sandmeier, E., Gehring, H., Christen, P., and Wilmanns, M. (2004) Structural studies of the catalytic reaction pathway of a hyperthermophilic histidinol-phosphate aminotransferase. *The Journal of Biological Chemistry*, **279**, 21478–21488.

295 le Coq, D., Fillinger, S., and Aymerich, S. (1999) Histidinol phosphate phosphatase, catalyzing the penultimate step of the histidine biosynthesis pathway, is encoded by *ytvP* (*hisJ*) in *Bacillus subtilis*. *Journal of Bacteriology*, **181**, 3277–3280.